wawi

INSTITUT FÜR WASSERWIRTSCHAFT, HYDROLOGIE
UND LANDWIRTSCHAFTLICHEN WASSERBAU

Mitteilungen Heft 103
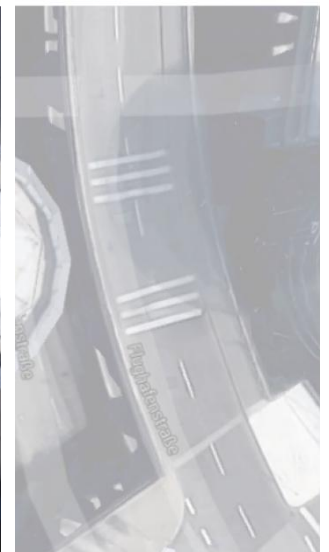
Imagery ©2016 Google, Map data ©2016 GeoBasis-DE/BKG (©2009), Google   10 m

E. RABIEI

Improvement of rainfall estimation using weather radar and RainCars for hydrological analyses

Improvement of rainfall estimation using weather radar and RainCars for hydrological analyses

Von der Fakultät für Bauingenieurwesen und Geodäsie
der Gottfried Wilhelm Leibniz Universität Hannover

zur Erlangung des akademischen Grades
Doktor-Ingenieur
- Dr.-Ing. -

genehmigte Dissertation

von

Ehsan Rabiei, M. Sc.

geboren am 27.07.1985 in Isfahan

2016

Referent: Prof. Dr.-Ing. Uwe Haberlandt
Korreferent: Univ.Prof. Dipl.-Ing. Dr.techn. Günter Blöschl

Tag der Promotion: 27. Juni 2016

Acknowledgements

First and foremost I would like to thank my supervisor Prof. Dr.-Ing. Uwe Haberlandt. It has been a great honor for me to be working in his team and under his supervision. I, not only learnt how to develop and present ideas from plans to structured texts, but also had the unique opportunity of bringing new ideas to the table. I would like to express my appreciation of the freedom I had to be able to spark my own creativity in his team.

I wish to thank all my colleagues in the institute with whom I spent a wonderful time during my research. I would like to express my thankfulness to Bastian Heinrich and Ehsan Mohammad-Pajooh for the help I received in the laboratory experiments. The scientific discussions I had with Christian Berndt and Markus Wallner helped me to develop ideas from the very first steps. My special thanks are due to Anne Fangmann, Sven van der Heijden and Alexander Verworn for their comments on my publications. In addition to others, I acknowledge all the good times I had with Ana Callau Poduje, Matthias Beyer, Bora Shehu, Stefan Plötner and Hannes Müller. It would have been a tougher journey without the friendly atmosphere we had in the institute.

The many friends and groups that became a part of my life in Hanover made my time indeed enjoyable. I am grateful for time spent with friends for camping, hiking, traveling, going out and playing football and table tennis.

Lastly, my very special thanks to my family for all their love and support. For my parents, who raised me in a way to be able to discover the world independently. And most of all for my loving, supportive, charming, and patient fiancée Sarva, whose support is very appreciated.

Thank you

Declaration

I, Ehsan Rabiei, hereby declare that:

1. I know the regulations for doctoral candidates and have met all the requirements. I agree with an examination under the provisions of the doctoral regulations.

2. I have completed the thesis independently, and where I have consulted other works, to the best of my knowledge and belief, this is always clearly attributed.

3. I have not paid any third party to contribute to the content of my dissertation (this means that the scientific work may has not been acquired or conveyed, either in part or in full, by a third party for payment or any other consideration).

4. This work contains no material which has been accepted for the award of any other degree or diploma at any other university or tertiary institution.

5. The same or partly similar work has not been submitted at any other university or academic institution.

6. I agree that my thesis can be used for verifying the compliance with scientific standards, in particular using electronic data processing programs.

The relevant permission that might be needed from the journals to reproduce the published works are granted from the copyright holders.

Hanover, March 7, 2016

Ehsan Rabiei

List of publications

This work consists of the following publications:

Chapter 3

Berndt, C., **Rabiei, E.**, Haberlandt, U., 2014. Geostatistical merging of rain gauge and radar data for high temporal resolutions and various station density scenarios. Journal of Hydrology, 508(0): 88-101.

My contribution to the paper:

- Programming and applying conditional merging (CM) interpolation technique in FORTRAN
- Preliminary investigation of the two interpolation techniques, KED and CM
- Preliminary results and pros and cons of KED and CM
- Writing a program for accumulating the radar data for coarser temporal resolutions
- Programming outlier detection for radar data and producing the related Fig .4
- Partly interpreting the results

Chapter 4

Rabiei, E., Haberlandt, U., 2015. Applying bias correction for merging rain gauge and radar data. Journal of Hydrology, 522(0): 544-557.

My contribution to the paper:

- Initial idea of correcting radar data using quantile mapping
- Developing the method
- Programming the method in FORTRAN
- Interpreting the results
- Writing the text and producing the figures

Chapter 5

Rabiei, E., Haberlandt, U., Sester, M., Fitzner, D., 2013. Rainfall estimation using moving cars as rain gauges - laboratory experiments. Hydrol. Earth Syst. Sci., 17(11): 4701-4712. [received the Jim Dooge best paper award in HESS]

My contribution to the work:

- Initial idea of building a rain simulator and a car speed simulator

- Designing the rain simulator for producing a range of rain intensities

- Defining the settings used in the study

- Setting up the laboratory - Teamwork

- Performing the tests in the laboratory - Teamwork

- Analyses of the data, interpreting the results

- Writing the text and producing the figures

Chapter 6

Rabiei, E., Haberlandt, U., Sester, M., Fitzner, D., Wallner, M., 2016. Areal rainfall estimation using moving cars - computer experiments including hydrological modeling. Hydrol. Earth Syst. Sci. Discuss., 2016: 1-38. [After First Revision]

My contribution to the work:

- Initial idea of evaluating the laboratory results in computer simulation combined with a hydrological model for a more general conclusion

- Developing all the techniques (except for the traffic model)

- Implementing all the techniques

- Carrying out all the analyses

- Interpreting the results

- Writing the text and producing the figures (except for figures related to traffic model)

Kurzfassung

Die Schätzung der Niederschlagsmenge ist eine anspruchsvolle Aufgabe, vor allem für hohe zeitliche Auflösungen. Räumliche Niederschlagsvariabilität ist schwer zu beobachten und wird oft als eine wichtige Fehlerquelle für Ermittlung des Gebietsniederschlags angesehen. Eine eingeschränkte Anzahl der Niederschlagsmesser auf der einen Seite, die Ungenauigkeit der Fernerkundung auf der anderen Seite, sind die Herausforderungen für die Ermittlung des Gebietsniederschlags.

In dieser Studie wird zuerst die Bedeutung der zeitlichen Auflösung der Regendaten und die Dichte des Niederschlagsmessnetzes für die Leistung von räumliche Interpolationsverfahren untersucht, wenn Wetterradar als zusätzliche Information berücksichtigt wird. Vier verschiedene Interpolationstechniken werden verglichen und mit Kreuzvalidierung ausgewertet. Kriging mit Externem Drift (KED), Indikator Kriging mit Externem Drift (IKED) und Conditional Merging (CM) untersuchen die Verwendung der Radardaten als zusätzliche Information, wobei Ordinary Kriging (OK) keine weiteren Informationen verwendet und als Referenzverfahren berücksichtigt wird. CM erbringt die besten Ergebnisse im Vergleich mit den anderen Interpolationsverfahren. Die Berücksichtigung von Radardaten scheint auch für sehr hohe zeitliche Auflösungen von Vorteil zu sein. Die Glättung der Radardaten verbessert die Leistung im Zusammenfügen mit den Regenschreiberdaten. Dies zeigt, dass Radardaten Probleme haben.

In Anbetracht der Tatsache, dass Radardaten von Fehlerquellen betroffen sind, wird ein neues Verfahren zur Korrektur der Radardaten vorgeschlagen, Quantile-Mapping. CM und KED werden verwendet, um die Korrekturmethode zu bewerten. Die Interpolationstechniken werden verglichen und mit Kreuzvalidierung ausgewertet. Die Korrektur durch Quantile-Mapping führt zu einer Verbesserung der Radardaten und der Leistung der Interpolationstechniken.

Aufgrund der Tatsache, dass Messgeräte nicht überall zur Verfügung stehen, werden im nächsten Schritt fahrende Autos als Niederschlagsmesser (RCs) untersucht. Scheibenwischer und optische Sensoren werden zur Messung von Niederschlagsintensitäten berücksichtigt. In Laborversuchen haben die Beziehungen zwischen Regenintensitäten, welche von konven-

tionellen Regenmessern aufgezeichnet wurde, und den entsprechenden Signalen von Scheibenwischer und optischen Sensoren vielversprechende Ergebnisse gezeigt. Die Messung mit Scheibenwischer wird als unpraktisch angesehen, da die Einstellung der Scheibenwischerfrequenz durch mehrere Faktoren beeinflusst wird. Im nächsten Schritt werden die Ergebnisse der Laborversuche in Computerexperimenten verwendet, um Gebietsniederschlag zu schätzen.

Aufgrund der geringen Anzahl von RCs auf Straßen und das Fehlen eines Bezugs werden die Computerexperimente durchgefürt. Im Anschluss werden die im Labor beobachteten Messfehler in Computerexperimenten verwendet um einen möglichen Vorteil der Ermittelung des Gebietsniederschlags mit RCs zu untersuchen. Danach werden die Gebietsniederschläge in einem hydrologischen Modell verwendet um zu untersuchen ob RCs eine Verbesserung der Modellierung ermöglichen. Zu diesem Zweck werden die Radardaten als Referenz betrachtet und die anderen Datenquellen werden daraus extrahiert. Die Ergebnisse zeigen, dass die RCs nützlichen Zusatzinformationen zur Ermittlung des Gebietsniederschlags sowie für die hydrologische Modellierung bereitstellen.

Allgemein lässt sich schließen, dass die Notwendigkeit für bessere Datenquellen zur Ermittlung des Gebietsniederschlages, insbesondere für feine zeitliche Auflösungen, offensichtlich ist. Dieser Bedarf kann durch alternative Quellen wie RCs befriedigt werden.

Schlagworte: Wetterradar, RainCars, Geostatistik

Abstract

Rainfall estimation is a challenging task, especially for high temporal resolutions. Spatial rainfall variability is difficult to observe and is often remarked as an important source of error for areal rainfall estimation. Restricted number of recording rain gauges, on the one hand, and inaccuracy of the remote sensing techniques, on the other hand, are the challenges for areal rainfall estimation using available sources of data.

In this study, firstly, the degree of importance of rainfall data temporal resolution and rain gauge network density on the performance of interpolation techniques is addressed, considering weather radar as additional information. Four different interpolation techniques are compared and evaluated by means of cross validation. Kriging with External Drift (KED), Indicator Kriging with External Drift (IKED) and Conditional Merging (CM) investigate the use of radar data as additional information, whereas Ordinary Kriging (OK) is used as the reference method in which no additional information is used. CM performed the best among the other interpolation techniques. Radar data is observed to be beneficial even for very high temporal resolution. Smoothing the radar data improved the performance in merging rain gauge and radar data. This can represent the difficulties original radar data has.

Considering the fact that radar data suffers from sources of error, next, a method is proposed to correct weather radar data using ground observations. The quantile mapping bias correction method is used to correct radar data. CM and KED are used in order to evaluate the correction method. The interpolation techniques are compared by means of cross validation. Implementing bias correction resulted in the improvement of the radar data and the performance of the interpolation techniques.

Rain gauges are not available all over a study area, therefore, moving cars measuring rainfall (RCs) are investigated in the next step. In laboratory experiments, windshield wiper frequency and optical sensors are considered for measuring rainfall intensities. For this purpose, a tipping bucket is placed as reference measuring true rainfall intensity. The sensor readings for both wiper frequency and optical sensors are analyzed against the reference. Wiper frequency

and optical sensors showed promising results indicating rain rate. However, since wiper frequency adjustment is affected by several factors, considering wiper frequency for rainfall measurement is impractical. Therefore, in the next step, the uncertainties only related to optical sensors derived from laboratory experiments are used in computer experiments for areal rainfall estimation.

Due to the low number of RCs in the streets and the lack of a reference source for them, computer experiments are carried out to investigate RCs for areal rainfall estimation and discharge simulation. The measurement errors explicitly observed in laboratory experiments are used for RCs. To this end, radar data is considered as the reference and the other sources of data, i.e. hypothetical RCs and rain gauges, are extracted therefrom. OK is used for estimating areal rainfall for all the sources. The areal rainfall estimations corresponding to each sources of data are evaluated by comparing with the reference. Additionally, the areal rainfall estimations are used in a hydrological model for discharge simulation to assess the need for such sources of data. The results show that the RCs provide useful additional information for areal rainfall estimation as well as for discharge simulation.

In general, it could be concluded that although using additional information, such as weather radar, for areal rainfall estimation improve the interpolation performances, the need for a better source of data in particular for fine temporal resolution is evident. This need might be satisfied using alternative sources such as RCs.

Keywords: Weather radar, RainCars, Geostatistics

Contents

List of Figures

List of Tables

Abbreviations

RC   RainCar - Moving car measuring rainfall

R   as a variable in W-R relationship: Rainfall intensity

W   Sensor reading

BC   Bias Correction

CDF   Cumulative Distribution Function

CM   Conditional Merging

IKED   Indicator Kriging with External Drift

KED   Kriging with External Drift

MFB   Mean Field Bias

OK   Ordinary Kriging

Q-Q   Quantile mapping

BASt   Bundesanstalt für Straßenwesen - Federal Highway Research Institute

DEM   Digital Elevation Model

DFG   Deutsche Forschungsgemeinschaft - German Research Foundation

DWD   Deutscher Wetterdienst - German Weather Service

OSM   Open Street Map

CV   Coefficient of Variation

NSE   Nash-Sutcliffe coefficient

Pbias   Percentage Bias

R   as a statistical measure: Correlation coefficient

RDev   Relative Deviation

RMSE   Root Mean Square Error

Z   Radar Reflectivity

Chapter 1

Motivation and objectives

The quality of climate data influences hydrological analyses significantly. Moreover, better input data, in general, help to improve our understanding about the hydrological processes. A better understanding of the processes results in improvement of the analyses. Rainfall data is an important input for hydrological analyses. Reliable precipitation information is required especially for highly dynamic and nonlinear processes such as floods. Rain gauges provide valuable information, but at irregularly spaced points with a certain density. On the other hand, rain gauges cannot be located overall because of the high cost. Interpolation techniques are used to estimate rainfall amount for locations where no observation is available. Observing spatial rainfall variability is difficult and is often addressed as an important source of error for areal rainfall estimation. The spatial variability of rainfall is rather significant for fine temporal resolution analyses, such as urban hydrology. The spatial configuration and the number of rain gauges are the factors influencing the quality of areal rainfall estimation. Improvement of the quality of short time rainfall estimation is the main concern in this study. This is accomplished by investigating, on the one hand, the current means of rainfall measurement, and, on the other hand, moving cars for measuring rainfall (RCs).

The spatial variability of rainfall could be captured using advanced technologies, such as weather radar. A weather radar device estimates precipitation intensity by analyzing the reflected energy from hydrometeors at a certain height above the ground. Radar data with high spatial and temporal resolution could be used directly, for example, as input in hydrological modeling, as additional information in interpolation techniques and for analyzing rainfall patterns. However, radar data contains errors because of its simple principle behind precipitation estimation. One of the objectives of this study is to investigate the importance of using radar data as additional information for areal rainfall estimation in different interpolation techniques.

In addition to the choice of interpolation techniques, several other factors, such as the temporal resolution of data and the number of observations in the study area influence the quality of areal rainfall estimation. As a result, the benefit of using radar data for different temporal resolutions and different network density scenarios is first addressed. Although radar data provide valuable information and are widely used, they are not without errors. On the other hand, rain gauges provide accurate point-information. Improving the quality of rainfall estimation by weather radar is another topic in this study. Consequently, a method for correcting radar data merged with observation data is developed. Increasing the number of observations results in a higher rain gauge network density. The number of observations could be increased by taking non-recording rain gauges with a daily observation interval into consideration. Therefore, a method is proposed for disaggregating non-recording rain gauges using weather radar data.

In addition to ordinary devices measuring rainfall, several alternatives are proposed in different studies to compromise the need for high quality data. The initial intention of those techniques is often not for rainfall measurement purposes. As a result, they are not as accurate as high quality observation devices, such as rain gauges. However, considering them as inaccurate economical alternatives, the number of observations could in fact be higher than accurate rain gauges. HABERLANDT and SESTER (2010) proposed for the first time the idea of using RCs. They considered wiper speed as an indicator for rain intensity. The initial intention was to investigate the use of RCs because of: (1) the ease of determining the coordinates by GPS and recording the required information on a small memory chip and (2) feasibility of transmitting the information via mobile phones for online access. A huge number of cars world wide represents the potential of such an approach. They investigated the benefit of using those moving sensors in a modelling study, using hypothetical uncertainties for RCs rainfall measurements. Investigating RCs for rainfall measurement purposes in details is another objective of this study. The possibility of using RCs for point rain measurement is first addressed with laboratory experiments. In other words, the main objective of this part of the study is to analyze the uncertainties related to RCs. Car speed, as an important factor influencing the rainfall estimation, is also investigated by a car speed simulator in laboratory. Verifying the benefit of using RCs for areal rainfall estimation and discharge simulation purposes is addressed next. Due to the insufficient number of RCs in field experiment and the lack of a reference data for them, computer experiments are set up. In addition to the number of RCs, several uncertainties are investigated to consider factors such as wind speed, road spray and tree coverage. The main objective of this part of the thesis is to describe a better understanding of how RCs could help for the need mentioned earlier. The research hypothesis is that inaccurate RCs are able to collect more information than rain gauges which could result in improving the quality of rainfall estimation.

Chapter 2

Introduction and overview

Hydrology studies the circulation of water and its elements through the hydrologic cycle. The evaporated water from oceans and land surface falls back as *precipitation* to the earth. The precipitation, is intercepted by plants and vegetation, produces runoff on the land surface, percolates into soil, recharges groundwater, becomes river discharge, and eventually, flows out into the oceans. Two basic precipitation mechanisms are convective and stratiform, describing precipitation formation. The main difference between the two mechanisms is the time needed until precipitation develops. The stratiform precipitation with weak vertical air motions needs quit long for developing precipitation (hours) and precipitation particles are initiated mainly at the top of the cloud system. On the other hand, the convective precipitation with strong vertical air motions are developed quite fast (approx. 45 min) and the precipitation particles are developed at cloud base during cloud formation (MAIDMENT, 1992). Estimation of precipitation amount, as one of the most important elements in the hydrologic cycle, plays an important role in the hydrologic analyses. Precipitation data is required for different purposes such as designing constructions like dams, dikes and sewage systems, plans for overcoming problems related to droughts or floods, and furthermore, for future scenarios such as climate change studies. Rainfall, as the most common *precipitation* type, is mainly discussed in this study.

Rainfall data with coarse temporal resolution could be obtained with the help of relatively dense non-recording rain gauge networks and new technologies such as satellites. Additionally, the spatial variation in coarse resolution is less than in fine resolution. Rainfall estimation in fine temporal resolution is still challenging. Improvement of the quality of short time rainfall estimation is the main focus of this study. Following the objectives of this dissertation, investigating ordinary means of rainfall measurement, i.e. rain gauges and weather radar, is

first addressed, while evaluating the new idea of using moving cars for measuring rainfall (RainCars) is discussed thereafter.

2.1 Rainfall measurement techniques

Precipitation intensity, as expressed by the World Meteorological Organization, is the amount of precipitation collected per unit time interval (LANZA et al., 2006). The current means for measuring rainfall can be categorized as remote sensing techniques, e.g. satellite and weather radar, direct measurement techniques, e.g. tipping bucket, and economical alternatives for increasing the observation network density such as acoustic disdrometers.

The definition of weather radar (**RA**dio **D**etection **A**nd **R**anging) describes the detection of "*anything in the atmosphere which returns to a receiver a detectable amount of power* " (BATTAN, 1973). Although the origin of using radar for meteorological purposes goes back to the end of the 19th century (GRIFFITH, 1995), the development of the devices is still in focus (e.g. LENGFELD et al., 2014). Quantitatively, rainfall amount (R) is expressed using its relationship with the reflectivity (Z) observed by a radar device. A transmitted pulse from the radar antenna is not completely returned to the radar depending on the number, size, shape, relative position, orientation and composition of the particles being observed by radar. The average received power can be expressed by the radar system characteristics, which is constant, and the radar reflectivity (Z) (GRIFFITH, 1995). Different parameter sets for the Z-R relationship are needed depending on several factors, such as the rain type (AUSTIN, 1987). The rainfall amount estimation is often inaccurate due to the simple principle of detecting any object in the atmosphere by weather radar. Inaccuracy of radar data can be explained by factors such as rain type or the existence of frozen particles. The attenuation is a common problem related to weather radar data. Several methods are proposed for correcting the attenuation. MAY (2014), for example, addressed the attenuation issue by following algorithms: Linear, ZPHI (reflectivity-differential phase shift), Self-Consistent, and Modified Self-Consistent. He suggests that using more sophisticated methods such as Self-Consistent is more preferable because of the sensitivity of the fixed-coefficient algorithms (Linear and ZPHI). However, he is of the opinion that validating the techniques by comparing radar rainfall estimations with observation gauges has problems due to the difference in temporal and spatial scales of the two sources. The strength of attenuation also depends on the radar type (X- or C-Band) (DELRIEU et al., 2000) where the X-Band radar is more sensitive. Radar clutter is expressed as unwanted echoes on radar display (HAYKIN et al., 1982). Statistical approaches are usually proposed

for detecting clutters such as by LI et al. (2014). Ground clutters could be identified using a clear-air condition; however, clutter locations appearing under anomalous propagation are hard to detect. The data often differs from ground observations due to the fact that the radar measurements take place at a certain height from the ground. This is more evident for high temporal resolution data.

Imagery ©2016 Google, Map data ©2016 GeoBasis-DE/BKG (©2009), Google   10 m
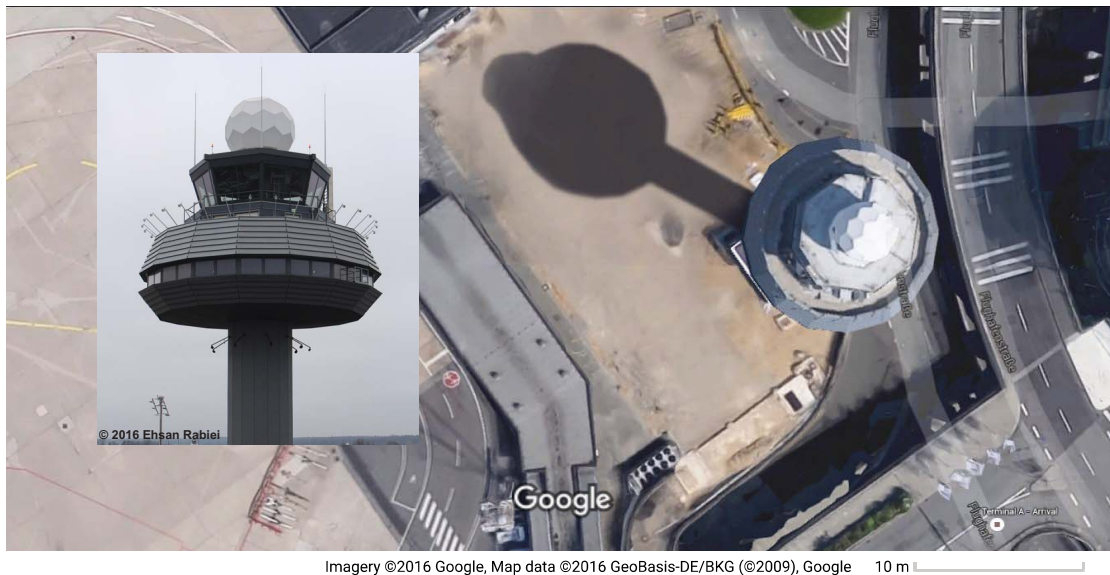
Figure 2.1: Hanover Weather Radar Station, located at Hanover airport

The German Weather Service (DWD) weather radar stations are sometimes located at airports because of the importance of weather data in aviation industry. Figure 2.1, for example, illustrates the weather radar location at Hanover airport.

Most of the weather radars in Europe are C-Band (freq. 5.6 GHz and wavelength 5.4 cm), S-Band (freq. 2.8 GHz and wavelength 10.7 cm) and X-Band (freq. 9.4 GHz and wavelength 3.2 cm) devices. DWD radar network provides rainfall information using C-Band weather radar systems with an azimuth resolution of $1°$, the spatial resolution along each beam of 1 km, and a temporal resolution of 5 min. S-Band and X-Band radar devices are for middle range and short range purposes, respectively. The inexpensive X-Band radar devices are implemented mainly for urban hydrology or regional catchments. The X-Band radar devices are also used for measuring rainfall in remote areas such as valleys (HAGEN, 2013).

Following the strategies for the DWD radar devices, in order to scan the entire atmosphere up to 18 km a total of eleven scans with different radar elevations, shown in Fig. 2.2, are carried out every 5 min. The bright blue precipitation scan shows the scan which takes place with

the radius of up to 150 km from radar device for estimating the rainfall amount. The other 10 scans with certain elevation settings reach the radius of up to 180 km in order to capture the 3D rainfall information for purposes such as now casting (WEIGL, 2013). Due to the principle behind rainfall estimation by weather radar, coarse temporal resolutions are expected to be more representative as the temporal variation of rainfall over a large time becomes less important.
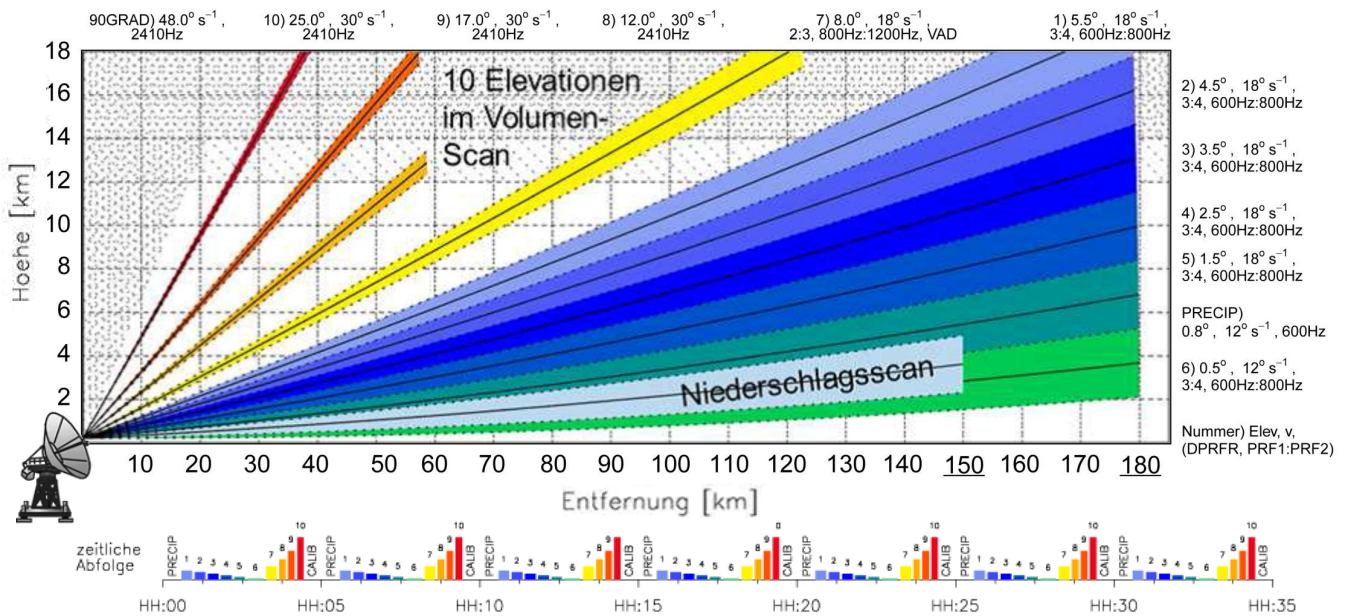
Figure 2.2: DWD Weather radar scan strategy (HELMERT et al., 2014)

The reflectivities associated with a radar cell represent an average value of a certain volume. Due to the fact that this volume becomes bigger when farther away from the radar origin, the spatial resolution of the captured rainfall information decreases. This could be more significant for high temporal resolution data and/or for convective rain events when the effects of non-uniform beam-filling are more in evidence. The non-uniform beam-filling phenomenon occurs when a radar cell is partly rainy. Hence, in addition to common problems radar data has, for example clutters and attenuation, the rainfall amount is often under- or overestimated by weather radar. Due to all the difficulties connected with radar data, several methods are proposed for correction. KITCHEN et al. (1994), for example, proposed a method to compensate for the effects of bright band, range, and orographic growth. Bright band appears when there exists a transition from ice crystal fall to rainfall.

Figure 2.3, for example, illustrates the spatial distribution of rainfall data observed by Hanover weather radar for January 1, 2006 at 00:55. The DWD parameters are used in the Z-R relationship for converting reflectivity to rainfall intensity (see Chapters 3 and 4). This figure
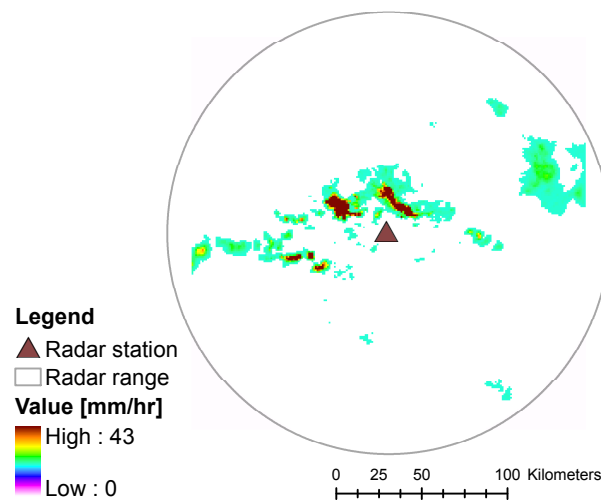
Figure 2.3: Rainfall spatial distribution observed by Hanover weather radar on January 1, 2006 at 00:55

shows that a relatively good spatial variability of rainfall amount over a large area can be observed by a weather radar. However, the radar observations can be not comparable with ground observations due to all the problems mentioned earlier.

In contrast to weather radar, rain gauges provide relatively accurate point information. However, they are located irregularly in the study area. There are several types of rain gauges used for rainfall measurement purposes, such as the tipping bucket, weighing rain gauge and disdrometer. The gauges are divided into two types of instrument by LANZA et al. (2006): catching and non-catching. The catching instruments collect precipitation through an orifice and measure the water volume over a certain time. The second group, e.g. disdrometers, estimate the precipitation amount by analysing the droplet size distribution (DSD).

Rain gauges could be classified into two main categories: (1) non-recording rain gauges with a daily temporal resolution and (2) recording rain gauges with finer temporal resolution. According to the DWD (DWD, 2016), the number of stations for recording rain gauges with hourly temporal resolution and non-recording rain gauges with daily temporal resolution in Germany are 1293 and 5538, respectively. Those numbers include also the stations that were only temporally in operation. Non-recording rain gauges provide accurate accumulative rainfall depth over a particular period of time, usually a day. The number of non-recording rain gauges is much higher than the number of recording rain gauges. Increasing the number of observations could be carried out by taking non-recording rain gauges into consideration. Disaggregating non-recording rain gauges is required before being merged with recording rain gauges.

| **(a)** tipping bucket | **(b)** weighing rain gauges | **(c)** disdrometer |
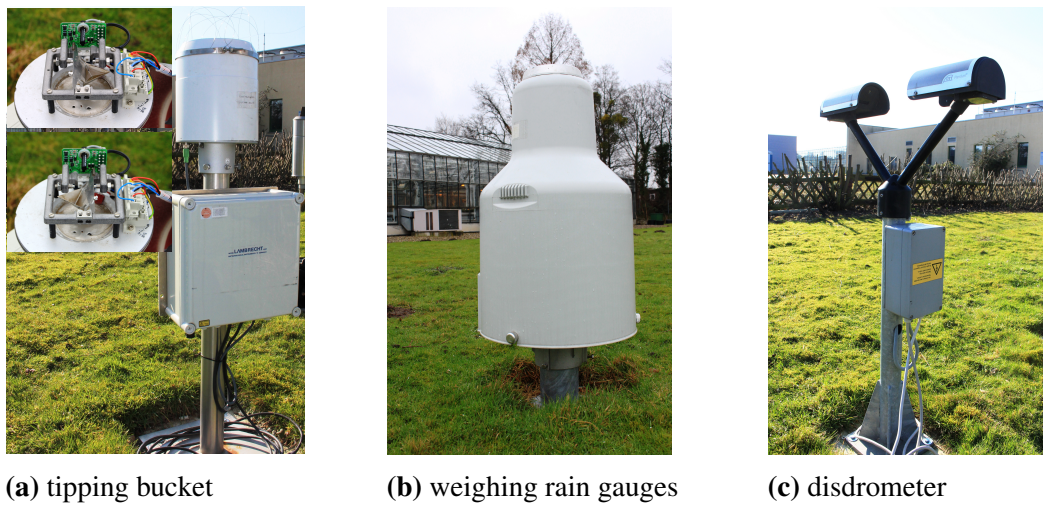
Figure 2.4: Ordinary rain gauges

One of the popular devices used widely for measuring the amount of rainfall is the tipping bucket, Fig. 2.4a. The tipping balance of the two buckets represents the rainfall amount collected between the two sequence tips. This restricts the accuracy of the device when it comes to measuring rainfall amount for low intensities. On the other hand, the rainfall amount collected could have evaporated between events. There are some standard correction methods proposed to overcome these issues. Self-siphoning rain gauges could have a higher resolution, but are subject to errors mainly because of the time needed for emptying the siphon (SERRA et al., 2001). The weighing rain gauges do not have the problems mentioned and are more accurate, Fig. 2.4b. The difference in weight of the rainfall amount collected in the storage represents the rainfall amount happening between the measuring time steps. The device is able to compensate noises such as evaporation and a significant weight change when, for example, unwanted particles fall into the storage. However, it has a time delay of 1 to 10 min for the rain intensity output. The resolution of the data is typically between 0.01 and 0.1 mm of rainfall amount. The DWD uses Pluvio OTT weighing rain gauges as the recording rain gauges in Germany. In general, wind can affect the rain gauges with orifice which could also introduce some errors for such devices. Disdrometers analyze the DSD parameters for estimating the rainfall amount, Fig. 2.4c. A similar way as explained for weather radar is used for estimating the rainfall intensity. A laser beam transmits from one side, where the particle size and speed is estimated depending on the voltage and the signal length at the receiver. The rainfall intensity is estimated using the Z-R relationship (CARACCIOLO et al., 2008). Although disdrometers provide valuable information, the data could contain errors because of indirect rainfall measurements.

In addition to local measurement techniques, the global need for frequent and accurate precipitation measurements could be satisfied using data obtained from satellite remote sensing. KUMMEROW et al. (1998) described the Tropical Rainfall Measuring Mission (TRMM) sensor package. It carried the TRMM Microwave Imager (TMI), the precipitation radar (PR), and the Visible and Infrared Radiometer System (VIRS). Additionally, to measure the total upwelling radiant energy, it carried two related Earth Observing System (EOS) instruments in the Clouds and Earth's Radiant Energy System (CERES) and the Lightning Imaging System (LIS). Although TRMM's precipitation radar (PR) suffered from similar uncertainties to ground-based radars for rainfall estimation, the TRMM PR has delivered a unique 17-year dataset of global tropical rainfall. The TRMM 3B42 product is available in 3-hour temporal resolution and a 0.25-degree by 0.25-degree spatial resolution. The data have a coverage of 50° N - 50° S. The TRMM satellite ended its journey on April 15, 2015. SMITH et al. (2007) described the mission of the International Global Precipitation Measurement (GPM) Program which is to provide observations of rain and snow worldwide every three hours. The design of the GPM was by following the knowledge and published findings of the TRMM. The GPM instruments are designed to detect falling snow, measure light rain, and provide quantitative estimates of microphysical properties of precipitation particles. The GPM Core Observatory satellite was launched on February 27th, 2014. The satellite data was evaluated in several studies. PRAKASH et al. (2016), for example, described the GPM-based multi-satellite IMERG precipitation estimates for the southwest monsoon season which is notably better than the TRMM Multi-satellite Precipitation Analysis (TMPA) in capturing heavy rainfall over India.

Several alternative ways are proposed for rainfall measurement such as acoustic disdrometer (JONG, 2010), microwave links (RAHIMI et al., 2006; UPTON et al., 2005; ZINEVICH et al., 2009) and optical sensors (HYDREON, 2012; XANONEX, 2012). The main objective of using these techniques is to improve the accuracy of rainfall estimation by increasing the number of observations in an economical manner. As the methods mainly mentioned are not initially aimed for rainfall measurement purposes, they are usually not as accurate as ordinary rain gauges. However, they could theoretically provide denser rainfall information than rain gauges. Unexpected problems arise when investigating new techniques in practice. A summary of analyzing acoustic disdrometer and microwave links for rainfall measurement is provided in the following.

JONG (2010) proposed using acoustic disdrometer as a cheap alternative for rainfall measurement. The device was meant to fulfill some of the following criteria: it (a) should not contain moving parts, to prevent clogging, (b) should be inexpensive and long-lasting, and (c) should

be easy to produce. The constraints considered for designing the device resulted in restrictions in rain rate measurements and accuracy of the device. The acoustic disdrometer analyzes the relationship between drop signals and drop diameters. Rainfall amount is estimated in a similar way to the Z-R relationship used for ordinary disdrometers. The sensor cover vibrates when a drop falls on it. A piezo detector converts the vibration into an electric pulse. The electric pulse depends on the size of the rain drop. However, the produced signal is not a sudden change and has a certain length. Consequently, he proposed an algorithm for peak detection. The calibration of the disdrometer was carried out at Delft University of Technology, using a reservoir at 12 m height and medical needles for producing drops. Assuming a constat drop size for each specific setting, the drop size was determined by collecting the drops with a small cup. Implementing the relationship between drop size distribution (DSD) and rain intensity, he examined the technique during a rainfall event. Implementing the device in Singapore and the Netherlands, he evaluated the disdrometer performance. A noticeable underestimation of rainfall amount was observed in both study areas. However, the rainfall estimations were synchronized with the reference. He concluded that the disdrometer encounters problems when the rain intensity becomes higher than a certain threshold. He suggests further investigations for a better rainfall estimation.

UPTON et al. (2005) pointed the fact that using microwave link could provide averaged continuously measured estimates of rainfall along a path close to the surface. The intended path, however, should be clear, i.e. not passing too close to any obstructions. They proposed a relationship similar to Z-R relationship for estimating rainfall. They explained that the coefficients of the proposed relationship depend on the frequency of the wave, the temperature of the raindrops and the size and shape of the raindrops passing between two antennas. Due to the difficulties when using single frequencies (the variation in coefficients), they suggest implementing dual frequency approach. They suggested using the difference in the attenuations at two frequencies resulting in a close to linear relation between rain rate and the difference in the attenuations. However, rain drops are not the only factors causing attenuation. Slight attenuations could be caused because of atmospheric absorption. Therefore, the strength of the received signal is not constant even for no-rain days. Furthermore, the signal strength can also vary during an event. The result of antenna-wetting, for example, results in change of the attenuation before and after an event. Although relatively good results were presented, further developments were suggested. A more recent investigation of the approach was carried out by OVEREEM et al. (2013). They explained the benefit of using cellular communication networks for rainfall measurements, in particular in urban areas because of high density. They proposed a methodology to exclude unwanted signal fluctuations. They estimated the mean 15-min path-

averaged rainfall intensities using the minimum and maximum attenuation. They evaluated the work using a gauge-adjusted radar dataset. The rainfall map is, thereafter, produced implementing OK. Even though they believed in the usefulness of the microwave links rainfall estimation, they were aware of the deficiencies of such an approach. For example, the tropics links, often working at lower frequencies, can have higher errors in rainfall estimates.

2.2 Rainfall interpolation techniques

Rainfall data, like other climate variables, is collected at certain locations by rain gauges rather than continuous surfaces. As a result, interpolation techniques are required to estimate the rainfall amount at points where no rain gauge is located. Several factors influence the quality of rainfall estimation, such as the data availability, temporal resolution of data, availability of additional information and the interpolation techniques used for rainfall estimation. There are many methods used for rainfall estimation, such as nearest neighbor (ISAAKS and SRIVASTAVA, 1990), inverse distance weighting (SHEPARD, 1968) and univariate Kriging techniques, e.g. Ordinary Kriging (OK). The principles of geostatistics is described by MATHERON (1963). Most of the mentioned methods smoothen the areal rainfall distribution which may not represent the actual structure. In order to overcome this deficiency, multivariate geostatistical approaches, such as KED, are suggested. GOOVAERTS (2000) divided the methods into two categories: (a) methods that use only rain gauge observations such as inverse square distance, Thiessen polygon and OK, and (b) the techniques combining rainfall data with additional information, for example elevation, such as KED. He compared different interpolation algorithms by evaluating the cross-validation results. The methods in which no additional information, i.e. elevation, are used failed compared with other techniques. High spatial rainfall variability could influence the performance of interpolation techniques. However, this could be captured by using additional information, such as elevation or weather radar. HABERLANDT (2007) proposed using radar data as additional information in KED. He observed a clear improvement in comparison to univariate interpolation techniques. SINCLAIR and PEGRAM (2005) proposed using CM for merging radar and rain gauge data. Radar data is also used as additional information in this method, but not in the same manner as KED. They concluded that using CM resulted in reducing the bias and variance of error estimates, using an artificial simulation experiment. Depending on the interpolation technique, the assumptions for additional information could be; having a linear relationship with the observation data (e.g. KED), representing the spatial variability of rainfall (e.g. radar in conditional merging: CM) and having different accuracy

(e.g. in Kriging with uncertain data).

The copula-based interpolation techniques are proposed by BÁRDOSSY and LI (2008) for interpolating observations of a large scale groundwater quality measurement network in Baden-Württemberg, Germany. They compared the performance of four different interpolation techniques: multivariate v-transformed normal copula, multivariate Gaussian Copula, OK and Indicator Kriging (IK). The following advantages for copula-based approaches were mentioned: 1) illustrating the dependence structure without the influence of marginal distribution, 2) suitable when encountering outliers and data transformations, and 3) using full distribution, resulting in obtaining more information than a variogram. The copula based interpolator is non-linear. The factors influencing the estimations are the configuration of the observation and target points, and their values. However, the copula approaches are demanding in terms of computational time when the number of observations is too big. They observed better cross validation results using copula approaches comparing with OK or IK. BÁRDOSSY and PEGRAM (2013) applied Gaussian copulas and unsymmetrical v-copulas for interpolating precipitation data for several temporal resolutions from a day to a year. Instead of using only traditional local elevation, a smoothed, shifted version is also considered to illustrate the topography-precipitation relationship. For copula approaches, they assumed that marginal distributions of precipitation at each site are unique for a chosen time step. Furthermore, they treated zero values like censored values. They treat zeros such that within a vicinity of each dry station all the values are zero. The results were compared with traditional methods, OK and KED. Validation of different techniques is carried out by a split sampling approach in a way that the stations are randomly separated into two groups with an equal size. By excluding one group, rainfall estimations for the excluded group are compared with the observations when implementing only the the existing group. They observed that the interpolation quality depends on the temporal resolution of the data under study. They believe that the uncertainties derived with copula approaches are more realistic than kriging methods. They concluded that Gaussian Copulas, combined with directional smoothing of topography performs better than the other techniques. For fine temporal resolution, the number of observations with zero values (censored values) would become very large such that copula techniques with the current approaches may face difficulties. The use of copula techniques for interpolating fine temporal resolution data should be investigated comprehensively in another study.

A short description of the assumptions made for Kriging methods represents the inherent difference of the techniques. From the second order stationarity or the intrinsic hypothesis, the expected value of the random function is constant over the domain. The Kriging system is

derived by minimizing the estimation variance with respect to the unbiasedness condition and with the help of the Lagrange multiplier. The main assumption in KED is the presence of a linear relationship between the additional information and the expectation of the observation data. This results in an inconstant expected value which is in contrast to the constant expected value over the domain (the assumption of OK). Dissatisfying the assumption in KED could result in deterioration of performance compared with OK. Furthermore, numerical instabilities can happen when using this method. In CM, first, interpolating radar values is carried out when implementing OK on the extracted radar values from the cells corresponding to the rain gauges. CM uses only the deviation between the interpolated radar values and observed radar values. The rain field is estimated by adding this deviation to the rain gauge interpolation field using OK (see Chapter 3).

Interpolation methods are also sensitive to network density and the temporal resolution of the data under study. HOFSTRA et al. (2010) investigated the influence of station network density on the distribution and trends in indices of two variables of area-average daily precipitation and maximum and minimum temperature. They observed that sparse network density leads to over-smoothing for both precipitation and temperature. The smoothing observed to be more significant for high percentiles. The temporal resolution of the data under study also influences the performance of interpolation techniques which is due to the larger spatial variability for high temporal resolution data.

The third chapter discusses the influence of network density, temporal resolution and interpolation technique on rainfall estimation by means of cross-validation. Consequently, temporal resolutions from 10 min to 6 h and different network densities are investigated. The following geostatistical approaches are applied to evaluate the advantages and disadvantages of using different interpolation techniques: KED, Indicator KED (IKED) and CM. The benefit of using radar data in geostatistical approaches, as additional information, is compared with the reference method, OK. A common problem regarding radar data is when encountering convective rain events. Unrealistic values could be expected for such events. In order to consider a non-linear relationship between the expectation of the observation data and the additional information, IKED is implemented when considering a stepwise implicit application of KED for different indicators. Additionally, implementing IKED might compensate the severe over- or underestimation of rainfall by radar. The same as KED, numerical instabilities can also occur using this technique. Furthermore, because of the problems associated with radar data, it was also decided to investigate the effect of temporal and spatial smoothing on radar data.

Applying quantile-quantile (Q-Q) transformation is usually used for scaling and bias correction

purposes in climate impact studies. INES and HANSEN (2006), for example, used this method for correcting the daily General Circulation Models (GCM) rainfall for crop simulation studies. A straight forward bias correction method is proposed to deal with the uncertainties of radar data and in order to compensate for the common problems, e.g. over- and underestimation of rainfall. Considering the fact that the rain gauges provide accurate data, radar data is assumed to follow the statistical rainfall variability observed by the rain gauge network. This was carried out by assimilating the cumulative distribution function (CDF) of radar data to the CDF derived from the rain gauge network. This method is discussed further in detail in Chapter 4. Applying the (Q-Q) transformation when considering the observation network data as the reference is the main objective in this part of the study. Furthermore, it is worth noticing that in this method, a direct relationship between the radar-point values and the corresponding observation data is not the main focus. This is in contrast to the usual approaches, where the observations are compared with the corresponding radar cell values for correcting radar data. This could result in a better performance of the method even if the radar-point values are very unrealistic. The radar data quality is investigated by comparing with the corresponding observation data before and after implementing the correction method. Evaluating the correction method is also carried out when implementing radar data in CM and KED interpolation techniques. Furthermore, due to the fact that the number of non-recording rain gauges with daily temporal resolution is usually higher than the recording rain gauges with finer temporal resolution, using radar data for disaggregating daily rain gauges is also investigated. Chapter 4 discusses using radar data for disaggregation purposes in more detail.

2.3 Moving cars for rainfall measurement purposes

As discussed previously, the need to map the spatial rainfall variability better is evident. In addition to weather radar, several innovative methods such as microwave links (UPTON et al., 2005) and acoustic rain gauges (JONG, 2010) are proposed to fulfill this demand.

The potential of using RainCars was addressed for the first time by HABERLANDT and SESTER (2010). The initial intention was to investigate the use of RainCars because of an easy approach for determining the coordinates by GPS and recording the required information on a small memory chip. Furthermore, the information could be transmitted via mobile phones for online access. This idea was justified due to the fact that the number of cars on streets in countries like Germany is relatively high and a huge potential exists for using them as moving sensors measuring rainfall. In that modeling study, the wiper speed was consider as an indication for

rainfall intensity on the front windshield. The two sources of data (RainCars and rain gauges) were extracted from the reference data source, radar data. The benefit of using RainCars was evaluated when comparing the areal rainfall estimation by RainCars with the areal rainfall estimation using only the rain gauge network in an event-based approach. Hypothetical errors were assumed for rainfall estimation by RainCars. This means that each wiper movement frequency was considered representing a certain range of rainfall intensities (classes). The traffic model provided the RainCars' locations and, according to the extracted point-rainfall intensity from radar, the RainCars' value would be then associated with a certain class of rainfall intensity. Indicator Kriging was used to estimate the areal rainfall estimation by RainCars and OK for rain gauge network. Although hypothetical inaccuracies were implemented in that study, it was shown that a large number of inaccurate devices could provide a better areal rainfall estimation than a couple of accurate rain gauges. This could be explained by the fact that RainCars measuring the rainfall amount could gather more information than a couple of accurate rain gauges. As a result, spatial rainfall variability could be captured in a better manner.

In order to evaluate the potential of using RainCars for practical use, the possibility of using RainCars for point-measurement purposes was first addressed. Consequently, laboratory experiments were designed and conducted. The main objective of this part of the study was to study the relationships between sensor readings (W) and rainfall intensity (R) by laboratory experiments. Sensor readings refer to wiper speed (adjusted either manually by a driver or automatically by optical sensors) and signals of optical sensors which are designed to be placed on cars for automating wiper activity. Investigating the relevant sensor reading uncertainties is the main purpose of this part of the study. A rainfall simulator with the ability of producing a wide range of rain intensities is designed and constructed. In addition to producing a wide range of rain intensities, homogeneous rainfall distribution over the desired area and replicating the properties of natural rain were the points considered when designing the rainfall simulator. A tipping bucket was considered as reference in order to analyze the sensor readings. The performance of RainCars could be influenced by several factors such as car speed, wind speed, wind direction, windshield angle, etc. Car speed, as an important factor influencing the rainfall estimation, is investigated with the help of a special car speed simulation. Chapter 5 describes the laboratory experiments from design to results in more detail.

It is worth mentioning that several factors could influence the performance of RainCars in practice. In addition to the car speed which was investigated by a car speed simulator, factors such as wind speed, wind direction, road spray and tree coverage could deteriorate the

performance of RainCars. Following approaches may be considered for compensating those factors. The wind speed could be analyzed in a similar way to car speed, having the wind direction. Statistical approaches such as those for detecting clutter in radar data may be used for compensating the influence of road spray and tree coverage. Such approaches require relatively large number of observations. It is worth noticing that some factors might be because of the car type and shape. However, identifying all the factors influencing the RainCars performance is difficult.

Figure 2.5: Schematic image of RainCars (Credit:iww.uni-hannover.de, Bastian Heinrich)

Figure 2.5 illustrates a schematic image of a RainCar. Optical sensors, such as the one shown in Fig. 2.5, are designed for automating the wiper activity. The readings from such a sensor could be considered as an indication of rainfall amount.

FITZNER et al. (2013) discussed the initial results of RainCars in field experiments. They investigated robust models for rainfall estimation using sensor readings and possible model for online calibration. They assumed that stationary rain gauges provide accurate information. Furthermore, they considered the vulnerability of W-R relationship in terms of the current wind direction and speed. Therefore, they proposed an exchange of information between RainCars, and also among RainCars and rain gauges for re-calibrating the W-R relationship. Because of that, not only the spatial distance was taken into consideration, but also the temporal lag between the measured and expected variable. They analyzed the manually adjusted wiper speeds of 6 cars and automatically adjusted wiper speeds of 4 cars with a sampling rate of 1 min.

However, they were of the opinion that due to the low number of data points, the results might not be reliable. Even though they limited the analyses to 4000 m distance to stations, relatively weak results were obtained. Applying the inverse distance weighted (IDW) interpolation technique for estimating the reference values for RainCars was given as an important issue for analyzing the results. Furthermore, a restriction of using upper level wiper speeds after certain car speeds was mentioned also as one of the deficiencies of such an approach.

2.4 RainCars for areal rainfall estimation as well as discharge simulation

As mentioned previously, one of the advantages of using RainCars is that the number of observations is relatively high. This could result in a better illustration of spatial rainfall variability and, consequently, better areal rainfall estimation. After analyzing the use of RainCars for point-measurement purposes in Chapter 5, Chapter 6 addresses the measurement uncertainties derived from laboratory experiments for (a) areal rainfall estimation and, afterwards, (b) discharge simulation. It is worth noticing that the interactions in hydrological modeling are not the focus of this part of the study. The hydrological model is used only as a tool simulating the discharges for different sources of data. However, several factors can influence the performance of a hydrological model. Some of the factors are summarized in the following.

Due to the low number of RainCars in field experiments and the lack of a reliable reference data for them, a computer experiment is designed to investigate the benefit of using RainCars for both areal rainfall estimation and discharge simulation. The wiper speed is not analyzed here because of all the mentioned limitations for this approach (FITZNER et al., 2013; RABIEI et al., 2013). The signal readings of an optical sensor is considered for further analyses. A continuous analysis of implementing RainCars for areal rainfall estimation over a long period of time, as well as using the data in a hydrological model, are the objectives addressed in this part of the study. For a more general conclusion, in addition to the uncertainties previously derived in laboratory experiments, higher and lower uncertainties are also taken into consideration. This could obtain the minimum required accuracy for the RainCars.

The computer experiments are set up to meet different objectives. The primary objective is to implement the uncertainties derived in laboratory experiments for areal rainfall estimation. Reference data is required from which the other sources of data are to be extracted. It is decided

that radar data covering a large area is a good source to be considered as the reference in this part of the study. The rainfall data for both hypothetical RainCars and rain gauges are extracted from the reference. The areal rainfall estimation determined by interpolating the extracted point-data (using OK) over the study area is then compared with the reference. Before interpolating RainCars' values over the study area, the error derived from the laboratory is randomly introduced into the data, whereas the extracted values for rain gauges are directly used.

In order to investigate the advantages and disadvantages of using a new data source, the data should be used directly as input in the analyses. The relationship between rainfall data and discharge simulation is not linear. Therefore, an improvement in the interpolation performance (e.g. by means of cross validation) should not necessarily result in an improvement of model performance simulating discharges. In the following, some factors influencing the model performance are summarized.

There are generally several factors influencing the model performance, such as calibration strategy, the quality of input data, temporal resolution of the data under study and the complexity of the model. GUPTA et al. (1999), for example, discussed the fact that using different automatic calibration strategies might lead to different model parameter sets. KAVETSKI et al. (2011) described the influence of temporal data resolution on parameter interference and model identification in conceptual hydrological modeling. He is of the opinion that having high-resolution data in more complex model structures results in a better overall performance both in terms of aggregate measures of model performance (such as Nash-Sutcliffe representing the goodness of fit) and reproducing important quantitative signatures. Spatial and temporal resolution of data is also a factor influencing the quality of analyses. OUBEIDILLAH et al. (2014) investigated the effect of four different datasets with different spatial and temporal resolutions on the VIC hydrologic model. They observed that the dataset with the finest resolution for high precipitation P95, annual 95% quantile, should report precipitation extremes more accurately. PRICE et al. (2014) compared the accuracy of the SWAT model for four spatial and five temporal scales using gauge data and radar data while keeping all other model inputs constant. They found that different data sources result in different parameterizations. They also concluded that the choice of whether to use radar, gauge, or other rainfall data should be decided mainly according to the spatial and temporal scales of interest. JASPER et al. (2002) investigated the use of two different datasets in the grid-based WaSiM-ETH hydrological model: (1) observations from rain gauges and weather radar and (2) forecast data from different numerical weather prediction (NWP) models. The runoff simulations by

radar data had significant quality differences. This was justified by the fact that the watersheds were located in very steep mountainous terrain. BIEMANS et al. (2009) quantified the global distribution of the uncertainty in annual as well as seasonal precipitation estimation on a basin scale and the resulting uncertainty in discharge simulations by the Lund-Potsdam-Jena managed land (LPJmL) model. They compared the variations between seven global gridded precipitation datasets of: the Climate Research Unit (CRU), CRU-Potsdam-Institut für Klimafolgenforschung (CRU-PIK), the global precipitation dataset (MW), the GPCC global precipitation dataset, the Global Precipitation Climatology Project (GPCP), the Climate Prediction Center Merged Analysis of Precipitation (CMAP) and The global precipitation dataset developed by ADAM et al. (2006) (ADAM) at a basin scale. Furthermore, they also evaluated the discharge simulations using those datasets on a mean annual and a mean seasonal time scale with observations for 294 basins around the world. Precipitation estimates observed to suffer from larger measurement errors. They also observed that areas with low precipitation uncertainty typically have simpler topography, are not snow dominated, and have a dense precipitation network. Moreover, the results showed that the uncertainty in precipitation has a significant impact on discharge estimations. They are of the opinion that the range of uncertainty in input data affects the output and may not be neglected in the communication of results. They believed that more accurate precipitation datasets can satisfy this need.

Another objective of this part of the study is to analyze discharge simulations when different rainfall data are used as inputs in a hydrological model. Therefore, all the other influencing factors, e.g. model parameters, are kept constant. This means that a general setting for the hydrological model is used for all the datasets. The HBV-IWW hydrological model simulates the discharges for all the scenarios mentioned earlier, where the reference data is used for simulating the reference discharge. The simulated discharges are then compared with the reference discharge. The benefit of using RainCars could be observed when comparing the results with when only rain gauges are used.

There are two main factors influencing the areal rainfall estimation quality using RainCars: (1) the number of RainCars available on the streets, and (2) the accuracy of the measurements. Different numbers of RainCars address their possible required number. Although using large number of RainCars may result in improving the quality of areal rainfall estimation, the minimum number of RainCars required for dominating rain gauges is very important. Higher and lower uncertainties than the one derived in the laboratory are investigated to obtain a threshold for the minimum requirements for the accuracy of the measurement devices. Higher uncertainties account for possible factors deteriorating the performance of RainCars that could

not be investigated in laboratory such as road spray, trees, wind, etc. This part of the study would show the potential of using the data for areal rainfall estimation and discharge simulation. Chapter 6 discusses the computer experiments and all the assumptions taken for this part of the study in more detail.

Chapter 3

Geostatistical merging of rain gauge and radar data for high temporal resolutions and various station density scenarios

S U M M A R Y

This study investigates the performance of merging radar and rain gauge data for different high temporal resolutions and rain gauge network densities.

Three different geostatistical interpolation techniques: Kriging with external drift, indicator kriging with external drift and conditional merging were compared and evaluated by cross validation. Ordinary kriging was considered as the reference method without using radar data. The study area is located in Lower Saxony, Germany, and covers the measuring range of the radar station Hanover. The data used in this study comprise continuous time series from 90 rain gauges and the weather radar that is located near Hanover over the period from 2008 until 2010. Seven different temporal resolutions from 10 min to 6 h and five different rain gauge network density scenarios were investigated regarding the interpolation performance of each method. Additionally, the influence of several temporal and spatial smoothing-techniques on radar data was evaluated and the effect of radar data quality on the interpolation performance was analyzed for each method.

It was observed that smoothing of the gridded radar data improves the performance in merging rain gauge and radar data significantly. Conditional merging outperformed kriging with an

external drift and indicator kriging with an external drift for all combinations of station density and temporal resolution, whereas kriging with an external drift performed similarly well for low station densities and rather coarse temporal resolutions. The results of indicator kriging with an external drift almost reached those of conditional merging for very high temporal resolutions. Kriging with an external drift appeared to be more sensitive in regard to radar data quality than the other two methods. Even for 10 min temporal resolutions, conditional merging performed better than ordinary kriging without radar information. This illustrates the benefit of merging rain gauge and radar data even for very high temporal resolutions.

3.1 Introduction

Rainfall data with a high resolution in space and time are of importance for the modeling of hydrological and other environmental processes. Rainfall is usually measured at irregularly spaced point locations with a certain density. The spatial density is often quite high for daily measurements, but there is regularly a lack of stations delivering a more frequent recording of precipitation. Radar data have a high resolution in space and time, but are in general strongly biased ("Real-time estimation of mean field bias in radar rainfall data"). A radar device does not measure the precipitation intensity directly, but rather the reflected energy from hydrometeors at a certain height above the ground. Sources of errors include variations in the relationship between reflected energy and rainfall intensity depending on rainfall type, changes in the precipitation particles before reaching the ground, anomalous beam propagation and attenuation (WILSON and BRANDES, 1979). Hence, it could be expected that the use of uncorrected radar data is not acceptable for many hydrological applications.

Considering only station data to obtain rainfall estimates, various interpolation methods have been applied (DUBOIS et al., 1998). A few examples include the nearest neighbor method (ISAAKS and SRIVASTAVA, 1990), inverse distance weighting, spline fitting techniques (HUTCHINSON, 1998a; HUTCHINSON, 1998b) and univariate kriging approaches like ordinary kriging. Some of these methods create strongly smoothed areal rainfall distributions which usually do not represent the actual spatial rainfall structure. Multivariate geostatistical methods, e.g. kriging with an external drift, were applied in several studies by using additional information in order to improve the interpolation performance. For instance, GOOVAERTS (2000) reported that implementing the elevation as a background information can improve the interpolation performance on a monthly and yearly time scale.

As a result of improved availability and higher accuracy of radar data, several methods for merging rain gauge data and radar data were proposed over the years. Merging approaches based on cokriging were applied in numerical experiments by KRAJEWSKI (1987) and AZIMI-ZONOOZ et al. (1989). The incorporation of simulated radar information improved areal rainfall estimations for simulated rainfall fields.

HABERLANDT (2007) used kriging with an external drift to interpolate hourly rain gauge data, using radar as the drift information. A clear improvement of interpolation performance in comparison to univariate interpolation methods was achieved. However, the usage of elevation as further additional information did not improve the quality noticeably. Another study by VERWORN and HABERLANDT (2011) showed the benefit of implementing radar data in kriging as an external drift.

A further technique to combine radar and rain gauge data is the so called conditional merging approach, which consists of combining an interpolated rain gauge field with rainfall variability information derived from radar data. The method was reported first in EHRET (2002) and it is referred as Conditional Merging in SINCLAIR and PEGRAM (2005).

GOUDENHOOFDT and DELOBBE (2009) evaluated several merging approaches with different complexity for daily rainfall data and preferred geostatistical merging over univariate rain gauge interpolation and radar data adjustment. Kriging with an external drift was the best approach. However, conditional merging performed only slightly worse. VELASCO-FORERO et al. (2009) evaluated ordinary kriging, kriging with an external drift and collocated cokriging in combination with a non-parametric and automatic technique to obtain correlograms from radar images. Kriging with an external drift performed best.

Statistical merging procedures were applied for combining rain gauge and satellite data as well. For instance, LI and SHAO (2010) proposed a nonparametric kernel merging technique for rain gauge and TRMM satellite data. An improvement in comparison to kriging methods was detected for the Australian study area. WOLDEMESKEL et al. (2013) used a combination of thin plate smoothed splines and inverse distance weighting to merge satellite and station data on a monthly time scale. In particular for regions with a sparse station network, an improvement of rainfall estimation was found out.

BÁRDOSSY and PEGRAM (2013) used copula techniques and kriging methods for the spatial interpolation of rainfall sums for 1 day, 5 days, 1 month and 1 year, while taking into account the elevation as the additional information. The best interpolation results were achieved by

using a shifted and smoothed version of the digital elevation model which accounts for the effects of directional advection. In general the copula-based techniques performed well for all temporal resolutions and provided a better estimation of uncertainty.

There are several uncertainties in the estimation of rainfall intensity by weather radar, e.g. variations of parameters in the Z-R-relationship in relation to rain type (GRIFFITH, 1995), attenuation of the radar beam and increasing measuring altitude depending on the distance from the radar station. The occurrence of these errors is crucial for high temporal resolutions and becomes less important with increasing accumulation time. Due to this, it could be expected that the advantage of incorporating radar data would be restricted to lower temporal resolutions. Additionally, it is generally assumed that the benefit of using radar data would increase by decreasing rain gauge network density. This assumption is supported by findings of KRAJEWSKI (1987), GOUDENHOOFDT and DELOBBE (2009) and YOON et al. (2012), where station density effects had been analyzed.

A different way of tackling the problem of the merging rain gauge with radar data is the assimilation of radar information to rain gauge measurements. The error variance of various uncertainty sources could be quantified and incorporated in the calibration procedures (CHUMCHEAN et al., 2003; CHUMCHEAN et al., 2004).

The objective of this study is to compare the performance of certain merging techniques between gauge and radar rainfall for a large and continuous data set. Most of the previous studies, which included merging or other interpolation techniques, used daily or hourly data for a specific area with a certain number of available rain gauges. This study evaluates a wide range of high temporal resolutions from 10 min to 6 h and various station network densities. It aims at providing information for different temporal resolutions and station densities, about whether the combined use of rain gauge and radar data is advantageous compared to univariate rain gauge interpolation. Inspired by BÁRDOSSY and PEGRAM (2013) it looks in particular at spatial and temporal smoothing options of the radar variable to improve the interpolation performance. In addition the effect of radar data quality on the merging result is investigated in this study.

The paper is organized as follows. After the Introduction, the section "Methodology" contains a description of all merging techniques that were applied for this study. Also, the general evaluation procedure followed in this case study and the performance assessment are explained. The study area and data are introduced in Section 3.3. In particular the radar data pre-processing is described here. Next, Section 3.4 contains the results and a corresponding discussion. The

findings are presented separately for the effect of radar data smoothing on the interpolation performance and the influence of station density and temporal resolution. Moreover, radar data quality aspects are discussed here. In the final section the conclusions are drawn and an outlook is presented.

3.2 Methodology

3.2.1 Merging methods for radar and rain gauge data

The geostatistical approaches used in this study for merging rain gauge and radar data include Kriging with External Drift (KED), Indicator Kriging with External Drift (IKED) and Conditional Merging (CM). The univariate method Ordinary Kriging (OK) is used as a reference, illustrating a possible benefit of radar data use. A detailed description of OK is provided in geostatistical textbooks (GOOVAERTS, 1997; ISAAKS and SRIVASTAVA, 1990). The Geostatistical Software Library (DEUTSCH and JOURNEL, 1992) with some modifications for the successive procession of time series was used for the computations in this study.

All kriging methods require the assumption of a theoretical semivariogram model that is to be fitted to an experimental one. The semivariogram $\gamma(h)$, which will be referred as variogram in the following text, is a measure indicating the spatial variability of a regionalized variable *Z*.

$$\gamma(h) = \frac{1}{2 \cdot N(h)} \sum_{i=1}^{N(h)} (Z(u_i) - Z(u_i + h))^2, \tag{3.1}$$

where *N(h)* is number of data pairs, which are located a distance vector *(h)* apart. Previous research of HABERLANDT (2007) and VERWORN and HABERLANDT (2011) showed that the variogram model has only a small impact on the estimation performance of OK and KED, though the distribution of rainfall can be highly dynamic in space and time. Similar results regarding the variogram influence were obtained by EHRET (2002).

Accordingly, two isotropic variogram models were used. They were fitted to experimental variograms, which were averaged separately over all summer and all winter time steps. This separation into one summer and one winter variogram is considered because of the assumed seasonal changes in rainfall type. Only radar data were used for the calculation of experimental

variograms. GERMANN and JOSS (2001) also conducted variogram estimation using radar data and reported that high resolution radar images provide good information about the spatial continuity of precipitation. The section "Variogram inference" contains further details. The main advantage of this procedure is that the visual fitting of the theoretical variogram model has to be done only twice for each temporal resolution and not for each single time step. All time steps with an average rain gauge rainfall exceeding a certain threshold were taken into account for the calculation of the season-specific experimental variogram (Eq. (3.2)). Prior to averaging, standardization by the variance was done for each time step:

$$\gamma_{season}(h) = \frac{1}{n} \cdot \sum_{i=1}^{n} \frac{\gamma(h,i)}{var(i)}. \tag{3.2}$$

In this equation, n is the number of time steps, $\gamma(h,i)$ is the variogram value for the distance class h of time step i and $var(i)$ is the variance of time step i. Next, an exponential variogram model was fitted visually.

$$\gamma_h = c_0 + c \left[1 - exp\left(-\frac{h}{a} \right) \right]. \tag{3.3}$$

Here, a is the range, c the sill and c_0 the nugget effect.

In terms of objectivity, a visual fitting procedure is considered as adequate because the fitting of the theoretical models was easy and obvious for the experimental variograms that were computed from radar data (see Section 3.4.1)

3.2.1.1 Kriging with an external drift

Kriging with external drifts allows the incorporation of one or more additional variables that are used as background information for the interpolation of the primary variable. Since the focus of this study is merging rain gauge data with radar data, radar data has been considered as the only additional information in this method. The basic assumption of KED is that the expected value of the estimated variable *Z(u)* has a linear relationship with an additional variable *Y(u)*:

$$E[Z(u)|Y(u)] = a + b \cdot Y(u) \tag{3.4}$$

So the intrinsic hypothesis (Eqs. (3.5 and 3.6) is relaxed:

$$E[Z(u+h) - Z(u)] = 0, \tag{3.5}$$

$$E[(Z(x+h) - Z(x))^2] = 2\gamma(h) \tag{3.6}$$

It states that the expected value of the estimated variable is independent of the location u. In consequence, the expected value is not constant within the interpolation area anymore,

$$E[Z(u+h)] \neq E[Z(u)]. \tag{3.7}$$

In the same way as for OK, the KED estimator for an unknown point (u_0) is defined as the weighted sum of the observations at n neighboring points:

$$Z^*(u_0) = \sum_{i=1}^{n} \lambda_i \cdot Z(u_i), \tag{3.8}$$

where $\lambda_i s$ are the kriging weights that must be determined by solving the kriging system:

$$\sum_{i=1}^{n} \lambda \cdot \gamma(u_i - u_j) + \mu_0 +_m u \cdot Y(u_i) = \gamma(u_i - u_0)i = 1, \ldots, n$$
$$\sum_{j=1}^{n} \lambda = 1 \tag{3.9}$$
$$\sum_{j=1}^{n} \lambda_j \cdot Y(u_j) = Y(u_0)$$

where n is the number of neighbors, Y the additional variable and μ are Lagrange multipliers. For further information regarding KED, the reader is referred to geostatistical textbooks and the manual of the Geostatistical Software Library (DEUTSCH and JOURNEL, 1992).

A considerable problem when applying kriging with an external drift for merging of station and radar data with a high temporal resolution is the frequent occurrence of numerical instabilities in the kriging system (Eq.3.9). According to DEUTSCH and JOURNEL (1992), this might happen when the drift variable does not vary smoothly in space, e.g. if many stations have

zero precipitation. The number of time steps having these instabilities could be reduced by increasing the number of data points used for the kriging process.

In general, 16 neighboring stations were considered in KED for estimating each point value. If the kriging system was ill-conditioned or singular, a next attempt was applied that took into account all available stations. In case this was still not successful, the affected time step was interpolated using OK.

3.2.1.2 Indicator kriging with external drift

Interpolating a continuous variable by indicator kriging with external drift (IKED) implies a transformation of the observed variable Z(u) into a corresponding binary indicator variable $I_\alpha(u)$, see (ISAAKS and SRIVASTAVA, 1990). Various thresholds α_k with *k = 1, . . . ,K*; were used to obtain a vector of rainfall indicator variables.

$$I_\alpha(u) = \begin{cases} 1 \text{ if } Z(u) \geq x \\ 0 \text{ otherwise} \end{cases} \tag{3.10}$$

The interpolation using indicator kriging with an external drift (IKED) is carried out as follows: first, the KED algorithms are applied for all indicators to get an estimate of the cumulative probability density function (cdf) of *Z(u)*. Thereafter, the estimate of the primary variable *Z(u)* is obtained by using the so called E-type estimate, which approximates the mean of the cdf (DEUTSCH and JOURNEL, 1992):

$$Z_E^*(u) = \sum_{k=1}^{k+1} \frac{\alpha_k + \alpha_{k-1}}{2} \cdot [I_{\alpha k}^*(u) - I_{\alpha k-1}^*(u)]. \tag{3.11}$$

Here, $\alpha_k, k = 1, \dots, K$ are the specified thresholds and $\alpha_0 = z_{min}, \alpha_{k+1} = z_{max}$ are the minimum and the maximum values of the Z-range. The experimental indicator variograms are calculated in the same way as for OK and KED. Nevertheless, variograms have to be estimated separately for all indicator variables. The absolute thresholds are calculated individually for each time step based on the non-exceedance probabilities of certain predefined quantiles. Thus, a set of average indicator variograms for a wide range of predefined absolute thresholds has to be calculated prior to the application of IKED (see also Section 3.4.1). An important feature of

IKED is the possibility to consider a quasi non-linear relationship between the expected value of the primary variable $E[Z(u)]$ and the additional information $Y(u)$ by the stepwise implicit application of KED for different indicators I_α. Another reason for applying IKED is the linkage of the estimated value to the predefined quantiles. Due to this, severe over- or underestimation which might be caused by poor radar data quality is limited. Numerical instabilities can also occur in IKED. Concerned time steps were treated in the same way as in KED. For further information on the application and the theory of IKED, the reader is referred to DEUTSCH and JOURNEL (1992)

3.2.1.3 Conditional merging

Another method to combine rain gauge and radar data is the conditional merging (CM) approach described by SINCLAIR and PEGRAM (2005). Fig. 3.1 shows a scheme of CM. The first step of the conditional merging procedure is to apply OK to the gauge observations (a) to obtain the best linear unbiased estimate of rainfall for all gridpoints (c). Next, radar rainfall values of gauge locations (a) are extracted from the gridded radar data (b) and interpolated by OK as well (d). This is followed by calculating the deviation between interpolated and observed radar rainfall values for each gridpoint, whereby it gives the value 0 at rain gauge locations (e). Finally, the deviation grid is added to the rain gauge interpolation field from the first step (f). The result is a rainfall field that follows the mean field of the rain-gauge interpolation while simultaneously preserving the rainfall pattern of the gridded radar information (g).
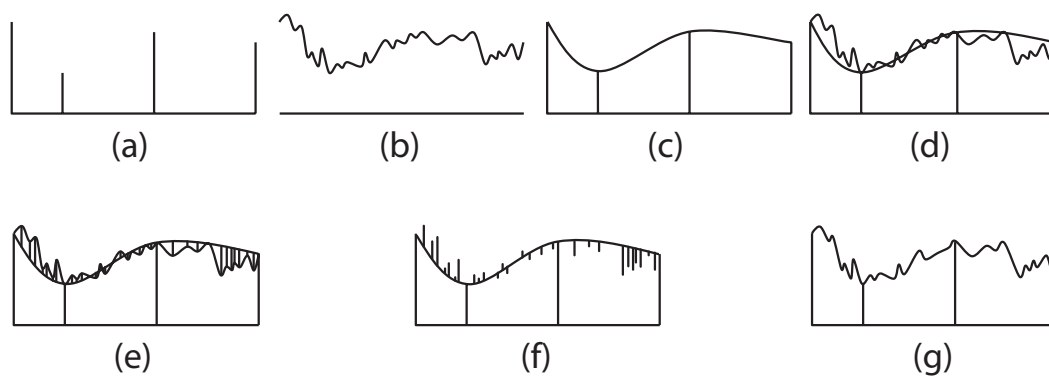
Figure 3.1: The conditional merging process. (a) Rain gauge observation at discrete points. (b) Radar observation on a regular grid. (c) Interpolation of rain gauge observations by using ordinary kriging. (d) Interpolation of corresponding radar pixel information. (e) Computation of deviation between observed radar grid interpolated radar grid. (f) Addition of deviation grid to the grid of rain gauge interpolation. (g) Resulting rainfall field (SINCLAIR and PEGRAM, 2005).

A straightforward approach was used for variogram estimation. As mentioned before, variograms were computed as average variograms for summer time steps and for winter time steps separately, i.e. the same variograms as estimated from radar data for KED and OK before were used here for all interpolations (see Section 3.2.1.1).

Conditional merging is computationally efficient and robust. Since it only uses OK it is not affected by numerical instabilities.

3.2.2 Performance assessment

The interpolation performance was assessed by applying the cross validation method. The so called "leave-one-out" method is based on a simple principle: A successive estimation of all sampled locations is done by using all other stations while always omitting the sample value at the regarded location. The following performance measures were used to compare estimation (Z^*) and observation (Z):

The simple bias criterion

$$Bias = \frac{1}{n} \cdot \sum_{i=1}^{n} [Z^*(u_i) - Z(u_i)], \qquad (3.12)$$

the root mean square error normalized with the average of the observations

$$RMSE = \frac{1}{\bar{Z}} \cdot \sqrt{\frac{1}{n} \cdot \sum_{i=1}^{n} [Z^*(u_i) - Z(u_i)]^2} \qquad (3.13)$$

and the *RVar* coefficient, which indicates the preservation of variance of the observed information

$$RVar = \frac{Var[Z^*(u_i)]}{Var[Z(u_i)]}. \qquad (3.14)$$

In context of the unwanted smoothing effect of rainfall interpolation, an *RVar* value close to 1 is preferable.

A slightly modified cross validation approach was used for all analyses regarding the rain gauge density scenarios (see Section 3.3.1). In order to obtain comparable performance criteria for different station densities, only the stations belonging to the scenario with the lowest station density are considered in calculating the cross validation performance criteria. This approach requires that the set of stations which is considered in the scenario with the lowest station density is present in all other scenarios as well.

3.2.3 General steps for analysis

The previously explained geostatistical merging techniques have been applied for different temporal resolutions and different station densities. In addition, the benefit of using radar data for different interpolation techniques was investigated by comparing the results with OK, which does not incorporate radar data.

According to BÁRDOSSY and PEGRAM (2013) there is no significant influence of the microtopography on the rainfall sums measured by gauges. However, the prevailing wind direction affects the rainfall sums. Due to this, they used a smoothed and shifted transformation of the elevation to improve the interpolation quality for daily up to yearly rainfall sums. Radar data usually contain a space-time variable bias in comparison to rain gauge data. An important source for bias between gauge and radar rainfall might be the spatial mismatch of the measuring domains, i.e. rainfall usually is captured directly above the ground while the radar reflectivity is measured in a certain height depending on the distance from the location of the radar device. Considering the advection of precipitation fields this bias might be larger for higher temporal and spatial resolutions. According to this, it is expected that spatial and temporal smoothing of radar data can improve the interpolation performance of geostatistical merging.

In the first part of the analysis, seven different smoothing techniques were applied on hourly radar grids and evaluated in terms of interpolation performance. For the second part, the technique that gave the best result was used to smooth the radar grids for all temporal resolutions. Then, cross validation was carried out for 10 min, 20 min, 30 min, 1 h, 2 h, 4 h and 6 h data. In order to obtain findings for a wider range of station densities, five different scenarios which took into account 100% , 80% , 60% , 40% and 20% of the available rain gauges were evaluated (see Section 3.3.1). In addition, the effect of radar data quality was analyzed by defining two cases for which the evaluations were done separately. In case A, all available time steps with significant rain were taken into account. Case B considered only the time steps of case A with

reasonable radar data quality (see Section 3.3.4).

The general procedure for the analyses conducted in this study is summarized as follows:

1. Aggregation of 10 min rain gauge data (highest avail. temp. resol.) to all required temporal resolutions.

2. Pre-processing of 5 min radar data (provided temp. res.) (see Section 3.3.2).

3. Smoothing of 5 min radar data grids (see Section 3.3.3)

4. Aggregation of smoothed and non-smoothed radar data (5 min temporal resolution) to all required temporal resolutions.

5. Estimation of variograms and indicator variograms for summer and winter season.

6. Cross validation of OK, KED, IKED and CM for hourly data and a scenario with a medium station density for all smoothing techniques to find out which is the best smoothing method.

7. Detection of time steps with poor radar data (see Section 3.3.4)

8. Cross validation for OK, KED, IKED and CM for all station density scenarios, temporal resolutions and the two data quality cases by using the best smoothing technique from step 6.

3.3 Study region and data

3.3.1 Study region and rain gauge data

The study region is located within the 128 km range of the radar station Hanover in Lower Saxony, North Germany. Due to the recent increase of the number of rain gauges with a high temporal resolution and the recent improvement in radar data quality, the 3-year time period from January 2008 until December 2010 was selected for this study. Altogether 90 gauges with a temporal resolution of 10 min were operated by the German Weather Service (DWD) during the complete period in the study area. The data of rain gauges which do not cover the complete study period were not considered. However, stations with time series that contained missing

values for single time steps were taken into account.

Fig. 3.2 shows the location of the study area and the rain gauge network. The northern part of the study area is to be characterized as flat. It is part of the North German Plain. In the southern part, there are some smaller elevations and the Harz Mountains. Those are located in the southeast of the study area and have a maximum elevation of 1141 m a.s.l. The average annual precipitation varies between 500 mm/yr and 1700 mm/yr, whereas the highest rainfall amounts occur in the Harz Mountains.
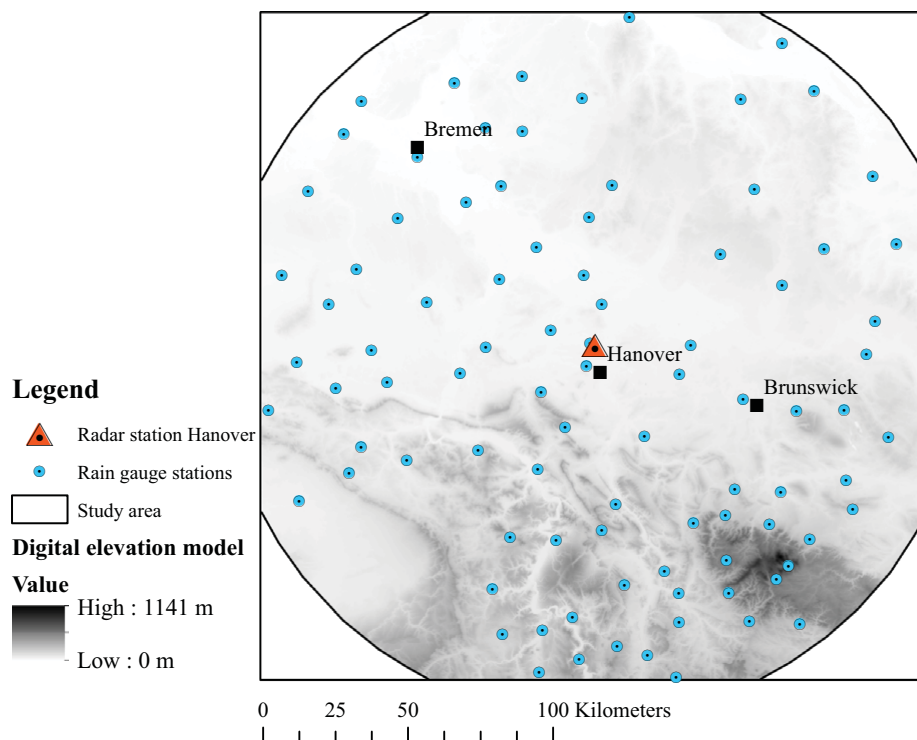
Figure 3.2: Location of the study area and rain gauge network.

In order to analyze the impact of network density on the interpolation quality, five scenarios were defined (Table 3.1). For each scenario a random selection of stations was done, where scenario 1 (100%) represents the complete available dataset. The selection was carried out in a way that the scenarios with higher station density always contain all stations of the 20% scenario. This procedure allows an objective comparison by cross validation using only the 20% subset for calculating the performance measures (see Section 3.2.2). Fig. 3.3 shows the randomly selected rain gauges for each station density scenario. Some cross validation tests for different station selections were performed in order to evaluate the influence of the random

Table 3.1: Rain gauge density scenarios.

No.	Used gauges	Percentage (%)	Gauges per 10.000 km^2	Scenario name
1	90	100	18.94	100% Scenario
2	70	78	14.73	80% Scenario
3	55	61	11.58	60% Scenario
4	37	41	7.79	40% Scenario
5	17	19	3.58	20% Scenario

selection on the interpolation performance. No significant influence was detected and therefore this random selection is considered as acceptable.

3.3.2 Radar data pre-processing

Radar data of the C-band instrument at Hanover were provided as raw reflectivities with an azimuth resolution of 1° and a time discretisation of 5 min (dx product of the German Weather Service, DWD). Accordingly, the data of each time step contained the measurements of 360 radar beam positions whereas the spatial resolution along each beam was 1 km. The raw reflectivities were transformed into rainfall intensities by using an average Z-R-relationship:

$$Z = a \cdot R^b \tag{3.15}$$

Z is here the reflectivity in $mm^6 m^{-3}$ and R is the rainfall intensity in mm/h. The parameters were set to a = 256 and b = 1.42 according to the Standard-DWD-relationship (RIEDL, 1986; SELTMANN, 1997). A simple clutter correction approach was applied as follows. A permitted range of the rainfall sum R_{sum} over the 3-year period (upper limit R_{max} and lower limit R_{min} was established according to the information in Table 3.2. Radar observation points with a higher or lower rainfall sum were identified as clutter. Additionally, a permitted rainfall duration and permitted dry spell duration is defined. Then, radar observation for a certain point is treated as clutter if the proportion of time steps with rainfall intensity of at least 0.1 mm/h exceeds a threshold of 70%, or if the percentage of time steps with rainfall intensity of lower than 0.01 mm/h exceeds a threshold of 98%. These empirically established thresholds were sufficient to provide adequate correction of clutter while not removing to many radar observation points. Blocked radar beams were identified visually and marked as clutter likewise.

Thereafter, a coordinate transformation of the radar data was performed. All non-clutter obser-
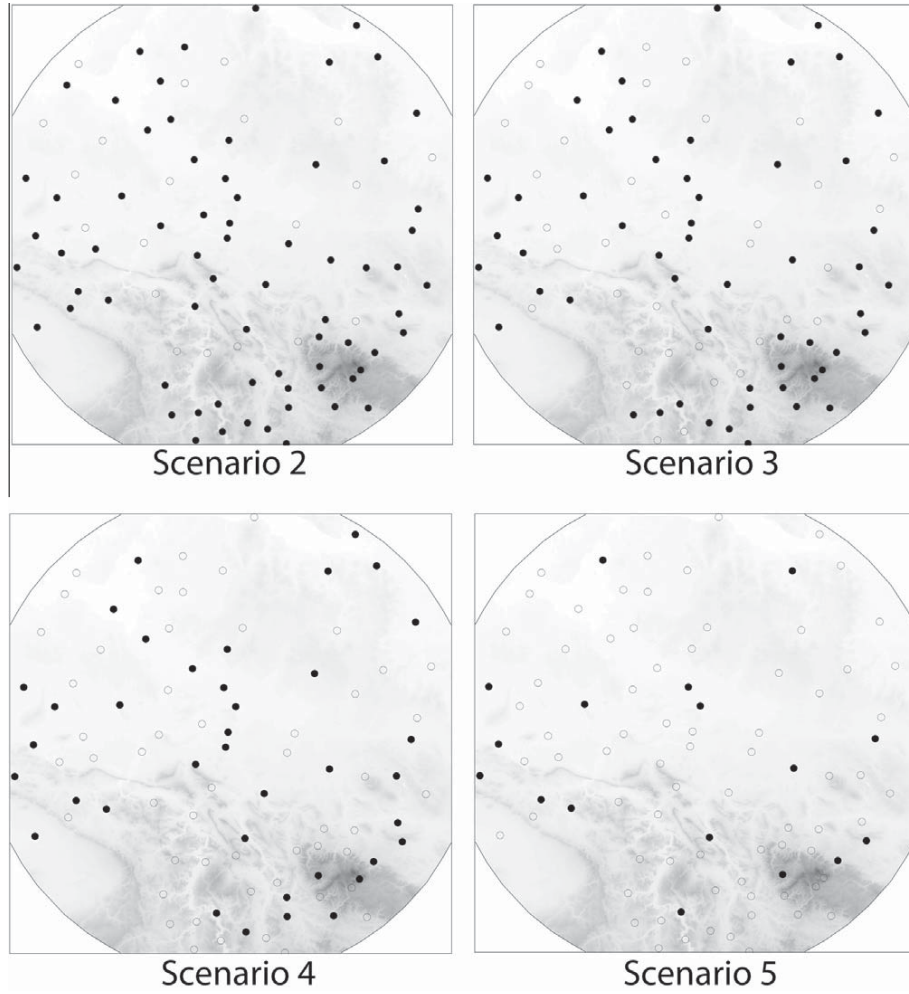
Figure 3.3: Random selection of rainfall stations for different density scenarios. The filled black dots indicate that the station is considered in the corresponding scenario.

Table 3.2: Clutter correction parameters. R_{sum}:rainfall sum 2008-2010; R_{max}: maximal allowed rainfall sum; R_{min}: minimal allowed rainfall sum; $R1_{lim}$: rainfall threshold for rain; $R0_{lim}$: rainfall threshold for no rain; $R1_{dur}$: allowed rain duration; $R0_{dur}$: allowed no rain duration, D: rainfall duration and no rainfall duration, respectively.

No.	Criterion	Parameter	
1	$R_{sum} > R_{max}$	$R_{max}(mm)$	2800
2	$R_{sum} > R_{mix}$	$R_{min}(mm)$	500
3	$D(Ri \geq R1_{lim}) > R1_{dur}$	$R1_{lim}(mm)$	0.1
		$R1_{dur}(\%)$	0.7
4	$D(Ri < R0_{lim}) > R0_{dur}$	$R0_{lim}(mm/h)$	0.01
		$R0_{dur}(\%)$	0.98
5	Erroneous beams	Visual inspection	

Table 3.3: Average correlation between radar and rain gauge data for each temporal data resolution.

10 min	20 min	30 min	1 h	2 h	4 h	6 h
0.37	0.46	0.51	0.57	0.60	0.62	0.62

Table 3.4: Smoothing techniques for gridded radar data.

Method	Type	Characterization
1	Spatial	Slight (9 grid cells)
2	Spatial	Stronger (25 grid cells)
3	Temporal	Simple moving average over 5 time steps (central)
4	Temporal	Weighted moving average over 5 time steps (central, $\lambda_0 = 0.4, \lambda_1 = 0.2, \lambda_2 = 0.1$)
5	Temporal	Weighted moving average over 5 time steps (central, $\lambda_0 = 0.7, \lambda_1 = 0.1, \lambda_2 = 0.05$)
6	Temporal	Weighted moving average over 3 time steps by only using past data (central, $\lambda_0 = 0.7, \lambda_1 = 0.2, \lambda_2 = 0.1$)
7	Spatio-temporal	Simultaneous application of method 2 and method 3

vation points were interpolated on a 1 km $\times$ 1 km grid by using inverse distance weighting. The gridded rainfall intensities in mm/h that were obtained by application of the Z-R-relationship were converted into the corresponding 5 min rainfall depths. A spatial, temporal and spatiotemporal smoothing of the radar data was carried out afterwards (see Section 3.3.2). Radar grids for all other temporal resolutions were produced by aggregating the 5 min grids.

To get a first impression of the linear relationship between rain gauge values and corresponding radar data grid points, Pearson's correlation coefficient was calculated and averaged over all stations and time steps for each temporal resolution (Table 3.3). As assumed the correlation coefficient decreases with increasing temporal resolution from 0.62 at 6 h resolution to 0.37 at 10 min resolution. This supports the assumption that the benefit of using radar data in combination with rain gauge data might be restricted to lower temporal resolutions.

3.3.3 Smoothing techniques for radar data

In order to evaluate the value of radar data smoothing, seven different techniques were applied on the 5 min radar grids. Afterwards, the data of all other temporal resolutions were produced by aggregating the 5 min radar grids. Table 3.4 shows the utilized approaches for smoothing the radar data.

Local spatial smoothing was applied with two different intensities, slight and strong spatial

smoothing. For slight smoothing (method 1) the grid cell values were recalculated by averaging the target cell value and the eight closest neighboring cells. The strong approach (method 2) consisted of averaging over the 24 adjacent grid cells.

The temporal smoothing was carried out by using a moving average approach that considered the data of 5 time steps and was applied on the 5 min gridded data.

$$P_s(t) = \omega_2 P(t-2) + \omega_1 P(t-1) + \omega_0 P(t) + \omega_1 P(t+1) + \omega_2 P(t+2) \qquad (3.16)$$

Here, $P_s(t)$ is the smoothed precipitation gridpoint value for the time step t. $P(t)$ represents the original precipitation grid point value and $P(t \pm j), j = -2, -1, \ldots, 2$ are the rainfall values of the adjacent time steps.

Different weights have been chosen, whereas the sum of all weights is 1. These temporal smoothing techniques (methods 3, 4 and 5) do not allow merging of rain gauge and radar data in real-time because future precipitation measurements would be required for this. In order to take into account a scenario where realtime interpolation is theoretically possible, method 6 was applied. This incorporates only the data of past time steps.

$$P_s(t) = \omega_2 P(t-2) + \omega_1 P(t-1) + \omega_0 P(t) \qquad (3.17)$$

The weights $\omega_0, \omega_1, \omega_2$ were selected to 0.7, 0.2 and 0.1, respectively.

Additionally, a spatio-temporal smoothing technique (method 7) was applied as a combination of method 2 and method 3. The temporal smoothing was carried out prior to the spatial smoothing.

High frequency signal is generally filtered out by the application of smoothing, i.e. some kind of noise removal is carried out implicitly by these simple and practical approaches. Theoretically, an existing noise could contribute to a possible over- and underestimation. PEGRAM et al. (2011) worked on the separation of signal and noise to generate ensembles for uncertainty analyses.

3.3.4 Detection of time steps with poor radar data

Radar data quality is of high importance regarding the interpolation performance. A simple approach using two criteria was applied here to filter out time steps with poor radar data quality. First, the standard error between rain gauge values and corresponding radar point information was computed for time steps in which rainfall was detected by rain gauges as well as by the corresponding radar pixels:

$$SE_{PR}(t) = \sqrt{\frac{1}{n}\sum_{i=1}^{n}(R_i(t) - P_i(t))^2} \ \forall t \text{ with } sum_{i=1}^{n}(P_i) > 0 \text{ and } sum_{i=1}^{n}(R_i) > 0 \qquad (3.18)$$

Here, *P* is the gauge rainfall, *R* radar rainfall and n the number of stations. The time steps in which the standard error exceeds the 98th percentile of the empirical distribution of the standard errors were defined as outliers.
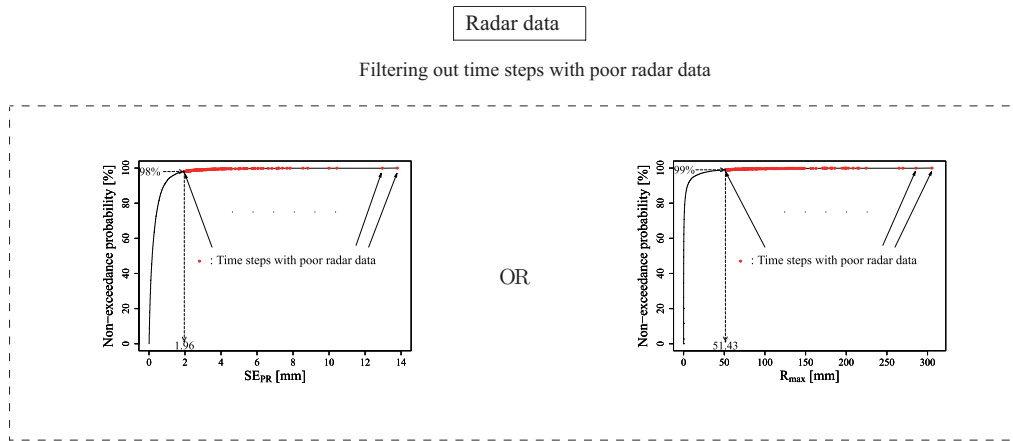
Figure 3.4: Detection method for time steps with poor radar data.

In some time steps, an implausible estimation of rainfall by radar occurs, which could not always be detected by the criterion described above. An additional criterion regarding the maximum radar rainfall grid cell was used to detect these time steps. This means that the maximum radar grid rainfall value is determined for each time step without a minimum rainfall threshold:

$$R_{max}(t) = \max_{i}[R_i(t)], \qquad (3.19)$$

where i is the number of grid points. Here, the 99th percentile of the empirical distribution of the maximum radar rainfall values is considered to detect those time steps with implausible high rainfall values. The time steps that meet one of these two criteria are treated as poor radar data time steps for further analysis. This detection procedure was applied separately to all temporal resolutions. Table 3.5 gives an overview about the number of removed time steps for each temporal resolution and Fig. 3.4 contains a scheme of the detection method. The 98th percentile threshold and 99th percentile threshold were established by manual tests. By this procedure, most time steps with poor radar data and hence a poor interpolation result could be excluded.

Table 3.5: Detected poor radar data time steps.

Temp. resolution (min)	No. of time steps (standard error method)	98th percentile of stand. errors (mm)	No. of detected time steps	No. of time steps (maximum value outliers)	99th percentile of radar max. val. (mm)	No. of max val. outl.	Total no. of outlies
10	49,032	0.65	981	143,329	15.18	1434	1956
20	27,596	1.03	552	71,814	26.79	719	1009
30	19,639	1.30	393	47,967	35.03	480	681
60	10,987	1.96	220	24,031	51.33	241	258
120	6162	2.89	124	12,051	69.54	121	190
240	3520	4.62	71	6048	102.03	61	103
360	2540	6.08	51	4045	119.13	41	73

3.4 Analyses and results

3.4.1 Variogram inference

Gridded radar data in different temporal resolutions were utilized for the inference of each experimental variogram. One thousand cells of the 1 km × 1 km radar grid were selected randomly to compute the variogram values for each time step. This number gave a sufficient estimation of the spatial rainfall structure. After that, the experimental variogram values were averaged for all winter time steps and all summer time steps separately. All time steps with an average radar precipitation higher than 0.1 mm were considered for this estimation of experimental variograms. By the use of this rather low threshold, it was ensured that a sufficient number of time steps were taken into account for the estimation of high temporal resolution variograms. Then, a fitting of the theoretical variogram model was carried out visually. Table

Table 3.6: Parameters for theoretical variogram models used in KED, CM and OK (exponential model).

Season		Temporal resolution (min)						
		10	20	30	60	120	240	360
Summer	$c_0(-)$	0.25	0.20	0.20	0.20	0.20	0.20	0.20
	$c(-)$	0.75	0.82	0.80	0.80	0.80	0.85	0.90
	$a_{eff}(km)$	30	45	45	60	75	96	99
Winter	$c_0(-)$	0.30	0.10	0.10	0.10	0.05	0.10	0.05
	$c(-)$	0.80	1	1.10	1.10	1.1	1.10	1.15
	$a_{eff}(km)$	48	60	75	90	28	105	105

3.6 contains the parameters of the variograms that were obtained for each temporal resolution and later used for the cross validation. Fig. 3.5 contains experimental variograms and fitted theoretical models for summer and winter season. Only 10 min, 60 min and 360 min variograms are pictured.
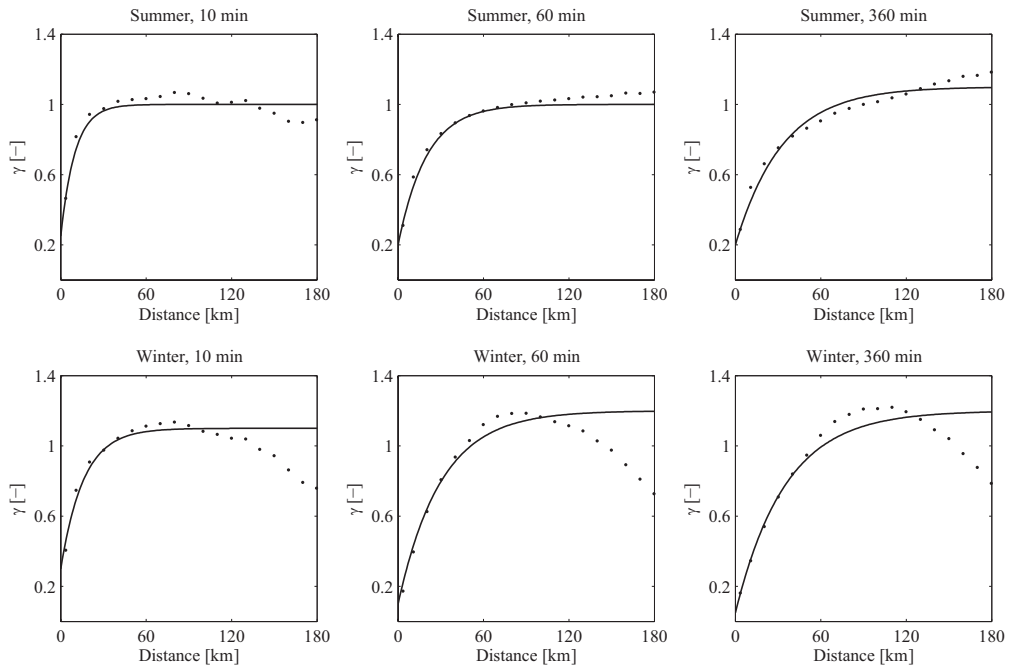
Figure 3.5: Selected experimental and theoretical variograms for OK, KED and CM.

In general, an increase of effective range (a_{eff}) with increasing temporal resolution was observed for both seasons. The nugget effect (c_0) is in summer always higher than in winter. This might result from the more frequent occurrence of convective rainfall events in summer.

The same procedure was used for the inference of indicator variograms. Again, only time steps with significant rainfall are used for the calculation of seasonal averaged experimental

variograms. The variograms were estimated separately for each temporal resolution and for five absolute rainfall thresholds τ at 0.1, 0.5, 1.0, 4.0 and 8.0 mm. Altogether 70 indicator variograms were fitted manually. Fig. 3.6 shows the season specific theoretical indicator variogram models for selected temporal resolutions. Each panel contains the theoretical variogram model for three different indicator thresholds. In general, a decrease in range (a_{eff}) and an increase in relative nugget effect $(c_0/(c_0+c))$ can be observed with a growing threshold for most temporal resolutions (see Table 3.7 and Fig. 3.6). This shows a weaker spatial persistence of extreme values.
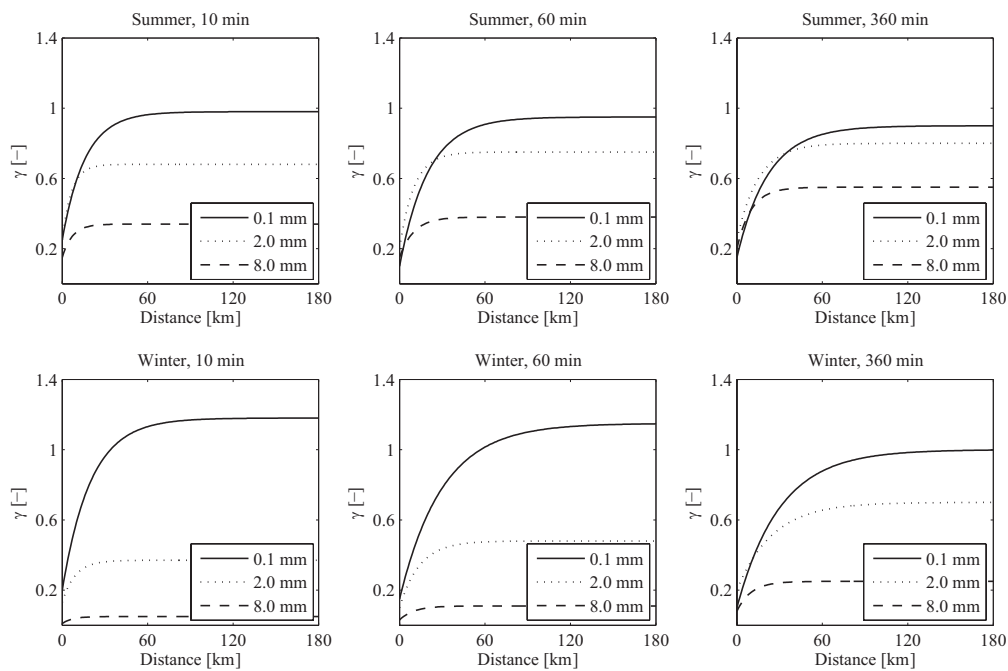
Figure 3.6: Selected theoretical variogram models for IKED.

For the IKED interpolation, relative thresholds from 13 quantiles with non-exceedance probabilities of p = 0.01, 0.05, 0.1, 0.2, 0.3, 0.4, 0.5, 0.6, 0.7, 0.8, 0.9, 0.95, 0.99 are used to calculate absolute thresholds α_P for each time step. Thirteen different indicator variables are then interpolated for each time step, based on the mentioned thresholds. For the interpolation of each variable, the closest indicator variogram is chosen automatically from the five previously inferred ones. This means that the indicator variogram is selected, for which the lowest difference between interpolation threshold α_P and inference threshold τ exists (see also HABERLANDT, 2007).

Table 3.7: Parameters of theoretical indicator variogram models used in IKED (exponential model).

Season	$\alpha(mm)$	Par.	Temporal resolution (min)						
			10	20	30	60	120	240	360
Summer	0.1	$c_0(-)$	0.25	0.18	0.15	0.10	0.10	0.15	0.15
		$c(-)$	0.73	0.80	0.80	0.85	0.85	0.75	0.75
		$a_{eff}(km)$	48	54	54	60	75	64	66
Winter	0.1	$c_0(-)$	0.20	0.15	0.15	0.15	0.10	0.10	0.10
		$c(-)$	0.98	1.00	0.97	1.00	1.00	0.90	0.90
		$a_{eff}(km)$	60	66	69	90	90	84	90
Summer	0.5	$c_0(-)$	0.25	0.25	0.25	0.2	0.2	0.15	0.2
		$c(-)$	0.66	0.68	0.68	0.75	0.75	0.7	0.7
		$a_{eff}(km)$	24	12	39	48	60	42	54
Winter	0.5	$c_0(-)$	0.3	0.25	0.2	0.2	0.2	0.2	0.2
		$c(-)$	0.72	0.76	0.8	0.83	0.75	0.8	0.9
		$a_{eff}(km)$	45	45	48	63	60	64	90
Summer	1	$c_0(-)$	0.35	0.2	0.25	0.25	0.2	0.23	0.25
		$c(-)$	0.48	0.65	0.6	0.6	0.65	0.62	0.6
		$a_{eff}(km)$	24	24	30	42	45	48	48
Winter	1	$c_0(-)$	0.25	0.2	0.16	0.2	0.2	0.18	0.2
		$c(-)$	0.48	0.5	0.6	0.55	0.55	0.65	0.65
		$a_{eff}(km)$	45	33	40.5	48	54	60	66
Summer	2	$c_0(-)$	0.25	0.25	0.25	0.2	0.25	0.25	0.25
		$c(-)$	0.43	0.43	0.45	0.55	0.5	0.55	0.55
		$a_{eff}(km)$	19.5	24	30	30	39	48	45
Winter	2	$c_0(-)$	0.13	0.15	0.1	0.1	0.13	0.15	0.2
		$c(-)$	0.24	0.28	0.32	0.38	0.42	0.45	0.5
		$a_{eff}(km)$	27	12	30	42	54	54	75
Summer	4	$c_0(-)$	0.25	0.2	0.2	0.15	0.2	0.2	0.25
		$c(-)$	0.25	0.3	0.31	0.43	0.4	0.45	0.45
		$a_{eff}(km)$	22.5	19.5	24	30	30	36	45
Winter	4	$c_0(-)$	0.05	0.05	0.05	0.075	0.12	0.1	0.15
		$c(-)$	0.12	0.14	0.16	0.175	0.21	0.3	0.35
		$a_{eff}(km)$	21	24	24	30	54	51	90
Summer	8	$c_0(-)$	0.15	0.15	0.15	0.15	0.2	0.2	0.2
		$c(-)$	0.19	0.21	0.21	0.23	0.25	0.3	0.35
		$a_{eff}(km)$	21	21	22.5	30	30	36	30
Winter	8	$c_0(-)$	0.01	0.02	0.02	0.03	0.05	0.1	0.08
		$c(-)$	0.04	0.06	0.06	0.08	0.1	0.13	0.17
		$a_{eff}(km)$	21	30	30	30	30	66	30

Table 3.8: Interpolation performance from cross validation using KED for various smoothing techniques on hourly data (314 considered time steps).

Smoothing method	$Bias(mm/h)$	$RMSE(mm/h)$	$RVar(-)$
No radar data use (OK)	0.097	1.075	0.258
Original radar data	0.047	1.025	0.752
1	0.034	0.953	0.673
2	0.025	0.921	0.609
3	0.045	0.992	0.783
4	0.045	1.005	0.768
5	0.046	1.016	0.760
6	0.046	1.005	0.776
7	0.026	0.892	0.649

3.4.2 Effect of radar data smoothing on the interpolation quality

In order to evaluate the effect of radar data smoothing on the interpolation performance, cross validation was carried out, using differently smoothed radar data in the merging process for a temporal resolution of 1 h. Different methods (KED, CM and IKED) were used to assess the effect of radar data smoothing on the merging performance, all of them showed similar results. Therefore, only the outcome of KED is presented here in detail.

All of the time steps with an average observed station rainfall intensity higher than 1.0 mm/h were considered in the calculation of the performance criteria. *Bias*, *RMSE* and *RVar* (Eqs. (3.12, 3.13 and 3.14)) were averaged over all time steps. The results of cross validation are presented for the complete period from 2008 until 2010 in Table 3.8.

Generally, smoothing of radar data improved the merging quality. At least a slight improvement in merging performance can be observed for all of the proposed spatial and temporal techniques. Using only spatial smoothing, the 25 cell approach (method 2) gave the best result, with an *RMSE* of 0.921 mm/h. Method 3 (simple moving average) was the best temporal smoothing approach with a *RMSE* value of 0.992 mm/h, which is only slightly lower than the *RMSE* value for using the original radar data (1.025 mm/h). Temporal smoothing resulted in general in a similar preservation of observation variance as when original radar data were used, whereas the spatial techniques showed a decline in the preservation of variance RVar. Though the reduction of observation variance for method 2 (RVar = 0.609) was higher than for method 1 (0.673), method 2 is regarded here as superior, since the *RMSE* measure is considered more important for the interpolation performance. Overall, the spatiotemporal smoothing approach, method 7, shows the best results. It gives the lowest estimation errors, with a *RMSE* of 0.892 mm/h. So

method 7 was applied for further investigations in this study.

In Fig. 3.7 the Bias and standard error are compared for the use of non-smoothed radar data vs. the use of radar data that was smoothed by method 7. Each dot represents one hourly time step here. It can be seen, that smoothing did not improve the merging performance consistently for all time steps. In particular, an improvement was detected for steps that have a high overestimation of rainfall by radar. It is assumed that this improvement is based on the reduction of rainfall peaks in the gridded radar data. It is also plausible that the improvement was higher for summer months than for winter months. The evaluations regarding the season are not shown here.
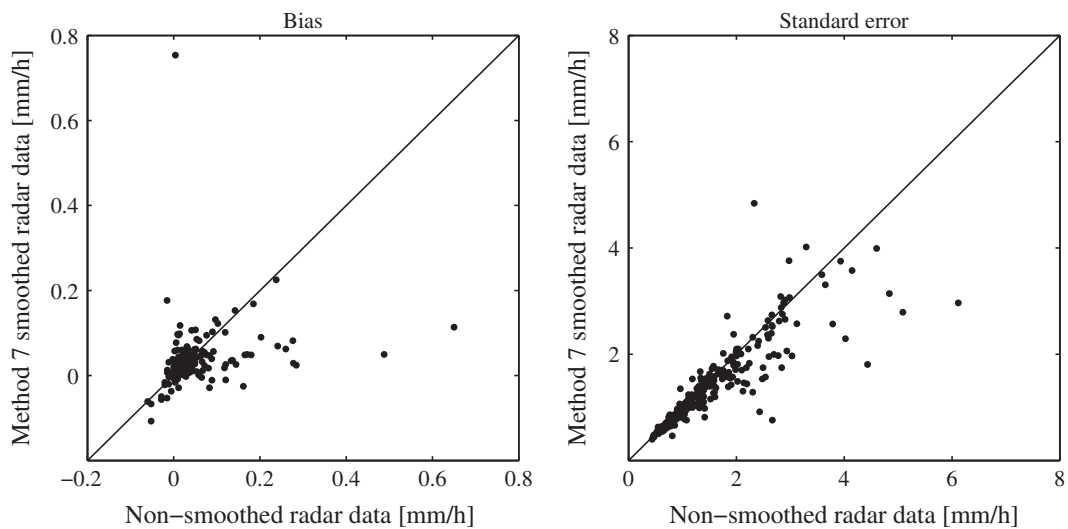
Figure 3.7: Scatter plots of bias and standard error for best smoothing method vs. original radar data.

3.4.3 Analysis of merging techniques regarding station density and temporal resolution

Many case studies, in which geostatistical interpolation techniques have been applied, e.g. GOUDENHOOFDT and DELOBBE (2009) and KRAJEWSKI (1987), conclude that the density of the rain gauge network is of importance regarding the interpolation performance. Furthermore, the spatial structure and dynamics of precipitation depend strongly on the temporal resolution, for instance, the ascertained variogram parameters show an increase of range with reduction of temporal resolution (see Section 3.4.1). Additionally, the correlation between rain gauge

Table 3.9: Number of time steps considered in interpolation performance evaluation and corresponding 95th percentile trimming limit (Case A: Considering all time steps for which rada rdata are available. Case B: Considering all time steps excluding outliers.).

Temporal resolution (min)	Case A		Case B	
	Number of time steps	95th percentile (mm)	Number of time steps	95th percentile (mm)
10	2884	0.139	2806	0.129
20	1562	0.263	1518	0.243
30	1091	0.385	1060	0.354
60	593	0.729	577	0.668
120	326	1.361	317	1.204
240	183	2.497	178	2.198
360	131	3.427	127	3.019

measurement and corresponding radar pixel was higher for low temporal resolutions (see Section 3.3.2).

Generally, it is assumed that the relative errors of radar rainfall measurements would be lower for coarser temporal resolutions. Advection effects and location mismatches between radar and gauge observation domains would be reduced with a decrease in temporal resolution.

The analyses were carried out using all available time steps with radar data (case A) and using only the time steps in which radar data provided a reasonable estimation of rainfall (case B). In the latter case, time steps with poor radar data were identified by the approach described in Section 3.3.4 and neglected in the calculations.

The cross validation results which are presented in the following consider only time steps with a significant amount of rainfall. In order to decide whether a certain time step is taken into account, the average rain gauge rainfall is calculated for all temporal resolutions, considering all of the 90 stations which are available for the total time period from 2008 until 2010. Hereafter all time steps with an average rainfall that is equal to zero were removed. Then, absolute rainfall limits were calculated as the 95th percentile of the remaining time steps, whereas this procedure is done separately for (A) and (B). In both cases only the 5% of time steps that exceed these trimming limits were taken into account for the evaluations (see Table 3.9).

The *RMSE* values (Eq. 3.13) representing the interpolation performance are provided in Fig. 3.8. Absolute values of the *RMSE* are plotted on the vertical axis while the horizontal axes contain the information about temporal resolution and station density. In addition the improvement

of interpolation quality relative to OK is illustrated by the surface color. An improvement of merging performance was achieved for all combinations of temporal resolution and station density that are colored in green, while a decline in performance is marked in red. All absolute *RMSE* values and all relative differences between each merging method and OK are interpolated linearly in the three-dimensional surface plots.
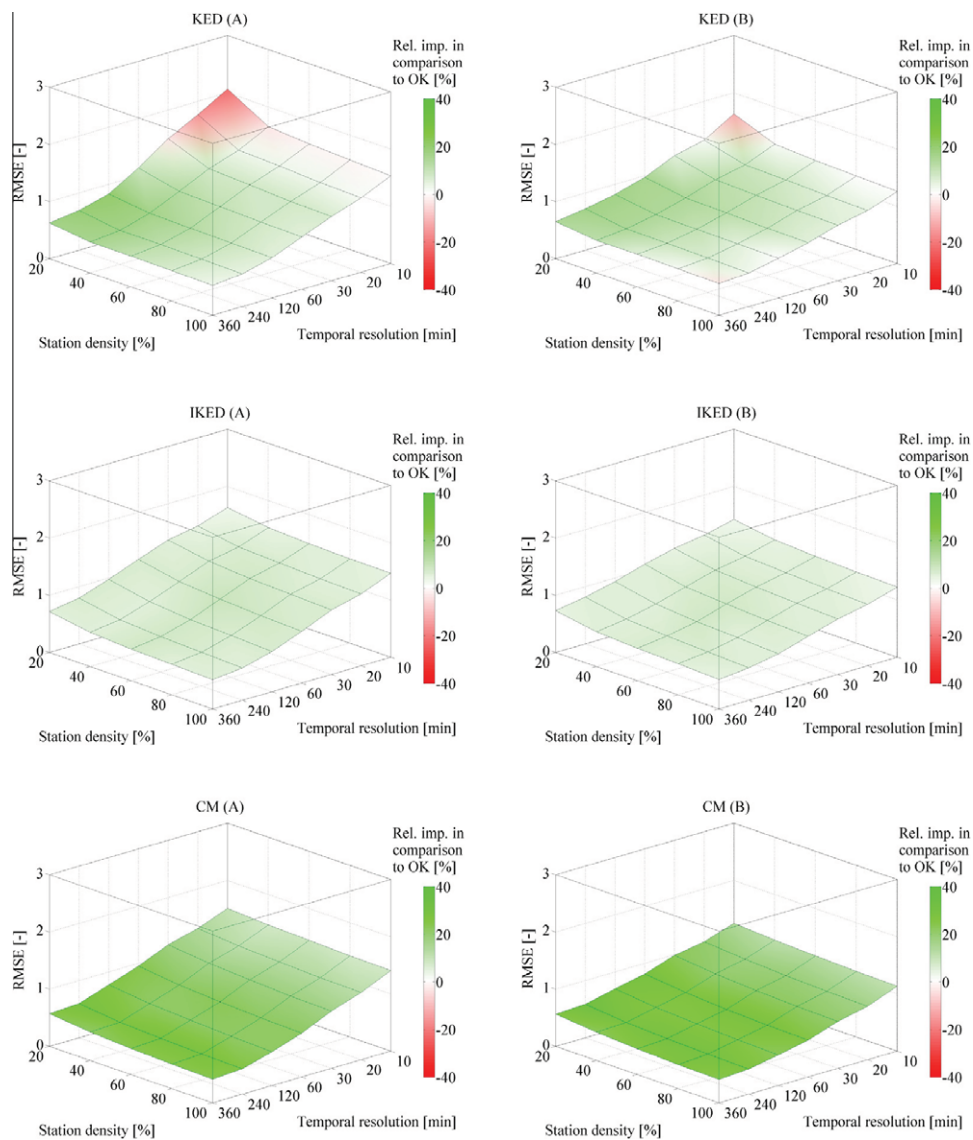
Figure 3.8: RMSE interpolation performance of KED, IKED and CM using smoothed radar data for (A) - no removal of time steps with poor radar data quality and (B) - removal of time steps with poor radar data quality. The colorbar indicates the relative improvement in comparison to OK.

Comparing the merging methods, it is clear that the CM approach performed best for almost all pairs of temporal data resolution and station density scenario concerning the *RMSE* criterion.

Table 3.10: Average interpolation performance (*Bias*, *RMSE*, *RVar*) over all station densities scenarios for each temporal resolution. Time steps with radar data outliers excluded (case B).

Temp. res. (min)		10	20	30	60	120	240	360
OK	*Bias(mm)*	0.006	0.012	0.017	0.028	0.049	0.066	0.055
	RMSE(−)	1.350	1.218	1.128	0.981	0.811	0.703	0.625
	RVar(−)	0.176	0.197	0.210	0.235	0.264	0.260	0.250
KED	*Bias(mm)*	0.007	0.012	0.014	0.013	0.016	0.064	0.017
	RMSE(−)	1.366	1.149	1.036	0.863	0.729	0.630	0.582
	RVar(−)	0.498	0.527	0.528	0.502	0.482	0.486	0.452
IKED	*Bias(mm)*	-0.033	-0.038	-0.039	-0.047	-0.061	-0.071	-0.118
	RMSE(−)	1.295	1.157	1.061	0.918	0.765	0.659	0.593
	RVar(−)	0.126	0.153	0.171	0.197	0.217	0.221	0.216
CM	*Bias(mm)*	0.003	0.005	0.008	0.005	-0.003	0.025	0.017
	RMSE(−)	1.181	0.992	0.885	0.709	0.602	0.495	0.467
	RVar(−)	0.432	0.510	0.548	0.585	0.577	0.696	0.690

As expected, the absolute values of *RMSE* are decreasing with decreasing temporal resolution and increasing station density. Using CM, an improvement in comparison to OK is achieved for the complete range of station densities and temporal resolutions.

KED performs significantly worse than OK for low station densities with high temporal resolution data. Only for temporal resolutions greater than or equal to 60 min, a consistent improvement over all station density scenarios was achieved considering all time steps including radar data outliers for the evaluation (case A). After removing these outliers (case B), a consistent advance in performance is observed for temporal resolutions greater than or equal to 20 min. For 360 min data and 100% station density, a slight decrease of merging performance in comparison to OK is detected for KED. This might be explained by the high station density, which allowed a good performance of OK in this case.

IKED performs relatively well for high temporal resolutions. The difference of *RMSE* in relation to OK is similar for all combinations of temporal resolution and station density. For combinations of small densities and low temporal resolutions, i.e. from 2 h to 6 h and the corresponding 20-60% scenarios, the merging performance is considerably lower than for KED. The relative improvement of the best approach (CM) in comparison to OK ranges from approx. 8% to approx. 30% for case A, and from approx. 10% to approx. 33% for case B.

In general, the benefit of incorporating radar data in the interpolation increases with decreasing temporal resolution, as can be observed in Fig. 3.8. Especially for KED, there is also a growth of radar data value with decreasing station density for temporal resolutions lower than 60

Table 3.11: Average interpolation performance ($Bias, RMSE, RVar$) over all temporal resolutions for each station density. Time steps with radar data outliers excluded (case B).

Station density		20%	40%	60%	80%	100%
OK	$Bias(mm)$	0.032	0.020	0.043	0.036	0.035
	$RMSE(-)$	1.125	0.998	0.958	0.913	0.875
	$RVar(-)$	0.027	0.171	0.270	0.313	0.357
KED	$Bias(mm)$	0.069	-0.010	0.024	0.018	0.002
	$RMSE(-)$	1.046	0.897	0.881	0.864	0.851
	$RVar(-)$	0.762	0.485	0.447	0.403	0.385
IKED	$Bias(mm)$	-0.160	-0.088	-0.033	-0.008	-0.002
	$RMSE(-)$	1.075	0.943	0.894	0.861	0.833
	$RVar(-)$	0.037	0.135	0.211	0.250	0.296
CM	$Bias(mm)$	0.009	-0.004	0.007	0.016	0.015
	$RMSE(-)$	0.856	0.787	0.746	0.717	0.701
	$RVar(-)$	0.401	0.556	0.619	0.645	0.663

min.

Mean interpolation performances for all temporal resolutions and station density scenarios are provided in Tables 3.10 and 3.11. The values of *RMSE*, *RVar* and *Bias* are averaged over all station density scenarios (Table 3.10) and temporal resolutions (Table 3.11). The tables contain only the results for case (B), i.e. time steps with poor radar data are excluded, since the objective is to provide a comparison of methods which is not influenced that strongly by radar data quality. The effect of radar data quality on the interpolation performance is discussed separately in Section 3.4.4.

Furthermore, it appears that CM and IKED are less sensitive than KED regarding the influence of the station density. In particular, the interpolation performance of KED for high temporal resolutions decreases much more from 100% to 20% station density in comparison to CM and IKED.

In terms of preservation of observation variance, CM outperforms all other interpolation techniques for most temporal resolutions and station density scenarios as well. Only for the lowest station density scenario and the highest temporal resolution KED outperforms CM. The observation variance preservation of IKED and OK is much lower, whereas OK even outperforms IKED in most cases. This means that rainfall fields interpolated by OK and IKED show a much smoother distribution than those interpolated using KED and CM.

The *Bias-criterion* is used as control criterion to test the implicit unbiasedness of the geostatistical methods. It is similarly low for all the merging methods.

In terms of computation time, CM and KED are preferable compared to IKED. CM needs a double application of OK as well as two simple arithmetical calculations. The KED calculations required a similar amount of computation time. In this study the number of indicator variables for IKED was selected to 13. Accordingly, the required computation time was 13 times higher than those of KED.
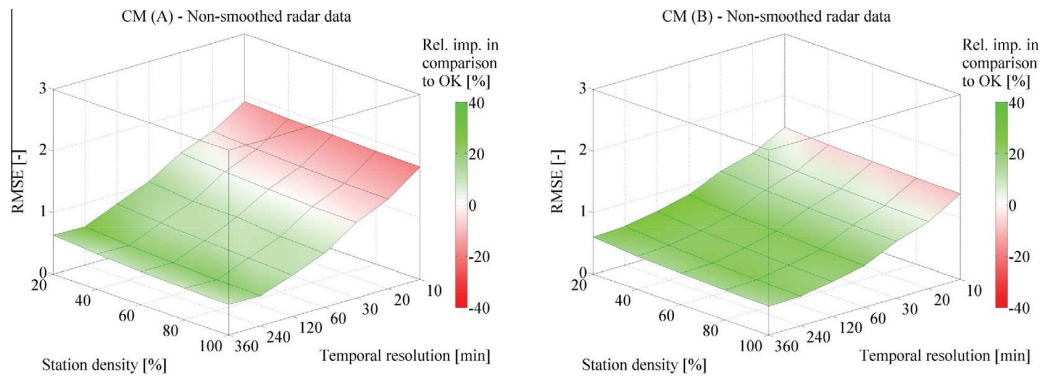
Figure 3.9: RMSE interpolation performance for CM using non-smoothed radar data for (A) - no removal of time steps with poor radar data quality and (B) - removal of time steps with poor radar data quality. The colorbar indicates the relative improvement in comparison to OK.

In order to highlight the importance of radar data smoothing, the cross validation calculations for CM were carried out using non-smoothed radar data as well. The results for different temporal resolutions and station density scenarios are shown in Fig. 3.9. Again, case (A) and case (B) are displayed. When comparing Figs. 3.9 and 3.8, it is obvious that CM performed significantly worse when non-smoothed radar data were used. In particular especially a significant weaker interpolation performance in comparison to OK for high temporal resolutions is evident. In this case a benefit of using radar data as additional information can only be seen for temporal resolutions lower than 30 min (A) and 10 min (B). Accordingly, radar data smoothing is in particular important for the merging of high temporal resolution data.

3.4.4 Effect of radar data quality - sensitivity of merging methods

This section discusses the influence of radar data quality on the interpolation performance. In general, high correlation between radar and rain gauge information is an important condition for successful merging of these two data sources.
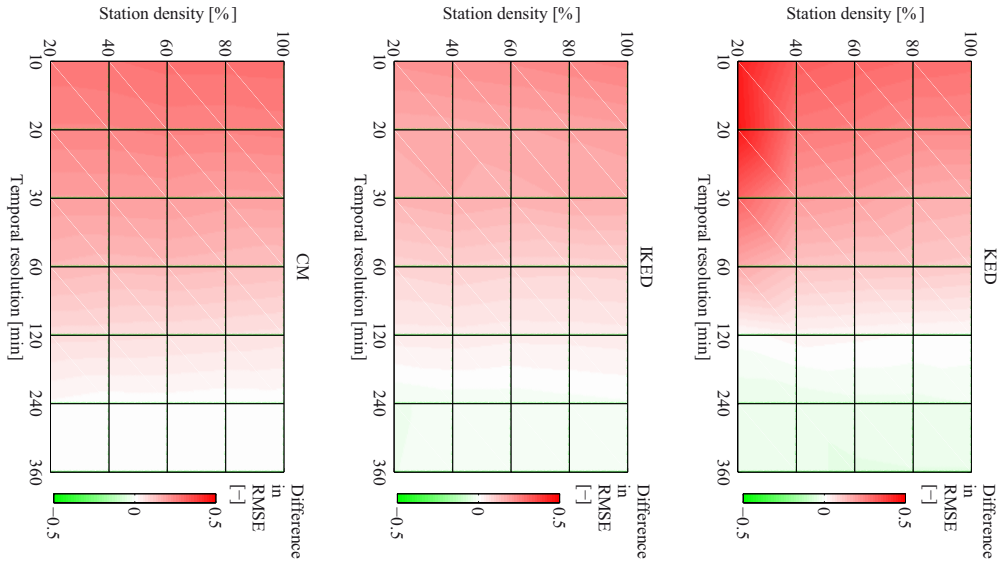
Figure 3.10: Difference between RMSE values from cross validation when including time steps with poor radar data quality (case A) and excluding time steps with poor radar data quality (case B) for KED, IKED and CM.

Fig. 3.10 shows the difference between *RMSE* values for case A when including and for case B when excluding time steps with radar data outliers for all merging methods:

$$D_{RMSE}(i,j) = RMSE_{(A)}(i,j) - RMSE_{(B)}(i,j). \tag{3.20}$$

Here, i is the temporal resolution and j the station density scenario. The color shading between the sampled points is interpolated linearly. Positive values (red color) indicate that the merging performance including the time steps with poor radar data is worse than those of excluding those time steps.

In general, the difference between the *RMSEs* of (A) and (B) increases with increasing temporal resolution. This shows that the detection and removal of radar data outliers is more important for high-resolution data.

For low temporal resolutions using KED and IKED, the RMSE values of case (B) are even a little higher than those of case (A). Thus, the green area in Fig. 3.6 indicates situations where the merging performance including all poor radar data time steps is slightly better than the interpolation performance without poor radar data time steps. This shows that radar data can be of value for the interpolation of low resolution rainfall although the rainfall estimation on a 5 min time scale is incorrect.

According to the difference in RMSE, i.e. the sensitivity regarding radar data quality, the methods were ranked as follows: IKED (lowest), CM (middle) and KED (highest). The sensitivity of KED in regard to radar data outliers was particularly high for some combinations of high temporal resolution and low station densities.

3.5 Summary and conclusions

The main objective of this study was a comparison of geostatistical methods for merging radar and rain gauge data considering different high temporal resolutions and station densities. Smoothing techniques were applied to radar data, which were then used in the merging process. Cross validation with these hourly data was carried out for KED, IKED and CM to evaluate the benefit of radar data smoothing. additionally, the cross validation computations were carried out with and without poor radar data time steps. Using this procedure, the effect of radar data quality on the interpolation performance was analyzed. The main findings and conclusions can be summarized as follows:

1. In case of hourly temporal resolution, smoothing improves the merging performance on average. However, a consistent improvement for all hourly time steps is not achieved. A spatio-temporal method is considered as the best approach to smooth the radar grids. The interpolation performance improves with stronger smoothing, but the preservation of the observation variance is reduced. Too strong smoothing is not recommended because this results in a loss of information about the spatial rainfall structure.

2. Radar data smoothing is strongly recommended for the merging of radar and rain gauge data with high temporal resolution. The application of CM with non-smoothed radar data led to significantly worse results than when using smoothed data and shows even no benefit of using radar data at all for the 10 min temporal resolution.

3. CM outperforms KED and IKED for all combinations of station density scenario and

temporal resolution.

4. An improvement of interpolation performance in comparison to OK was achieved even for radar and rain gauge data with the highest temporal resolution of 10 min. Although the correlation between rain gauge values and the corresponding radar pixels is much lower for these high temporal resolutions, the merging process benefitted from the incorporation of those smoothed radar grids.

5. CM is more appropriate for the interpolation of continuous time series, since numerical instabilities do not occur in contrast to the application of KED and IKED.

6. CM and IKED are not as sensitive as KED to poor radar data quality. Single time steps with high deviations between rain gauge values and corresponding radar rainfall values have a significantly higher impact on the KED interpolation performance.

7. Regarding computation time, CM performs slightly better than KED. IKED requires much more computation time which depends on the number of indicator variables used for the interpolation.

EHRET (2002) ranked CM as the best merging technique for rain gauge and radar data with 10 min temporal resolution, whereas different criteria were used to assess the interpolation performance. However, in contrast to the finding of this present study, an improvement of RMSE in comparison to OK was not achieved (EHRET (2002), p. 97). GOUDENHOOFDT and DELOBBE (2009) preferred KED to CM for the merging of daily data. Here, the interpolation performance of KED for 6 h was only a little weaker than those of CM. So, it might also be possible for the dataset of this study that KED performs better than CM on a daily time scale.

Generally, it is assumed that the results of this paper are valid for regions with similar topography as well. Nevertheless, a different behavior might be possible in regions which are predominantly mountainous. Furthermore, the results of this study are related to the merging of continuous time series. Combining radar and rain gauge data for a specific event may lead to different findings. The interpolation performance of all methods was evaluated in terms of averaged error statistics, i.e. the spatial distribution of the rainfall estimation error was not assessed. For all methods, temporal resolutions and station density scenarios, it has to be assumed that the spatial distribution of the prediction uncertainty is not constant within the study area. The spatial interpolation uncertainty could be a topic for further investigation.

The results encourage further work on merging high temporal resolution rainfall, which is

important for e.g. rainfall estimation in urban hydrology (BERNE et al., 2004). It is still a matter of research how the improvement in areal rainfall estimation affects the modeling of hydrological processes.

Acknowledgements

Chapter 4

Applying bias correction for merging rain gauge and radar data

S U M M A R Y

Weather radar provides areal rainfall information with very high temporal and spatial resolution. Radar data has been implemented in several hydrological applications despite the fact that the data suffers from varying sources of error. Several studies have attempted to propose methods for solving these problems. Additionally, weather radar usually underestimates or overestimates the rainfall amount. In this study, a new method is proposed for correcting radar data by implementing the quantile mapping bias correction method. Then, the radar data is merged with observed rainfall by conditional merging and kriging with external drift interpolation techniques. The merging product is analysed regarding the sensitivity of the two investigated methods to the radar data quality. After implementing bias correction, not only did the quality of the radar data improve, but also the performance of the interpolation techniques using radar data as additional information. In general, conditional merging showed greater sensitivity to radar data quality, but performed better than all the other interpolation techniques when using bias corrected radar data. Furthermore, a seasonal variation of interpolation performances has in general been observed. A practical example of using radar data for disaggregating stations from daily to hourly temporal resolution is also proposed in this study.

4.1 Introduction

Advanced technologies like weather radar help to increase our knowledge regarding the spatial structure of rainfall events. Although weather radar provides rainfall data with relatively high spatial and temporal resolution, the data is subject to several sources of error. Beside common problems associated with weather radar, e.g. existence of clutters and attenuation, the data suffers from the fact that weather radar usually either overestimates or underestimates rainfall. There are several physical factors affecting the accuracy of rainfall measurement which are not all recognised quantitatively, but rather qualitatively. Errors related to weather radar data have been investigated by several studies. AUSTIN (1987) studied the complexity of the relationship between rain intensity derived from radar reflectivity and surface rainfall. She discussed the influence of precipitation type, the existence of frozen particles and several other influential factors on the relationship between radar reflectivity and rain intensity, or the *Z-R* relationship. Others proposed methods trying to compensate common problems like detecting ground clutters by analysing radar pixels, implementing sophisticated algorithms for transforming reflectivity to intensity (ALFIERI et al., 2010), attenuation calibration (RAHIMI et al., 2006), etc. ALFIERI et al. (2010) studied a simple procedure for using continuously updated *Z-R* relationships in time to produce real time rainfall estimation.

Despite the difficulties that radar data has, several studies (e.g. QUIRMBACH and SCHULTZ, 2002) tried to use radar data directly as an input for water management purposes. In such circumstances, the radar data quality plays a significant role considering the above mentioned problems. On the other hand, merging radar data and rain gauge data is a traditional way to describe rainfall fields when considering the rain gauge network as providing true information. In order to combine the rainfall estimation from radar and the accurate point information from stationary rain gauges, a variety of methods including co-kriging (KRAJEWSKI, 1987), kriging with external drift (HABERLANDT, 2007; VERWORN and HABERLANDT, 2011), conditional merging (EHRET, 2002), have been proposed. Most of the methods consider the radar data as secondary information to estimate the rainfall field. In kriging with external drift, it is assumed that the expected value of the primary variable is linearly related to the additional variable. This assumption is not always fulfilled. Although EHRET (2002) did not assume linearity of radar data to the primary variable in conditional merging, the quality of radar data is still an important factor in this method. BERNDT et al. (2014) excluded time steps with poor radar quality in order to take into account the influence of radar data quality for merging. They used two criteria: (1) maximum radar rainfall values and (2) standard errors (between the gauge rainfall values and the corresponding radar-pixel values) for detecting time steps with poor

radar data. The poor radar data are detected when exceeding either the 99th percentile of the empirical distribution of the maximum radar rainfall values or the 98th percentile of the empirical distribution of the standard errors.

In addition to merging radar and station data, several studies attempt to adjust the radar image according to rain gauge information. ERDIN et al. (2012) implemented a Box-Cox transformation of radar and station data to improve the compliance with model assumptions. However, they recommend attention in implementing this method to avoid excessive transformation which can introduce positive bias. CHUMCHEAN et al. (2006) corrected radar data for the mean field bias which resulted in improving radar data quality. Besides, they used different parameters in *Z-R* relationship for different types of rainfall which also improved the radar data quality. VOGL et al. (2012) assimilated radar and gauge information to derive bias-corrected precipitation fields implementing copulas. This method requires calibration and fitting of the marginal distribution functions. THORNDAHL et al. (2014) investigated the use of mean field bias adjustment for correcting radar data. They found that a larger bias exists during summer periods compared to winter. This seasonal variation of error was justified by rainfall type, where a larger bias belongs to convective storms and a smaller to stratiform events.

Quantile-quantile (Q-Q) transformation is usually employed in climate impact studies for scaling and bias correction purposes. INES and HANSEN (2006) corrected the daily General Circulation Models (GCM) rainfall for crop simulation studies. They fitted the data into the gamma distribution function and corrected the daily GCM rainfall accordingly. JAKOB THEMESSL et al. (2011) found quantile mapping to have the best performance, especially at high quantiles, compared to seven other methods they implemented for reducing regional climate model error characteristics. CHEN et al. (2013) compared the performance of six bias correction methods for hydrological modelling over 10 North American river basins. They conducted bias correction on a monthly basis and applied two quantile mapping methods based on (a) an empirical distribution, and (b) a gamma distribution. BÁRDOSSY and PEGRAM (2011) implemented this method for downscaling regional climate model precipitation to observed values. Additionally, they used double Q-Q transformation for future scenarios. To our knowledge, all of these studies consider a long time period of the observation and target data, which is here radar data, for estimating the bias. The length of this considered time period accordingly plays an important role. For points where no observation data is available, one may use interpolation techniques which introduce uncertainty into the work. This means that the final result depends not only upon the length of the time period, but also the performance of the interpolation techniques. TEEGAVARAPU (2014) implemented two different quantile-

based bias-correction methods as well as an optimal single best estimator (SBE) method for corrections of spatially interpolated missing precipitation data. They figured out that using bias-correction methods overcomes the over and underestimation of low and high extremes. Among them, the equi-distance quantile-matching performed the best. GYASI-AGYEI and PEGRAM (2014) used Q-Q transform to normalise the daily rainfall data for later determination of marginal frequency distribution of rainfall at all sites on the day.

Correcting radar data by applying a quantile mapping transformation and considering the observation network data as the reference is the main objective in this study. In this paper, the bias is defined as the difference between the radar-pixel values and the rain gauge corresponding values.

This paper is organized as follows. After Section 4.1 the methodologies implemented in this study, are described. Section 4.3 is then provided. Section four discusses the results. A short summary of the work, comparison of different scenarios and possible use of the method in practice is provider thereafter.

4.2 Methodology

Considering the value of each radar pixel representing its average rainfall amount occurring over a certain time and space, a large deviation between radar-pixel data and the accurate point-measurement devices like ordinary rain gauges can be detected. Because of this deviation, merging these two data sources might not be optimal, especially for the time steps where this deviation is highest. In the following, by implementing quantile mapping technique on the radar data, the radar image for each time step is corrected assuming that the spatial bias in the radar data dominates. In Section 4.3 part, the reasons for taking this assumption are discussed.

The methods, assumptions, and definitions used in this study are explained in this section.

4.2.1 Q-Q transformation

As described in several studies, the basic idea of this method is to correct one data source considering another data source as true by comparing their probability distribution functions. In this study, first theoretical distribution functions are fitted to the two data sources. Then, the

quantile for each radar pixel value is estimated (the data source which will be corrected) from its cumulative distribution function (CDF). Thereafter, by considering the estimated quantile and using the inverse CDF of observed station data, the radar-pixel value is replaced. As mentioned earlier the primary assumption is that the rain gauge network is providing true information. Eq. (4.1) formulates the correction procedure:

$$Z'_R(x,t) = F^{-1}_{obs,t}(F_{rad,t}(Z_R(x,t))) \tag{4.1}$$

where $Z_R(x,t)$ is the value of radar cell at position x and time t, $F_{rad,t}$ is the cumulative distribution function estimated from radar data at time t, and $F^{-1}_{obs,t}$ is the inverse cumulative distribution function derived from the rain gauge network at time t which converts the quantiles estimated by $F_{rad,t}$ back to rain intensities, $Z'_R(x,t)$. The inverse cumulative distribution function is estimated from observed rainfall data.

In contrast to conventional implementation of the quantile mapping method where a certain time period from the two data sources is considered, in this study the radar image is corrected for each time step separately. This means that each radar image is corrected independently. There are two general ways to estimate the quantiles for each value in a data source, either implementing an empirical distribution function or fitting a theoretical distribution function to the data and estimating the quantiles accordingly. Using empirical distribution functions introduces uncertainties when too few points from the data source exist. This problem could be solved by applying an interpolation method, e.g. linear interpolation, but estimating quantiles between the points which are located far from each other might be an unrealistic approach. Instead of implementing empirical distribution functions with unknown uncertainties introduced when an interpolation method is applied, it is decided to use a theoretical distribution function. Fig. 4.1 illustrates the method visually.

The first step is to choose the time steps to correct. For this, different criteria need to be considered. Since there is usually enough data from the radar data source, the time steps chosen for correction depend on: (a) the number of available stations for each time step and (b) the average rainfall recorded at the available stations. In order to increase the sample size from the rain gauge network (to decrease the uncertainty in CDF curve fitting) several time steps after and before the current time step will be considered. The number of time steps and a detailed explanation about the way the number of time steps is estimated are provided in Section 4.4. The second step is to fit a distribution function to the data. The method of moments
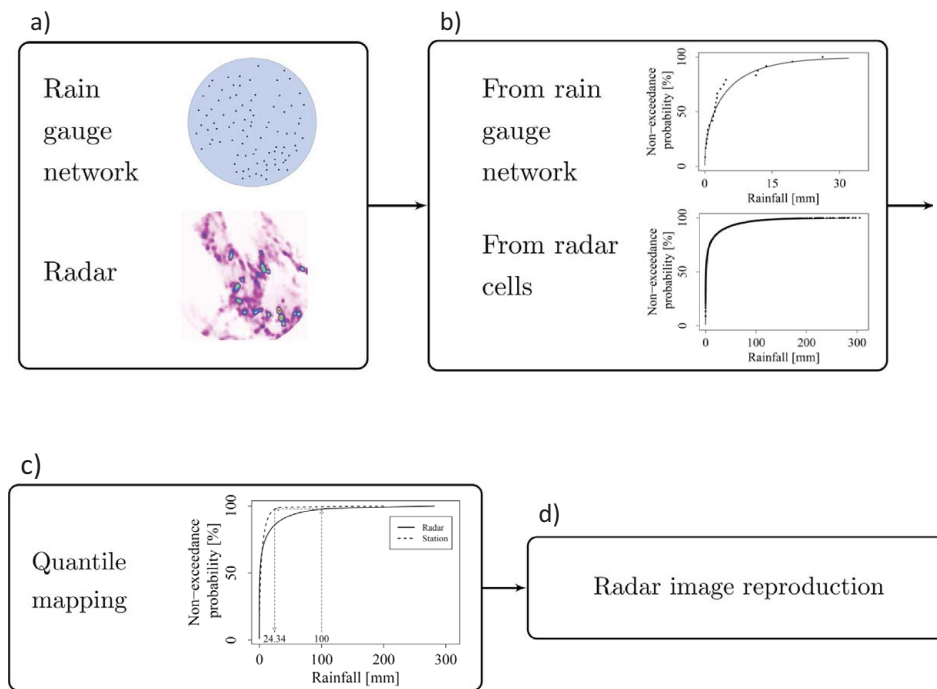
Figure 4.1: Different steps in correcting the radar data by quantile mapping. (a) Selecting the target time step, (b) fitting a cumulative distribution function to the data, (c) quantile mapping and (d) reproducing the radar data.

is implemented in this study. After fitting the distribution function to the data, each radar cell value is corrected by quantile mapping. The final step is to produce the radar image with the corrected values. As is clear from the described method, the locations of the maxima remain, however the values will change. In other words, the structure of the radar image does not change after implementing quantile mapping.

In contrast to the approach explained above, another way for implementing quantile mapping is when the distribution function is fitted for a certain time period. In this case, the distribution function parameters would be estimated either for each station separately or pooling the data of the stations i.e. a similar approach to THORNDAHL et al. (2014). Following this approach, there is a need to estimate the distribution function parameters for the points where no station is available from the observation points. Implementing interpolation techniques might be a possible solution for estimating the distribution function parameters for these points, which however introduces uncertainty to the work. This might lead to destruction of the radar image due to the following two reasons. Firstly, the bias is not dependent on the location of the stations (see Fig. 4.4).

This means that the distance from the radar origin to the observation points, or in general where the station is located, does not play an important role. Estimating the parameters from neighbouring stations might then lead to an incorrect distribution parameter set. Secondly, the radar cells are corrected independently. This means that the correction depends only on the distribution function derived from the rain gauge network and the radar cell value. This leads to increasing or decreasing radar cell values of a time step simultaneously which might result in changing the structure of radar image. It has been observed by VERWORN and HABERLANDT (2011) that applying a uniform non-linear attenuation correction does not improve merging performance using kriging with external drift. This indicates that the attenuation is not significant here. On the other hand, the latter point might result in changing the location of the maxima in the adar image as well.

4.2.1.1 Distribution function

As discussed, it is decided to fit a theoretical distribution function to the data instead of using an empirical distribution function. This decision is primarily based on the availability of the data. Instead, one might implement suitable interpolation technique for the time steps with less information, but this method introduces unpredictable uncertainties to the data. The gamma distribution function is used in the following:

$$F(Z(x,t);r,\lambda) = \frac{\lambda^r Z(x,t)^{r-1} exp(-\lambda Z(x,t))}{\Gamma(\alpha)}; \; Z(x,z) > 0 \qquad (4.2)$$

$Z(x,t)$ is the value of radar cell at position x and time t. For the CDF from radar data, $F_{rad,t}$ in Eq. (4.1), all the pixels of one time step are considered. On the other hand, for the rain gauge data several time steps are considered when estimating the CDF, $F_{obs,t}^{-1}$ in Eq. (4.1). The two parameters r and λ are determined using the Method of Moments.

All positive values are considered for fitting the theoretical distribution function and deriving the quantiles afterwards. The resolution of the rainfall data from rain gauge network is 0.1 mm/h and from radar data 0.01 mm/h. Radar rainfall is estimated using constant parameters for the reflectivity to rain intensity relationship. This relationship is explained in Section 4.3. In order to fit the CDFs to the rain gauge network data, all rainfall intensities larger than 0 mm/h are considered. For the radar data, different thresholds are defined meaning that values larger than the threshold are corrected and all values smaller than the threshold remain

unchanged. Five thresholds are considered: (a) 0.0 mm/h (b) 0.02 mm/h (c) 0.05 mm/h (d) 0.07 mm/h and (e) 0.1 mm/h. The reason for testing different thresholds is that the radar data contains very small values, of 0.01 mm/h, which is one-tenth of the smallest value of rain gauge network. Considering these below threshold values in quantile mapping would result in an overestimation of areal rainfall when estimated by radar and an underestimation when not. Under/over estimation of the applied method is investigated by comparing a radar cell with its corresponding station.

4.2.1.2 Temporal dependency of the station data

Due to a lack of data from the rain gauge network for some time steps, these time steps would not be corrected. This problem usually occurs when it rains strongly over a small area and the rest of the radar circle remains almost dry. Thus, it is necessary to increase the information from the rain gauge network by using more relevant time steps. As the main goal of this study is to correct each radar image separately, it would be inappropriate to use the rain gauge network information for longer periods of time. In order to investigate the temporal dependency, it is decided to use a temporal variogram (KITANIDIS, 1997). The empirical variogram is defined as follows:

$$\gamma_k(h) = \frac{1}{m} \sum_{k=1}^{m} \left[\frac{1}{2N(h)} \sum_{x_i - x_j = h} (Z(x_i) - Z(x_j))^2 \right] \tag{4.3}$$

where γ_k is the variogram averaged over all stations $k = 1, \ldots, m$, $N(h)$ represents the number of pairs separated by the vector h and Z the measured values at time x. As the temporal resolution of the rain gauge network data in this study is 1 h the separating vector (h) starts from 1 h.

The number of additional time steps to increase the information from the rain gauge network is estimated assuming that beyond the variogram range the data pairs become independent. In other words, the time length shorter than the variogram range is more likely to be representing time steps that could be considered for correcting a radar image. All calculations mentioned above are carried out using rainfall data for radar and gauges with 1 h temporal resolution.

4.2.2 Disaggregation of stations with daily data

BERNDT et al. (2014) showed that by increasing the rain gauge network density, the interpolation performance improves. Several studies tried to increase the rain gauge network density by combining the denser daily rain gauge network with the coarser hourly rain gauge network. For example, WALLNER et al. (2013) combined the daily rain gauge network by implementing a simple method of taking the nearest station and preserving its temporal pattern for disaggregating the daily stations. BÁRDOSSY and DAS (2008) analyzed the hydrological model performance as a function of the rain gauge density. They observed that the number and spatial distribution of rain gauges are influential in simulation results. In this study two methods are proposed: (a) using original radar data and (b) using radar data after bias correction. A daily time series from the radar-pixel corresponding to each station is extracted from the two sources mentioned above for testing disaggregation of daily gauge observations conditioned on radar data.

4.2.2.1 Disaggregation using radar data

Disaggregating daily rain gauge network data is carried out by using radar-pixel data. By extracting time series for the radar cells belonging to each station, the stations can be disaggregated:

$$Z_{dis}^h(i,t) = w(i,t) \times Z_{obs}^d(i,t) \text{ where } w(i,t) = \frac{Z_{rad}^h(i,t)}{\sum_{t=1}^{24} Z_{rad}^h(i,t)} \tag{4.4}$$

where w is the weight used for each time step, $Z_{dis}^h(i,t)$ is the disaggregated hourly value for time t and station i. $Z_{obs}^d(i,t)$ is the hourly rainfall intensity from the radar cell corresponding to the rain gauge and $Z_{obs}^d(i,t)$ is the observed daily station rainfall for disaggregation. Since the main objective of this paper is to investigate the influence of the bias correction method for different applications, two different radar data sources are compared (a) original radar data and (b) bias corrected radar data. Daily rain gauges are disaggregated by following the hourly fluctuation of radar-pixel data. In order to test the disaggregation, the rain gauge stations with hourly temporal resolutions are aggregated first to daily stations and then disaggregated back to hourly time steps following radar-pixel fluctuation.

4.2.3 Interpolation techniques

Accurate estimation of areal rainfall plays an important role in hydrological analyses. Areal rainfall is mainly estimated through interpolation techniques. The influence of radar data and bias correction methods on interpolation techniques is investigated by implementing radar data in two different methods, (a) conditional merging and (b) kriging with external drift. By comparing the results when using station data alone, the benefit of using radar data can be estimated. The performance of each interpolation method is investigated by means of cross validation.

Ordinary kriging (OK) is a standard interpolation method with the best linear unbiased estimator property (BLUE). This method is widely used in different studies for several datasets like temperature, wind, precipitation, soil properties etc. OK is considered as reference in this study to investigate the importance of the additional information from radar data and the importance of the radar data correction method. A detailed description of OK can be found in geostatistical textbooks such as ISAAKS and SRIVASTAVA (1990).

As the pre-requirement for all kriging methods, a theoretical semivariogram model is fitted to an experimental one using Eq. (4.3) $N(h)$ is the number of data pairs and in contrast to the earlier reference (in Section 4.2.1.2), h is the distance vector and x the location. Semivariograms are estimated for each season separately due to the assumption of seasonal changes in rainfall type. As a representative semivariogram for each season, the averaged semivariograms for all time steps within each season are used. In this study the year is split into two seasons, from March 21st to September 21st is considered as the summer time and winter from September 22nd to March 20th. Altogether, 11 semivariograms from January 2004 to January 2009 are estimated, fitted and employed for the interpolation. Radar data is used to estimate the experimental semivariograms. A set number of random radar-pixels (here 1000 points) for time steps with an average rainfall above a defined threshold are considered for estimating the season-specific experimental semivariogram. The average semivariograms are estimated by the following equation:

$$\gamma_{st}(h) = \frac{1}{n} \sum_{i=1}^{n} \frac{\gamma(h,i)}{var(i)} \tag{4.5}$$

where n is the number of time steps within the season, $\gamma_{st}(h)$ is the standardized variogram, $\gamma(h,i)$ is the calculated semivariogram for the distance vector of h and $var(i)$ is the variance

of time step *i*. The fitting procedure is carried out visually using an exponential theoretical variogram:

$$\gamma(h) = c_0 + c \left[1 - exp(-\frac{h}{a}) \right] \tag{4.6}$$

where *a*, *c*, and c_0 represent range, sill and nugget respectively. The objectivity of fitting experimental variograms visually is discussed by BERNDT et al. (2014).

4.2.3.1 Kriging with external drift

A common method for implementing additional information in interpolation procedures is kriging with external drift (KED). LIU et al. (2013) used a digital elevation model (DEM) as additional information for areal rainfall estimation whereas ROGELIS and WERNER (2013) used the effective elevation of a larger area. HABERLANDT (2007) proposed using radar data as the additional information in KED. BERNDT et al. (2014) implemented radar data and smoothed radar data as additional information which provided better results than using the original radar data alone. However it was also noted that the method is quite sensitive to radar data quality. By excluding time steps with poor radar data, the interpolation performance improved. Original radar data and bias corrected radar data are used here as additional information in KED to investigate the importance of bias in the correction method.

The fundamental principle of KED is the implementation of an additional variable $Y(x)$, assuming a linear relationship to the expected value of $Z(x)$.

$$E\left[Z(x)|Y(x)\right] = a + b \cdot Y(x) \tag{4.7}$$

As a result, the expected value is no longer constant over the study area. This is in contrast with the assumption taken for OK.

An important point in KED is the assumption of a linear relationship between the additional variable and expected value. This means that the performance depends more on how the two variables are correlated than the value of drift. For instance, VERWORN and HABERLANDT (2011) investigated the benefit of directly using radar reflectivity in KED and not derived rainfall intensity. They concluded that implementing log-transformation for radar reflectivities

improves the interpolation performance. More detailed information of the method could be found in GOOVAERTS (1997) and HABERLANDT (2007).

An important decision influencing the estimation of areal precipitation for kriging methods is the number of stations taken into account. The location of stations with available data also plays an important role. Since the number of stations and hence the network density varies between 2004 and 2008, it is decided to change the number of neighbours in the interpolation accordingly. As mentioned earlier, 11 time periods are defined assuming seasonal changes in rainfall type. Further information regarding the number of neighbours in interpolation for different time periods is provided in Section 4.3.

It is worth mentioning that the interpolation using KED might face numerical instabilities depending on the value of the additional information at the observation points. This problem can be solved by utilizing more stations in the interpolation process. Thus, in this study, the number of observations is first increased and if this is not possible, KED is replaced by OK for those time steps with numerical instabilities.

4.2.3.2 Conditional merging

Conditional merging (CM) is another method implemented in this study. It was first proposed by EHRET (2002) and later used by SINCLAIR and PEGRAM (2005) for rainfall field simulation. BERNDT et al. (2014) compared its performance with KED and concluded that CM performs better than KED for all station density scenarios and temporal resolutions used in their study. In contrast to KED, with the assumption of a linear relationship between the additional variable and expected value, no such assumption is necessary in CM. However the point-value in this method plays an important role. The main objective in CM is to preserve the radar pattern occurring between observation points. This is achieved by implementing OK on radar-pixel values first and then on observation points separately. Afterwards, the deviation between radar cells and interpolated values is applied on the rain gauge network OK result. Thus, these steps should be performed: (1) rainfall interpolation of observation points (rain gauges) by OK, (2) rainfall interpolation of radar-pixel data extracted for each station location by OK, (3) calculation of the deviation between radar cell values (original radar values for each cell) and rainfall interpolation of radar-pixel values on each radar cell and (4) applying the deviation (step 3) on the interpolated rainfall from observation points by OK (step 1) to produce the output image.

All the properties, such as variogram values, implemented in CM are the same as the ones used in OK.

4.2.4 Performance measures

4.2.4.1 Evaluation of radar data

Each station in the study area is located on a radar cell. In order to investigate the existence of bias, rain gauge data is compared with the corresponding radar-pixel data. The difference between the two sources illustrates the quality of radar data. As the sum of deviations might be close to zero (when underestimation and overestimation compensate each other), the root mean square error (RMSE) is considered as an appropriate measure of radar data quality. The RMSE is estimated for two scenarios (a) spatially and (b) temporally.

As the deviation between the observed values and radar-pixel values may change between stations, the RMSE value is estimated for each station separately and averaged over the number of time steps, called the temporal ($RMSE_t$) at station x (see Fig. 4.4):

$$RMSE_t(x) = \sqrt{\frac{\sum_{j=1}^{J}(Z(x,t_j) - Z_R(x,t_j))^2}{J}} \qquad (4.8)$$

where J is the number of time steps and $Z_R(x,t)$ and $Z(x,t)$ are the value of radar cell and rain gauge data at station x, respectively. The missing data are not considered for $RMSE_t$ estimation.

The spatial error is investigated by calculating the RMSE value for each time step over all stations, called the spatial RMSE ($RMSE_t$) (see Fig. 4.3). Here, n represents the number of stations with available data for each time step:

$$RMSE_s(t) = \sqrt{\frac{\sum_{i=1}^{n}(Z(x_i,t) - Z_R(x_i,t))^2}{n}} \qquad (4.9)$$

There are several factors like rain type and the existence of frozen particles (AUSTIN, 1987) which influence the quality of estimating rainfall from radar data when using constant param-

eters for transforming reflectivity to rain intensity (this relationship will be explained in the Subsection 4.3.1). As the rain type, or in general the type of precipitation, changes usually seasonally, investigation of $RMSE_s$ values for different time periods will illustrate the influence of rain type on the performance of radar data. On the other hand, investigation of temporal RMSE values ($RMSE_t$) will indicate whether the location of stations plays an important role in the bias magnitude.

The radar data quality before and after implementing bias correction is investigated by averaging the spatial $RMSE_s$ over all time steps, $RMSE_{\bar{s}}$. Besides, the average bias ($\bar{B}$) is also estimated:

$$\bar{B} = \frac{1}{J} \sum_{j=1}^{J} \left[\frac{1}{n} \cdot \sum_{i=1}^{n} \left[Z(x_i, t_j) - Z_R(x_i, t_j) \right] \right] \tag{4.10}$$

The average correlation coefficient ($\bar{R}$) is also estimated:

$$\bar{R} = \frac{1}{J} \sum_{j=1}^{J} \left[\frac{\sum_{i=1}^{n} (Z_R(x_i, t_j) - \bar{Z}_R(x_i, t_j))(Z(x_i, t_j) - \bar{Z}(x_i, t_j))}{\sqrt{\sum_{i=1}^{n} (Z_R(x_i, t_j) - \bar{Z}_R(x_i, t_j))^2 \sum_{i=1}^{n} (Z(x_i, t_j) - \bar{Z}(x_i, t_j))^2}} \right] \tag{4.11}$$

where n is the number of stations J is the number of time steps. Z and Z_R are the rain gauge data and the corresponding radar cell values, respectively.

More detailed information about the strength of temporal and spatial bias is provided in Section 4.3.

4.2.4.2 Evaluation of interpolation

The performance of the applied interpolation techniques is quantified by cross validation. The main goal is to estimate rainfall values on the observation points neglecting the observation value. Basically, one observation point is excluded from the dataset and the value for each time step is estimated using other available observation points. This procedure is performed for all the stations.The resemblance between the two time series, observed and estimated, is compared measured by the following criteria.

The root mean square error is estimated by:

$$RMSE_I = \frac{1}{J} \sum_{j=1}^{J} \left[\sqrt{\frac{\sum_{i=1}^{n} (Z(x_i, t_j) - Z^*(x_i, t_j))^2}{n}} \right] \tag{4.12}$$

The bias is estimated by:

$$B_I = \frac{1}{J} \sum_{j=1}^{J} \left[\frac{1}{n} \cdot \sum_{i=1}^{n} \left[Z(x_i, t_j) - Z^*(x_i, t_j) \right] \right]. \tag{4.13}$$

The preservation of variance is estimated by:

$$RVar = \frac{Var\left[Z^*(x,t)\right]}{Var\left[Z(x,t)\right]}. \tag{4.14}$$

The correlation coefficient is estimated by:

$$\bar{R} = \frac{1}{J} \sum_{j=1}^{J} \left[\frac{\sum_{i=1}^{n} (Z^*(x_i,t_j) - \bar{Z}^*(x_i,t_j))(Z(x_i,t_j) - \bar{Z}(x_i,t_j))}{\sqrt{\sum_{i=1}^{n} (Z^*(x_i,t_j) - \bar{Z}^*(x_i,t_j))^2 \sum_{i=1}^{n} (Z(x_i,t_j) - \bar{Z}(x_i,t_j))^2}} \right] \tag{4.15}$$

where Z^* is the rainfall estimation and Z is the rainfall observation. J and n are the number of time steps and number of stations considered in cross validation, respectively.

It is important to note that evaluating the performance of the bias correction method (see Section 4.2.1) is not carried out by means of cross validation because of the negligible influence of excluding a station on the final results.

4.3 Study area and data

The range of the weather radar located at Hannover airport describes the study area (Fig. 4.2), which is here a circle of 128 km radius. ll data is provided by the German Weather Service (DWD). Radar data has a temporal resolution of 5 min and rain gauge data are provided with 10 min temporal resolution. Both datasets are aggregated to an hourly temporal resolution. As

the *Z-R* relationship converts reflectivity to rainfall intensity in mm/h, aggregation of radar data is carried out by first dividing the values by 12 (as 12 time steps are considered) and then summing up the values for each pixel.
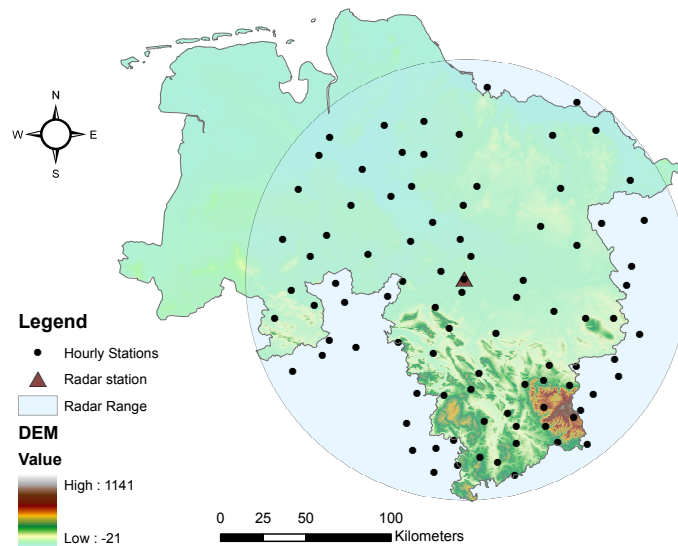
Figure 4.2: Study area and station network.

The number of stations and accordingly the density of rain gauge network for each time period (TP) is provided in Table 4.1. The main reason that different numbers are considered in crossvalidation is to avoid undesirable smoothening effect when stations are located with long distances to the interpolation point. As mentioned, the time periods are created considering seasonal variation of rainfall type.

Altogether, 105 stations with hourly temporal resolution are taken into consideration for this study. The transparent blue circle shows the area being scanned by the Hannover weather radar. In contrast to the flat northern part of the study area, the southern part contains the Harz Mountains with elevations of up to 1141 m a.s.l. The average annual precipitation varies within the study area, from around 500 mm/yr in the north-east part to around 1700 mm/yr in the Harz Mountains.

As mentioned earlier, in contrast to most studies where the quantile mapping is applied over a certain period of time, here Q-Q transformation is applied on each time step separately in order to correct a radar image. Considering the spatial rain variability of precipitation (see above), the benefit of applying quantile mapping on one time step instead of taking a certain

Table 4.1: Number of stations for each time period.

		1	2	3	4	5	6
Time	Start	Jan.04	Mar.04	Sep.04	Mar.05	Sep.05	Mar.06
period	End	Mar.04	Sep.04	Mar.05	Sep.05	Mar.06	Sep.06
Av. St.		23	34	43	49	57	64
No. St.		4	6	7	8	9	10
		7	8	9	10	11	
Time	Start	Sep.06	Mar.07	Sep.07	Mar.08	Sep.08	
period	End	Mar.07	Sep.07	Mar.08	Sep.08	Jan.09	
Av. St.		74	80	88	91	93	
No. St.		10	10	10	11	11	

*Av. St and No. St represent the number of available observation points and the number of stations used in cross-validation, respectively.

time period becomes evident. In other words, as the average annual precipitation varies in the study area significantly, applying the Q-Q transformation temporally (separately for each station) may result in destroying the structure of radar image. Additionally, there might be some other technical difficulties when convective rainfall occurs as some stations may have no rainfall recorded over a certain time. Further discussion on the benefits of implementing this method on each time step separately is provided in Section 4.4.

Assuming the rainfall type changes seasonally, the entire time period is divided into 11 time periods where each time period has its specific variogram properties. Table 4.1 provides the number of stations with available data (Av. St.) and the number of stations used in cross-validation (No. St.) for each defined time period with no constrains for the search radius. The properties of variograms implemented in this study is provided in Section 4.4.

4.3.1 Radar data

The C-band radar instrument located in Hanover has a 5-min temporal resolution and an azimuth resolution of 1°. The spatial resolution along each beam is 1 km. In this study, the dx-radar product provided by the German Weather Service (DWD) is used. Considering 128 km as the radius of the circle being scanned by the radar instrument, each radar image contains 46080 (128×360) cells. The reflectivity provided by DWD is transformed to rain intensity using the following *Z-R* relationship:

$$Z_r = a \cdot Z_R^b \qquad\qquad (4.16)$$

where Z_r is the reflectivity in $mm^6 m^{-3}$, and Z_R is the corresponding rain intensity in mm/h. The reflectivities are transformed using the standard DWD parameter set (RIEDL, 1986; SELTMANN, 1997), with $a = 256$ and $b = 1.42$. After estimating rainfall intensity, a clutter map for each month is estimated following the principles proposed by BERNDT et al. (2014). Radar cells with the rainfall sum outside of the defined acceptable range are considered as clutters. In contrast to Berndt et al., here the clutters are detected for each month separately and a clutter map is produced for each year accumulating all the cells detected in all months of the year. Subsequently, an interpolation on rectangular grid is carried using inverse distance interpolation to produce 1 km $\times$ 1 km grid cells.

4.3.2 Temporal and spatial bias in radar data

The temporal and spatial bias is analysed using Eqs. 4.8 and 4.9. As mentioned earlier, the spatial bias is analysed by estimating the RMSE for each time step. This means that the observation data from the rain gauge network is compared with the corresponding radar cell for each time step. Figs. 4.3 and 4.4 illustrate the existence of spatial and temporal bias respectively.

Black lines in Fig. 4.3 illustrate the hourly RMSE_s value for each year and the average during five years. Spatially averaged bias between the radar-pixel data and station data is estimated considering time steps in which rain is recorded from either data source. The highest spatial RMSE_s values mostly occur in summer. The red line in Fig. 4.3 indicates the temporal variation of average rainfall. Here, the average rainfall (arithmetic mean) is estimated by taking only stations with recorded rainfall into consideration. This value increases in summer, showing that intensive rainfall occurs mainly over a lower number of stations. Thus, this indirectly indicates the rainfall type. Convective rain events or possible sudden storms can be easily distinguished as they usually cover a smaller area with high intensity. The parts of red lines with higher values indicate intense rain events covering lower number of stations. On the other hand, rainfall events in winter are usually less intense and cover a larger area. Assuming the values of average rainfall (red line in Fig. 4.3) are an indicator of rain type, the bias seems to be strongly dependent on the rain type.
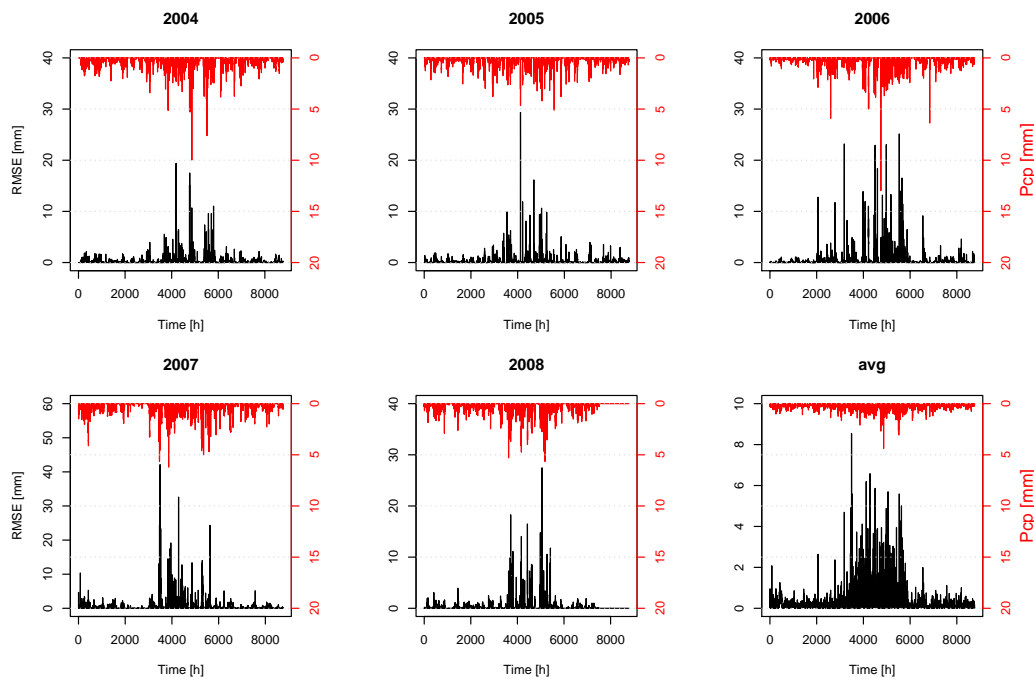
Figure 4.3: Black line (the lower line): temporal distribution of spatial RMSE$_s$ over the study area, red line (the upper line): temporal variation of average rainfall considering only stations with recorded rainfall for 2004, 2005, 2006, 2007, 2008 and averaged over five years.

Beside spatial bias, radar data are subject to temporal bias as well. In order to investigate the existence of temporal bias, a similar method to the spatial bias investigation is considered. In contrast to spatial bias where the RMSE was estimated for each time step separately, here the RMSE value is estimated for each year and each station separately. Thus, each station (observation point) receives a value for each year. Fig. 4.4 illustrates the spatial distribution of the temporal bias over the study area where the Inverse Distance Weighted (IDW) method is used for producing this figure.

Like spatial bias investigation, temporal bias is investigated considering the time steps in which the rain amount from both of the sources is not missing. The points in Fig. 4.4 represent the stations considered for each year. The darker cells illustrate higher RMSE values. Comparing the spatial distribution of temporal RMSE among the years, the locations of high bias value do not remain constant in space over different years. By comparing Figs. 4.3 and 4.4, it can be concluded that although temporal bias exists, the spatial bias (magnitude and variation) is much stronger and more straightforward to handle.
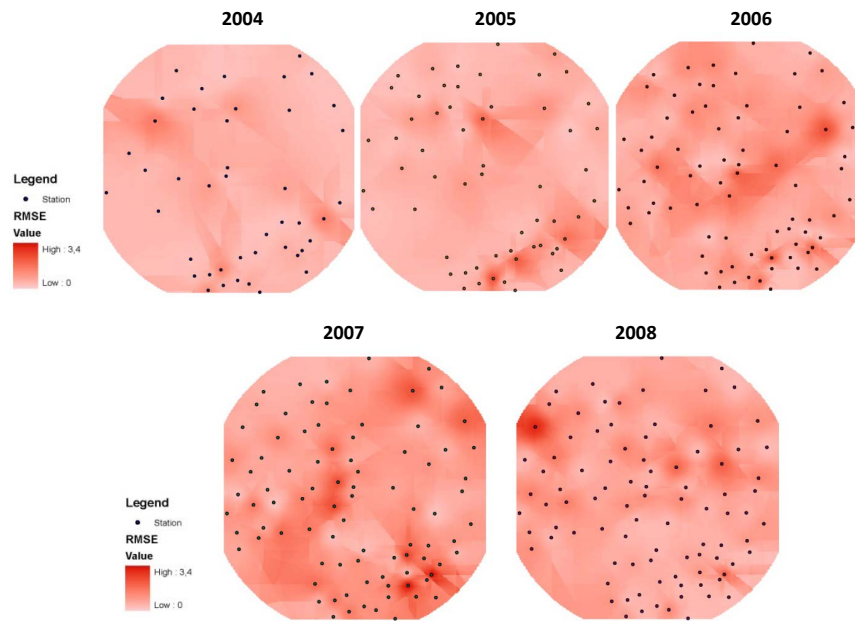
Figure 4.4: Spatial distribution of yearly average temporal RMSEt over the study area, each year separately.

4.4 Results and discussion

The main objective of this study is to investigate the performance of interpolation techniques using radar data before and after bias correction by means of cross validation. Before illustrating the interpolation performance, the quality of the radar data is compared with observation points. Finally, the use of radar data for disaggregation purposes is also investigated in this study.

4.4.1 Time window considered for bias correction

Some time steps cannot be corrected due to the lack of data from the rain gauge network. This problem usually occurs when it rains strongly over a smaller area and the rest of the radar circle stays almost dry. Thus, the goal in this part is to increase the information from the rain gauge network by using adjacent time steps from the rain gauge network for the purpose of fitting the distribution function. The number of required time steps is determined by assuming that the variogram range represents the time length having independent data pairs. Fig. 4.5 illustrates the estimated temporal variogram for each of the five years averaged over the stations.

Fitting the theoretical variogram to the empirical variogram is carried out visually. The ranges
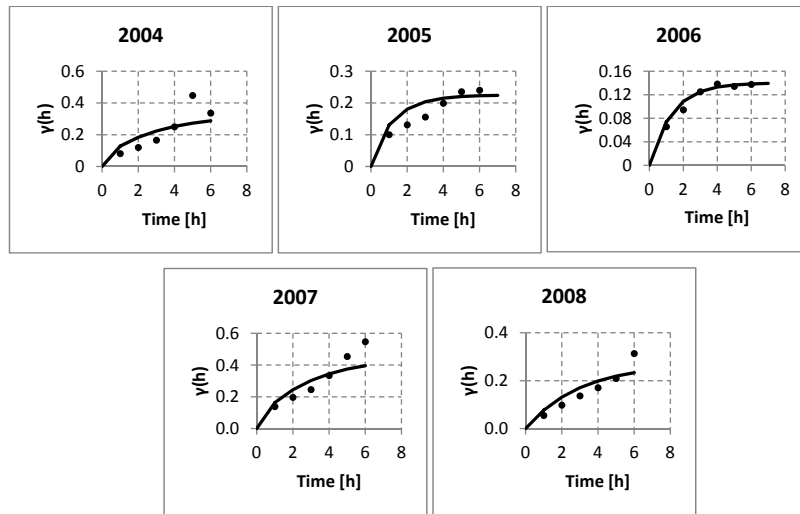
Figure 4.5: Temporal variogram estimated for each year separately.

estimated for the temporal variograms are between 4 and 9 h for the years 2004-2008. It is assumed that the time steps within 6 h are likely to be dependent. Thus, besides the current time step, 3 time steps before and 3 time steps after are considered to increase the number of observation points from the rain gauge network.

4.4.2 Radar data analysis before and after bias correction

In order to analyse the radar data quality, observation points from the rain gauge network are compared with the corresponding radar pixels. The quality of radar data is described by bias ($\bar{B}$), RMSE ($\text{RMSE}_{\bar{s}}$), and correlation coefficient ($\bar{R}$) which are provided in Table 4.2. The seasonal average value of each statistical measure is also provided in Table 4.2. Different thresholds are considered for selecting the radar pixels for the bias correction process. For instance, if the threshold is set to 0 all the radar cells having values greater than 0 will be considered. Five classes, BC1-BC5, with different defined thresholds 0.00, 0.02, 0.05, 0.07 and 0.10 mm/h are considered.

For evaluating the rainfall estimation by radar no such thresholds are defined meaning that all the time steps with available data from both data sources are considered in order to estimate the statistical measures given in Table 4.2. As discussed earlier, the bias (B) is not necessarily a

Table 4.2: Radar data quality before and after implementing bias correction, considering different thresholds 0.00, 0.02, 0.05, 0.07 and 0.10 mm/h, from BC1 to BC5.

Time period		1 Win.	2 Sum.	3 Win.	4 Sum.	5 Win.	6 Sum.	7 Win.
Original	$\bar{B}$	-0.06	-0.01	-0.05	0.00	-0.03	0.03	-0.01
radar	$RMSE_{\bar{s}}$	0.31	0.66	0.28	0.81	0.32	1.12	0.43
	$\bar{R}$	0.64	0.67	0.61	0.65	0.62	0.64	0.68
	$\bar{B}$	0.02	0.06	0.02	0.06	0.03	0.06	0.04
BC1	$RMSE_{\bar{s}}$	0.28	0.46	0.24	0.40	0.23	0.51	0.30
	$\bar{R}$	0.71	0.76	0.76	0.78	0.75	0.71	0.77
	$\bar{B}$	-0.02	0.02	-0.02	0.02	-0.01	0.03	0.01
BC2	$RMSE_{\bar{s}}$	0.26	0.4	0.23	0.35	0.21	0.44	0.27
	$\bar{R}$	0.72	0.78	0.74	0.79	0.75	0.74	0.78
	$\bar{B}$	-0.04	0	-0.04	0	-0.02	0.01	-0.01
BC3	$RMSE_{\bar{s}}$	0.27	0.39	0.24	0.33	0.21	0.42	0.26
	$\bar{R}$	0.7	0.78	0.71	0.8	0.74	0.74	0.78
	$\bar{B}$	-0.05	-0.01	-0.04	-0.01	-0.02	0	-0.02
BC4	$RMSE_{\bar{s}}$	0.27	0.39	0.25	0.33	0.21	0.41	0.26
	$\bar{R}$	0.68	0.77	0.69	0.79	0.74	0.74	0.77
	$\bar{B}$	-0.05	0	-0.04	0	-0.02	0.01	-0.01
BC5	$RMSE_{\bar{s}}$	0.28	0.4	0.25	0.33	0.21	0.46	0.27
	$\bar{R}$	0.67	0.77	0.67	0.8	0.73	0.73	0.77

Time period		8 Sum.	9 Win.	10 Sum.	11 Win.	μ Sum.	μ Win.
Original	$\bar{B}$	0.02	-0.05	0.01	-0.04	-0.04	0.01
radar	$RMSE_{\bar{s}}$	1.48	0.33	0.94	0.26	0.32	1
	$\bar{R}$	0.59	0.68	0.67	0.74	0.66	0.64
	$\bar{B}$	0.08	0.03	0.06	0.03	0.03	0.06
BC1	$RMSE_{\bar{s}}$	0.56	0.29	0.46	0.22	0.26	0.48
	$\bar{R}$	0.79	0.77	0.78	0.83	0.77	0.76
	$\bar{B}$	0.03	-0.01	0.02	-0.01	-0.01	0.02
BC2	$RMSE_{\bar{s}}$	0.5	0.27	0.38	0.2	0.24	0.41
	$\bar{R}$	0.8	0.78	0.81	0.82	0.77	0.78
	$\bar{B}$	0.01	-0.02	0	-0.03	-0.03	0
BC3	$RMSE_{\bar{s}}$	0.48	0.27	0.37	0.21	0.24	0.4
	$\bar{R}$	0.8	0.77	0.81	0.79	0.75	0.79
	$\bar{B}$	0	-0.03	0	-0.03	-0.03	0
BC4	$RMSE_{\bar{s}}$	0.47	0.27	0.36	0.22	0.25	0.39
	$\bar{R}$	0.8	0.76	0.81	0.78	0.74	0.78
	$\bar{B}$	0.01	-0.03	0	-0.03	-0.03	0
BC5	$RMSE_{\bar{s}}$	0.48	0.27	0.37	0.22	0.25	0.41
	$\bar{R}$	0.8	0.75	0.81	0.77	0.73	0.78

good criterion to represent the quality of the radar data. The main reason is that the rainfall over-estimation and underestimation by radar may occur during the time period under investigation which may have a cancelling effect. As can be seen, the B does not change significantly after implementing bias correction while the other two criteria change considerably. The correlation coefficient (R) measures the linear association between the two sources and becomes higher for all defined time periods when bias correction is applied. This shows that the linearity increases after implementing the bias correction method. As in KED where the linearity plays an important role, it could be expected that implementing radar data after correction results in improving the interpolation performances. Also, the $RMSE_{\bar{s}}$ improves after implementing bias correction. In general, the quality of the radar data improved as the deviation between the two sources decreased.

As the rain gauges have a measurement accuracy of 0.1 mm and the values derived from radar have a 0.01 mm resolution, considering all radar cells in bias correction may lead to rainfall overestimation. From the five defined thresholds, one threshold is selected for further analysis according to its performance. Although in general the radar quality improves after implementing bias correction, the results in Table 4.2 show a minor improvement when considering 0.05 mm/h as the threshold comparing with other examined thresholds. Therefore, bias correction will be implemented in interpolation techniques (see Section 4.4.4) by considering 0.05 mm/h as the threshold.

The improvement of radar data quality in summer is more noticeable than in winter. This could be expected as the RMSE value before bias correction was higher in summer (see Section 4.3.2).

4.4.3 Interpolation performance

Before discussing the interpolation performance, the effect of implementing bias correction on theoretical variogram parameters is first presented.

Table 4.3 illustrates the parameters of theoretical variogram before and after implementing bias correction. Although there is a minor influence on the sill (c_c) and nugget effect (c_0), the effect on the effective range (a_{eff}) is greater. As expected, implementing bias-correction results in smoothening radar data where the effective range gets larger after implementing bias correction.

Table 4.3: Theoretical variogram model parameters before and after implementing bias correction, a_{eff} is the effective range, c_c the sill and c_0 the nugget effect.

		Time period										
		1	2	3	4	5	6	7	8	9	10	11
Original	$c_0(-)$	0.05	0	0	0	0	0.1	0	0.05	0.05	0.05	0
radar data	$c_c(-)$	1.25	1.05	1.25	1.05	1.23	0.93	1.15	0.95	1.15	0.95	1.06
	$a_{eff}(km)$	75	45	75	45	75	39	69	45	69	42	75
Bias-corrected	$c_0(-)$	0	0	0	0	0	0.05	0	0	0	0	0
radar data	$c_c(-)$	1.3	1.05	1.2	1.05	1.2	1	1.1	1	1.2	1	1.1
	$a_{eff}(km)$	90	54	75	57	81	51	75	60	75	54	90

The performance of each interpolation technique is investigated by means of cross validation considering only time steps with a significant amount of rainfall. Thus, after excluding time steps with zero average value, only time steps having an average value higher than 95th percentile of all time steps are considered in estimating the statistical measures resulting in 1055 time steps in total. As explained earlier, in order to analyse the performance of each interpolation technique using different sources of data, 0.05 mm/h is considered as the threshold for applying bias correction for radar data (see Section 4.4.2).

BERNDT et al. (2014) discovered that conditional merging performs better than KED. In this study, the main objective is to analyze the sensitivity of the two methods to radar data quality.
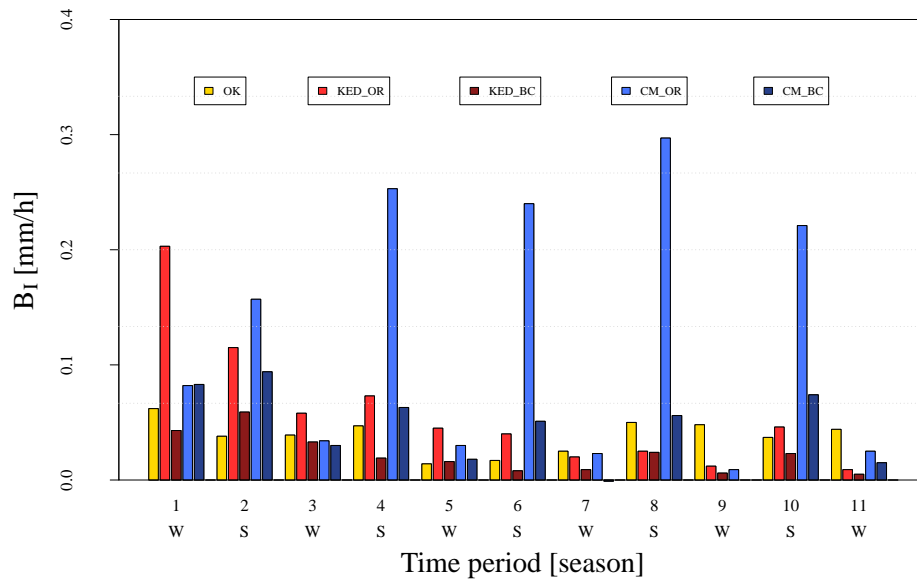
Figure 4.6: Cross validation results, averaged bias over all stations and all considered time steps. W: Winter, S: Summer, OK: ordinary kriging, KED_OR: kriging with external drift using original radar data, KED_BC: kriging with external drift using bias corrected radar data, CM_OR: conditional merging using original radar data and CM_BC: conditional merging using bias corrected radar data. (The order of the bars is as mentioned in this caption.)

Fig. 4.6 illustrates the B_I criterion for all 11 defined time periods. As expected, OK performs consistently well regardless of season. In contrast to OK, all the methods using radar data as the additional information are strongly dependent on radar data quality. As can be clearly seen, the radar data quality is more significant when implementing CM. It is also clearly visible that the interpolation performance improved when using radar data after bias correction. On the other hand, as the number of stations changes over time, the interpolation performance (each season separately) is shown to improve when implementing more stations (the number of stations for each time step is provided in Table 4.1).
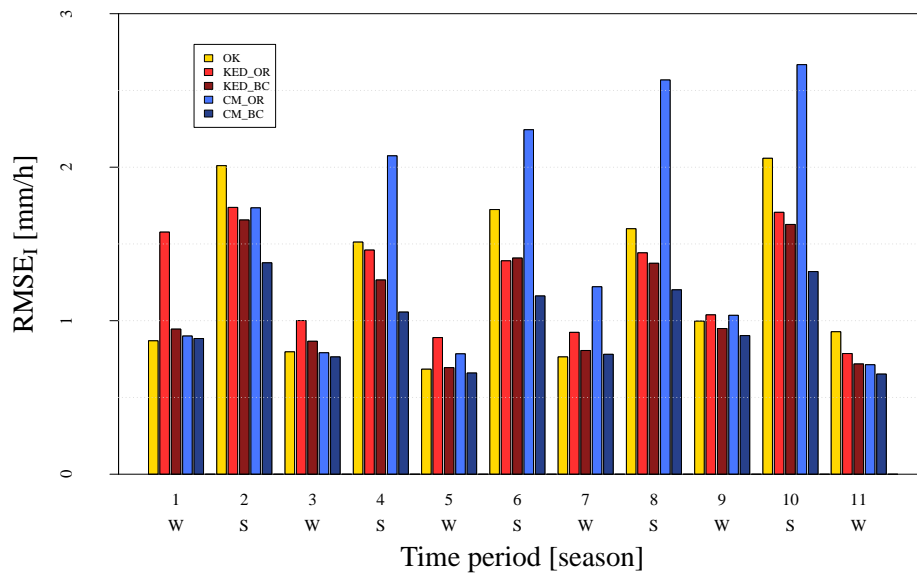
Figure 4.7: Cross validation results, averaged RMSE over all stations and all considered time steps. W: Winter, S: Summer, OK: ordinary kriging, KED_OR: kriging with external drift using original radar data, KED_BC: kriging with external drift using bias corrected radar data, CM_OR: conditional merging using original radar data and CM_BC: conditional merging using bias corrected radar data. (The order of the bars is as mentioned in this caption.)

Fig. 4.7 illustrates the estimated $RMSE_I$ for all 11 defined time periods and interpolation techniques implemented in this study. The interpolation performance changes seasonally for all the implemented techniques. In general, the interpolation performance is better in winter which shows the dependency of the interpolation performance on rainfall type (see Section 4.3.2).

The $RMSE_I$ improves when using radar data after implementing bias correction as was for the bias criterion in Fig. 4.6. VERWORN and HABERLANDT (2011) found that implementing radar data in summer is more significant. The same can be concluded here, with KED using original radar data performing better than OK in summer. On the other hand, KED after bias correction performs better in winter than in summer, which again illustrates the importance of radar data quality. Fig. 4.3 showed that radar data quality is better in winter time. The sensitivity of CM to radar data quality is greater when comparing the results with KED. It is evident that KED performs better than CM when implementing the original radar data. In contrast, the performance of CM is superior to KED when implementing bias corrected radar data. BERNDT et al. (2014) also concluded that CM performs better when excluding poor radar data quality.

Although the interpolation performance is better for winter, the use of radar data in summer is more significant. Also, the improvement in radar data quality in summer is more noticeable than

for winter. This illustrates the importance of applying bias correction, especially in summer.
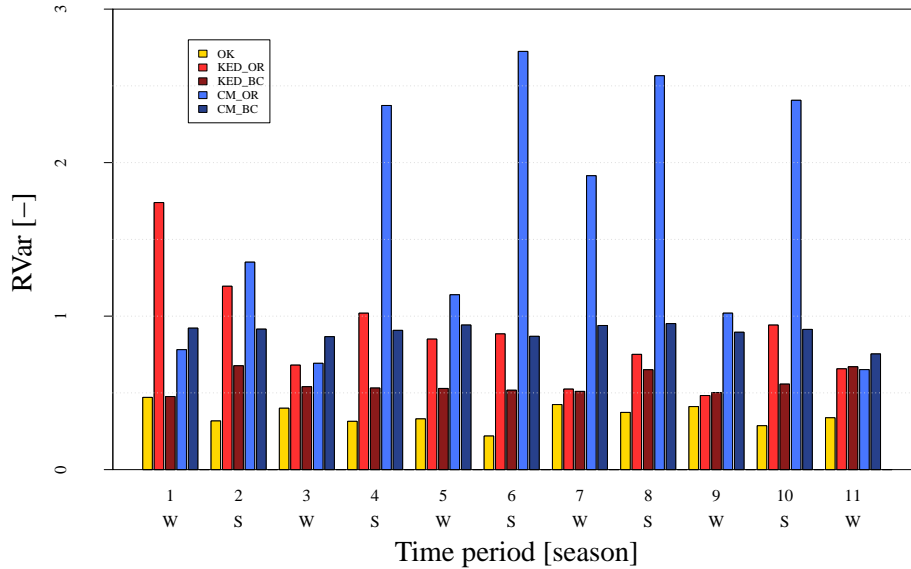
Figure 4.8: Cross validation results, averaged RVar over all stations and all considered time steps. W: Winter, S: Summer, OK: ordinary kriging, KED_OR: kriging with external drift using original radar data, KED_BC: kriging with external drift using bias corrected radar data, CM_OR: conditional merging using original radar data and CM_BC: conditional merging using bias corrected radar data. (The order of the bars is as mentioned in this caption.

Fig. 4.8 illustrates the RVar criterion representing the preservation of variance of the observations. The closer the value is to 1, the better the variance is preserved. Interpolation usually has smoothening effect and often a value smaller than 1 is expected. A value larger than 1 indicates more variability of rainfall estimation compared with nature. This can only happen when outliers from radar influence the interpolation performance. This phenomenon is more obvious when implementing CM representing the importance of radar data quality in this method.

As seen previously, CM fails when implementing original radar data compared with KED. Although in some time periods KED is closer to 1, in general CM performs better when implementing bias corrected radar data.
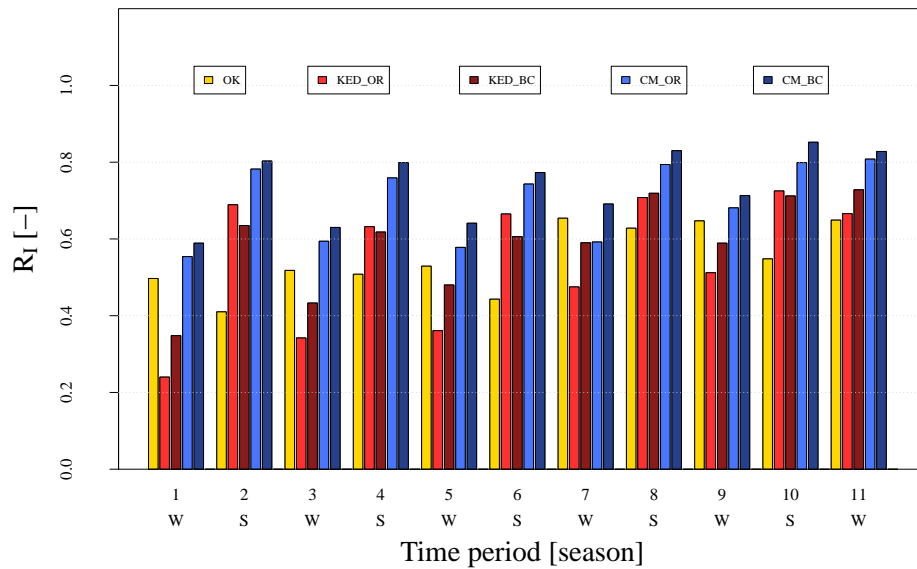
Figure 4.9: Cross validation results, averaged correlation coefficient over all stations and all considered time steps. W: Winter, S: Summer, OK: ordinary kriging, KED_OR: kriging with external drift using original radar data, KED_BC: kriging with external drift using bias corrected radar data, CM_OR: conditional merging using original radar data and CM_BC: conditional merging using bias corrected radar data. (The order of the bars is as mentioned in this caption.)

Fig. 4.9 illustrates the correlation coefficient estimated for each interpolation technique. CM using bias corrected radar data performs better than all the other interpolation techniques. R_I helps comparing the performance of interpolation techniques in which the $RMSE_I$ is similar. The estimated $RMSE_I$ in winter time is similar for different interpolation techniques, especially for the 1st, 3rd and 5th time period.

It could be concluded that CM is more sensitive toward the quality of radar data when comparing the results before and after bias correction. On the other hand, the best performance was CM after implementing bias correction of the radar data.

4.4.4 Evaluation of disaggregated station data against radar data

Table 4.4: Disaggregating daily stations using radar data.

Time period		1 Win.	2 Sum.	3 Win.	4 Sum.	5 Win.	6 Sum.
Original	Bias	0.00	0.00	0.00	0.00	0.00	0.00
Radar	RMSE	0.24	0.29	0.22	0.24	0.19	0.26
	R	0.79	0.88	0.81	0.89	0.83	0.87
BC3	Bias	0.00	0.00	0.00	0.00	0.00	0.00
	RMSE	0.26	0.26	0.24	0.23	0.18	0.25
	R	0.76	0.88	0.78	0.89	0.82	0.87

Time period		7 Win.	8 Sum.	9 Win.	10 Sum.	11 Win.
Original	Bias	0.00	0.00	0.00	0.00	0.00
Radar	RMSE	0.23	0.35	0.25	0.27	0.20
	R	0.85	0.89	0.83	0.90	0.85
BC3	Bias	0.00	0.00	0.00	0.00	0.00
	RMSE	0.21	0.30	0.24	0.24	0.21
	R	0.85	0.90	0.83	0.90	0.84

As discussed earlier, in addition to investigating the influence of bias correction on interpolation performance, original radar data and bias-corrected radar data are used for disaggregating daily stations. The disaggregation performances is investigated by first aggregating the hourly stations to daily time steps and then disaggregating back to hourly time steps using original and bias-corrected radar data. The main advantage of using rain gauges with hourly temporal resolution is the availability of hourly fluctuation from rain gauges meaning that the disaggregated time series would be evaluated by observed time series. Table 4.4 provides details on disaggregating daily stations once by original radar data and once by radar data after implementing bias correction. The statistical measures are estimated considering the observation data as true.

Disaggregating daily station rainfall with radar data shows a better performance when compared against cross validation results from interpolation (comparing with Table 4.4 and Fig. 4.9). For instance, the *R* is usually larger than 0.8 in Table 4.4 whereas it hardly reaches 0.8 in Fig. 4.9. The same is valid for the RMSE where larger values were obtained by the cross validation. In contrast to the radar data quality investigation for interpolation (Section 4.4.2) where there exists a significant improvement after implementing the bias correction method, the performance of disaggregating daily stations is not significantly influenced when implementing radar data after bias correction. The main reason is that the disaggregation using different radar

products does not change the daily rainfall amount but only the contribution for each hourly time step. Thus, the final result is not significantly influenced by the quality of radar data rainfall estimation, but more the correct temporal patterns of the radar data for each station. As the lower values are also influence by the bias correction method, i.e. leading to higher weights than needed, this might result in minor deterioration of the disaggregation results. In general, it can be concluded that using radar data is an important source for disaggregating daily stations as the density of non-recording stations is often higher than recording stations.

4.5 Summary and conclusion

The main objective of this study was to introduce a new method for correcting radar data. The radar data quality is investigated seasonally by means of the spatial RMSE between radar and station data. Implementing a simple quantile mapping method on each time step was proposed for correcting radar images considering rain gauge data as true. Radar data is implemented for areal rainfall estimation by two interpolation techniques, *conditional merging* and *kriging with external drift*. The importance of using radar data in the interpolation is investigated by comparing the performance when no radar data is considered, i.e. using the *ordinary kriging* method. Additionally, radar data was also considered for disaggregation of daily stations.

The results and findings of this study are summarized as follows:

1. The quality of radar data is improved after implementing the bias correction method. Since the method used in this study is applied on each time step separately, the number of observation data points from the station network might be insufficient. As a result, in order to correct a radar image, 3 time steps before and after the current time step are taken into account for station data to create a meaningful Q-Q transform relationship (7 time steps altogether).

2. It has been shown that radar data is a useful source for disaggregation purposes, but the influence of correcting radar data on disaggregation performance is insignificant.

3. The radar data quality changes seasonally. By comparing the radar-pixel data with observation values, it has been observed that the radar data has a better quality in winter compared to summer.

4. A seasonal variation in interpolation performances is also observed. All the interpolation

techniques perform better in winter than in summer. It can be justified when considering the fact that rainfall types change mostly seasonally.

5. In general using radar data improves the interpolation performance in summer, despite better interpolation performance in winter. On the other hand, the improvement of radar data quality after applying bias correction is more significant for summer rainfall events. It can thus be concluded that applying the bias correction method is more important for summer.

6. Beside the improvement of radar data quality after implementing bias correction, the interpolation performance also improved when using bias corrected radar data compared to using original radar data. Although CM showed greater sensitivity to radar data quality, CM performed better than KED when implementing bias corrected radar data.

The seasonal variation observed in the results may be due to the seasonal variation of rainfall type. Convective rain events occur mostly in summer and stratiform rain events in winter. In general, CM using bias corrected radar data performed better than all the other implemented interpolation techniques, although a seasonal variation in performance exists.

An important difference between the proposed method in this study and other similar studies (e.g. the method proposed by THORNDAHL et al., 2014) is that this study corrects each radar image, individually. Although THORNDAHL et al. (2014) have taken a constant mean field bias to correct the radar data which conserves the radar data structure, the performance of this correction is dependent on the time interval considered for the mean bias estimation. This phenomenon is not evident when using the method proposed in this study since no such time interval is considered for bias correction. It should be emphasized again that instead of considering different parameter sets for different types of rainfall, e.g. in CHUMCHEAN et al. (2006), the method presented in this study considers non-stationarity in radar-rainfall relationships indirectly. This is due to the fact that radar data is being corrected for each time step considering a new rain gauge data as true and under/over estimation of rainfall is compensated accordingly.

The method presented in this study is an offline calibration considering the presumptions explained earlier. This is due to the fact that in order to increase the sample size from the station network, a couple of time steps before and after the current time step are considered. Although depending on the number of time steps, one may consider the method as a close to real-time approach. Further investigations might help for real-time assimilation approaches if,

for example, similar CDFs could be observed for certain events.

Although this method is implemented in Lower Saxony, the same results might be derived in other study areas. Further investigation is required for investigating the influence of implementing bias correction for practical purposes such as hydrological modelling.

Acknowledgements

Chapter 5

Rainfall estimation using moving cars as rain gauges - laboratory experiments

Abstract

The spatial assessment of short time-step precipitation is a challenging task. Low density of observation networks, as well as the bias in radar rainfall estimation motivated the new idea of exploiting cars as moving rain gauges with windshield wipers or optical sensors as measurement devices. In a preliminary study, this idea has been tested with computer experiments (HABERLANDT and SESTER, 2010). The results have shown that a high number of possibly inaccurate measurement devices (moving cars) provide more reliable areal rainfall estimations than a lower number of precise measurement devices (stationary gauges). Instead of assuming a relationship between wiper frequency (W) and rainfall intensity (R) with an arbitrary error, the main objective of this study is to derive valid (W-R) relationships between sensor readings and rainfall intensity by laboratory experiments. Sensor readings involve the wiper speed, as well as optical sensors which can be placed on cars and are usually made for automating wiper activities. A rain simulator with the capability of producing a wide range of rainfall intensities is designed and constructed. The wiper speed and two optical sensors are used in the laboratory to measure rainfall intensities, and compare it with tipping bucket readings as reference. Furthermore, the effect of the car speed on the estimation of rainfall using a car speed simulator device is investigated. The results show that the sensor readings, which are observed from manual wiper speed adjustment according to the front visibility, can be considered as a strong indicator for rainfall intensity, while the automatic wiper adjustment show weaker performance. Also the sensor readings from optical sensors showed promising

results toward measuring rainfall rate. It is observed that the car speed has a significant effect on the rainfall measurement. This effect is highly dependent on the rain type as well as the windshield angle.

5.1 Introduction

Accurate spatial precipitation assessment for short time steps has been of research interest for some time. However, due to its high variability in time and space, rainfall observation is still a challenging task. For instance, SCHILLING (1991) has discussed the need for higher resolution data with 1 min time resolution and 1 km^2 spatial resolution in urban hydrology. Recent developments regarding modern instrumentation of recording gauges as well as the implementation of weather radar revealed a bright prospect for estimation of areal precipitation in short time steps. Recording gauges provide valuable point rainfall depths, but these are still often poor in density. Weather radar has become an essential source for rainfall estimation. For example, CHANDRASEKAR et al. (2012) showed the importance of high-resolution rainfall data using a X-band radar network for urban flash flood application. Despite its high spatial resolution, radar data has often a large space-time variable bias in rainfall estimation (JAVIER et al., 2007). There are several innovative methods which discuss new measurement techniques for rainfall intensity such as satellites (DIOP and GRIMES, 2003), microwave links (UPTON et al., 2005), and acoustic rain gauges (JONG, 2010). LEIJNSE et al. (2007) and MESSER et al. (2006) are the pioneers in using radio links from cellular communication networks for rainfall measurement purposes. This is quite a new way of measuring rainfall and has been under study by several researchers recently (OVEREEM et al., 2013; ZINEVICH et al., 2009). Most of the mentioned methods seek to use alternative devices which were intended originally for other purposes. JONG (2010) has also developed a low cost disdrometer to make measuring rainfall affordable with a very high spatial and temporal resolution.

The combination of data from different sources can improve the estimation of areal rainfall. For instance HABERLANDT (2007) and HABERLANDT and SESTER (2010) implemented kriging with external drift in order to combine radar data with rain gauge network data. EHRET (2002) applied another method for merging radar data with rain gauge data, called conditional merging. Other approaches for merging radar data with rain gauge data were suggested by ERDIN et al. (2012) and VOGL et al. (2012).

The idea of using moving cars as rainfall measurement devices was proposed for the first time

by HABERLANDT and SESTER (2010). They use wiper speed (*W*) as an indication of rainfall rate (*R*) by applying a hypothetical (*W-R*) relationship with an assumption about the rainfall rate estimation error. A traffic model has been applied to generate car trajectories on roads in a river basin. Radar data has been used as reference rainfall to evaluate the work. The rain rate for rain gauges and moving cars has been extracted from the radar data. Afterwards, the results of assessing areal rainfall by implementing ordinary kriging for rain gauges and indicator kriging for moving cars have been compared. These results show that a large number of inaccurate measurement devices would improve the spatial precipitation assessment in comparison to a couple of accurate devices. Besides, this new rainfall information will provide a good possibility to use this data for merging with other sources of data like radar or station data.

The main objective of this study is to develop and analyze the relationships between sensor readings (*W*) and rainfall intensity (*R*) by laboratory experiments. Sensor readings in this paper involve wiper speed, which is controlled either manually by a driver or automatically by optical sensors, as well as signals from optical sensors which can be placed on cars and are designed to automate the wiper activity. Within an experimental setup the relevant sensor reading uncertainties are to be investigated. For that reason a rainfall simulator with the ability to produce a wide range of rain intensities is designed and constructed. Rain simulators are a subject of different studies, for example, erosion (FIENER et al., 2011), agriculture, horticulture, hydrology, etc. Soil erosion experiments mainly use rain simulators which aim to reproduce, as near as possible, the properties of natural rain (SALLES and POESEN, 1999). The rain simulator used in this study should have the capability of producing different rain intensities with homogeneous distribution over the desired area as well as replicating the properties of natural rain. Analyses of rainfall measured by car sensors are accomplished considering a tipping bucket as reference device. There are many different environmental factors influencing the estimation of rainfall by cars in nature like car speed, wind speed, wind direction, windshield angle, etc. In this study, only the influence of the car speed on the estimation of rainfall is investigated with the help of a special car speed simulator.

The paper is organized as follows. Section two describes the rainfall simulator and the way it is designed. The description of the rainfall measurement devices and their functionality are provided in the third section. Section four discusses the results including the analyses of the produced rainfall and the derived (*W-R*) relationships. The last section presents a summary and conclusion.

5.2 Rainfall simulator - sprinkler irrigation system

Considering the addressed purposes of the study, a wide range of rainfall intensities needed to be produced by a rainfall simulator. The points guiding the design of the system are (1) producing homogeneous rainfall in the laboratory, and (2) the ability of testing cars with measurement devices under different rain intensities. According to the design principles of the sprinkler irrigation system, given in FAO (PHOCAIDES, 2000) or other handbooks, sprinkler spacing depends on the wetted diameter produced by each specific nozzle. Figure 5.1 shows the design of the rain simulator used for the laboratory experiments. It consists of two layers that have the capacity of positioning eight nozzles in total. All the measurement devices as well as the tested cars are placed under the rain simulator, which has a height of approximately 3 m from the ground. "P" in Fig. 5.1 shows the pressure controller which controls each layer's pressure. Considering the specifications for each nozzle provided by the manufacturer, the design of the rain simulator is based on a pressure of 2 bars and neglects head losses in pipes. To reproduce a larger range of rain intensities, pressures of 1 bar and 2.5 bars are also applied.
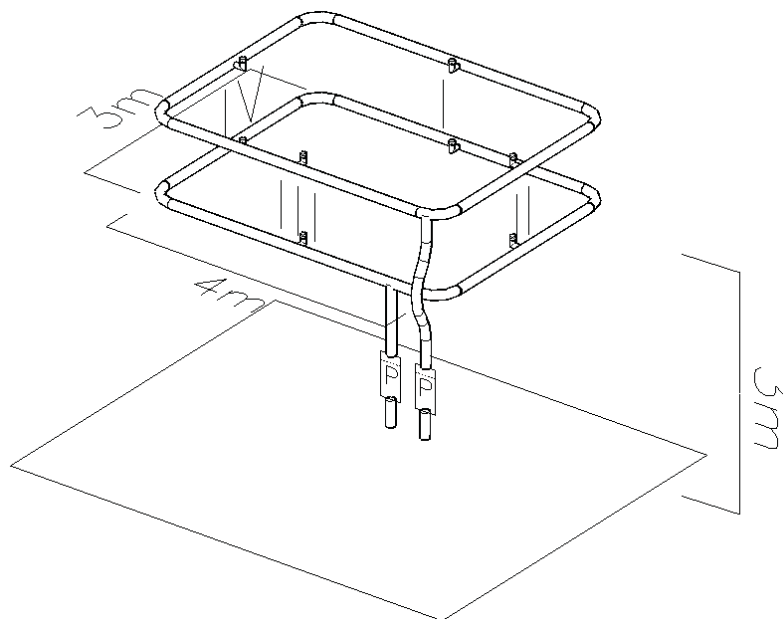
Figure 5.1: Rain simulator, two layers with 8 nozzles.

Producing different rain intensities is achieved by activating different sets of nozzles and applying different pressures on the nozzles. Table 5.1 presents detailed information about the three different nozzle models used in this study regarding their mean rainfall intensity and the maximum wetted radius under different pressures. It should be pointed out that in contrast

Table 5.1: Specification of the nozzles used in this study, given by the manufacturer.

Nozzle model	Pressure [bar]	Precipitation [mm h^{-1}]	Radius[m]
	1.37	62.2	2.13
S-8A	2.06	50.8	2.43
	2.41	52.1	2.43
	1.37	15	4.57
S-16A	2.06	18.3	4.88
	2.41	17.8	5.18
	1.37	45.2	2.13
8A	2.06	42.9	2.43
	2.41	36.8	2.74

to natural events, where the environmental factors influence the rain drops and fast rain rate variations can occur in a short period of time, the rainfall produced in the laboratory is constant over a certain time.

The numbers from I to IV in Fig. 5.1 shows the four spots available for placing the nozzles on each layer. Considering the water distribution pattern of the nozzles and the goal to produce homogeneous rainfall, the positions for the different nozzle types can be selected. Taking into account the mentioned factors and principles for sprinkler irrigation design, Table 5.2 shows different combinations of the nozzles used in this study. Altogether 8 classes of nozzle combinations are defined.

In Table 5.3 the Cartesian product of the set of pressures with the set of different nozzle combinations is given, excluding duplicates, which results in 39 pairs. Due to the capacity of the pump, only 32 pairs are applied. The stars in Table 5.3 show the sets where the demand is higher than the pump capacity. The rainfall intensities given in Table 5.3 for the 32 cases are measured with the tipping bucket reference device and cover a range between 9.2 and 98.1 mm h^{-1}. For instance, the lowest produced rainfall intensity of 9.2 mm h^{-1} belongs to the nozzle combination class 1 applying a pressure of 1 bar using 2 nozzles of the type S-16A on positions I and III on the 1st layer. The highest rainfall intensity of 98.1 mm h^{-1} belongs to the nozzle combination class 5 with an application of 2.5 bar pressure using 8 nozzles of the type S-8A on positions I, II, III and IV for both layers.

Most of the rain simulators are not able to generate low rainfall intensities, for example, SHARPLEY and KLEINMAN (2003) were also able to produce rainfall intensities starting from 17.0 mm h^{-1}. The generation of rainfall intensities lower than 9.2 mm h^{-1} in the laboratory is hardly possible because available nozzles providing uniform rainfall distribution usually cannot

generate lower intensities. However, given that the application is intended primarily for flood producing situations, this lower rainfall intensity limit is considered sufficient for this initial study.

The following analyses are performed using a constant rainfall intensity produced by the sprinklers in a time period of 15 min for all the possible 32 cases.

5.3 Rainfall measurement devices

Two kinds of measurement instruments are used in the laboratory, a reference gauge and devices which are meant for rainfall measurement with cars. The reference gauge provides the reference rainfall (R) in relation to the car sensor readings (W). The rainfall measurement devices are explained in the following.

5.3.1 Reference gauge

Tipping bucket

One of the most common devices of measuring rainfall depths is the tipping bucket rain gauge. Although the device is widely used for different purposes, it is subject to systematic and random instrumental errors (CIACH, 2003). However, wind as the most important factor influencing the measurement accuracy has no relevance in the laboratory. The tipping bucket used in this study has a minimum measurement resolution of 0.1 mm rainfall. The size of the bucket and rain intensity are the critical factors in estimating the rainfall for low intensities (LANZA et al., 2006). Since, in this study, only higher and constant rainfall intensities are applied in the laboratory, these uncertainties can be neglected. However, they are very critical for field measurements with finer temporal resolutions. So, it is suggested to implement, instead, more accurate rainfall measurement devices such as weighing rain gauges, as the reference for field experiments.

Table 5.2: Different nozzle combinations implemented in this study.

		Class							
		1	2	3	4	5	6	7	8
1st	I	S-16A	S-16A	S-8A	S-8A	S-8A	8A	8A	8A
layer	II	–	–	S-8A	S-8A	S-8A	8A	8A	8A
	III	S-16A	S-16A	S-8A	S-8A	S-8A	8A	8A	8A
	IV	–	–	S-8A	S-8A	S-8A	8A	8A	8A
2st	I	–	S-16A	–	S-16A	S-8A	–	S-16A	8A
layer	II	–	–	–	–	S-8A	–	–	8A
	III	–	S-16A	–	S-16A	S-8A	–	S-16A	8A
	IV	–	–	–	–	S-8A	–	–	8A

5.3.2 Sensors considered for rainfall measurement by cars

5.3.2.1 Wiper frequency analysis

The initial idea was to use the windshield wiper frequency as an indicator for rainfall intensity. The main goal here is to find a relationship between wiper speed (W) and rainfall intensity (R). This relationship is determined with the help of a stationary car placed under the rain simulator. Each car has a specific protocol for the wiper system, but the wiper systems are, in general, similar. The results of one car as a representative are presented in the following.

Two different scenarios of adjusting the wiper speed have been investigated. In the first scenario, the wiper activity is adjusted according to the visibility through the front screen, which is done completely manually by a driver. The manual adjustment of the wiper activity is applied by a person sitting in the driver's seat and the front visibility is adjusted by the clear view of lamps placed on the front wall, a similar condition to car's rear lights on the streets. This means, an individual person decides when to apply each single wipe, depending on the front visibility. In the second scenario, an automatic wiper speed adjustment option is used that considers different sensitivities. It's worth mentioning that the sensitivity settings can change from one car to another. This depends on the specific protocols implemented by the manufacturers. Different sensitivities are mainly defined for drivers' comfort in different precipitation conditions. In this case, the wiper system controls the adjustment of the wiper activity. The analysis concerning wiper frequency is solely carried out for one stationary car here which does not move under the rainfall simulator. In reality, the wiper speed could change for the same rain intensity depending on the car type, car speed, rain type, and windshield angle. It should be noted that different car types have different dimensional characteristics which may influence the aerodynamics of

Table 5.3: Applied pressures and corresponding produced rain intensities.

		Class							
		1	2	3	4	5	6	7	8
layer	P [bar]	PCP [mmh^{-1}]	PCP [mmh^{-1}]	PCP [mmh^{-1}]	PCP [mmh^{-1}]	PCP [mmh^{-1}]	PCP [mmh^{-1}]	PCP [mmh^{-1}]	PCP [mmh^{-1}]
1st	1	9.2	–	12.8	–	–	24.4	–	–
1st	2	16.8	–	37.7	–	–	34.4	–	–
1st	2.5	20.4	–	55.2	–	–	48.4	–	–
1st / 2nd	1 / 1	–	14.4	–	11.6	40.7	–	33.4	60
1st L. / 2nd L.	1 / 2	–	15.2	–	20.4	42	–	39.2	*
1st L. / 2nd L.	1 / 2.5	–	17.6	–	20.4	59.2	–	43.7	*
1st L. / 2nd L.	2 / 2	–	23.1	–	45.2	66.4	–	45.9	*
1st L. / 2nd L.	2 / 2.5	–	22.7	–	49.7	84.6	–	*	*
1st L. / 2nd L.	2 / 2.5	–	27.4	–	53.6	98.1	–	*	*

Stars indicate the sets where the demand is higher than the pump capacity.

the raindrops and, accordingly, the sensor readings. Besides, different cars have specific wiper systems which lead to dissimilar classes of wiper frequency. According to the functionality of the optical sensors measuring the rainfall (i.e., change in beam intensity), any foreign object passing the optical sensor might have influence on the signals coming from the device. It is thus important to mention that in automatic wiper systems, each time the wiper cleans off the windshield it passes in front of the optical sensor, which may affect the signals coming from the optical sensors controlling the wiper speed. However, in practice this noise could be filtered out because of a similar effect on the signals every time the wiper blade passes the optical sensor.

5.3.2.2 Optical sensors

As alternative to the wipers, the utilization of optical sensors as measurement devices which are available on modern cars for automating the wiper activities is investigated here. Two optical sensors have been employed in this study for measuring rainfall intensity. The output of the sensors is a function of the amount of water sensed on the surface of the device. The functionality of the two devices is similar, but the output is different. The two optical sensors are presented in Fig. 5.2.

The Hydreon sensor (HYDREON, 2012) is fully calibrated by the manufacturer and ready to

Figure 5.2: Optical sensors, left: Xanonex, and right: Hydreon (HYDREON, 2012; XANONEX, 2012)

be used for different purposes, for example, measuring rainfall, wiper control on the vehicles, irrigation control, etc. This device is capable for multipurpose use and is, according to the specification, able to sense raindrops smaller than half a millimeter. The device bounces infrared beams within its lens. The effect of drops on the surface allows some of the beams to escape. This can be explained by the principles of light refraction. The change in beam intensity is considered as an indication of rain amount on the surface. Here, each sensor reading corresponds to 0.01 mm of rainfall. Figure 5.3 illustrates how the Hydreon works. As can be seen, a raindrop on the surface results in escaping some beams and, accordingly, changing in beam intensity.
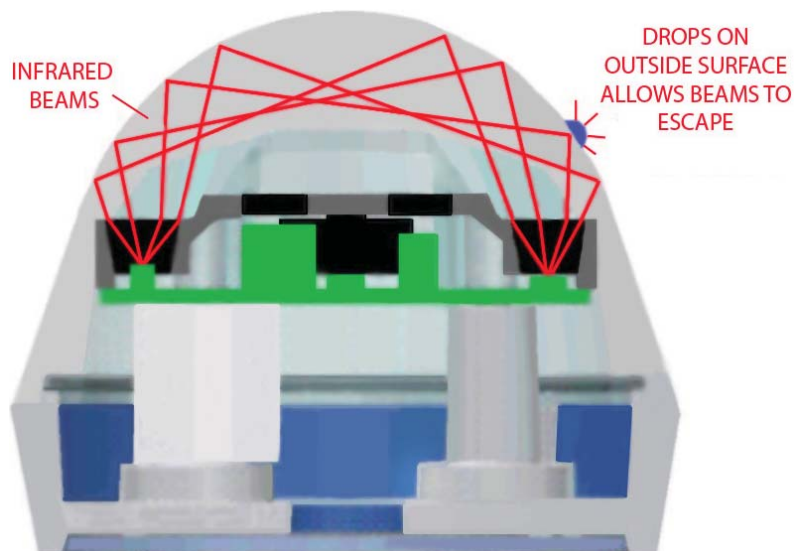
Figure 5.3: The functionality of the Hydreon sensor (HYDREON, 2012).

The Xanonex sensor (HYDREON, 2012) is especially made to be used on cars for automating

the wiper activities. For this purpose, it can be attached directly to the front windshield. This device works in a similar way as the Hydreon. Eight LEDs placed in a circle and the sensor in the center form the main parts of the device. The LEDs emit infrared beams out of the device. Depending on the water amount on its surface, which acts as obstacles on the windshield, part of the emitted beam is reflected back to the sensor. In principle, the sensor is implemented in an electrical circuit where a direct current flows and the flow is blocked for a certain time. This blockage appears as a signal length, which is a function of water amount. Here, the accumulation of the signals over a minute [s min^{-1}] is analyzed.

According to the sensing principles of the devices, it is postulated that the rainfall measured by the optical sensors is solely a function of water amount on the sensors' surfaces. As a result, it is assumed here that the droplet size distribution of the artificial rainfall is not relevant for measuring the correct rainfall intensity by the optical sensors.

5.3.3 Car speed simulator

One of the main influencing factors on the estimation of rainfall by a car is its speed. Analyzing an object with a certain velocity under rain has been investigated by physicists and other scientists. BOCCI (2012) has proven that the amount of water hitting an object under rain depends on its shape, its orientation, wind direction and rain intensity. The main purpose of the car speed simulator is to investigate this effect in the laboratory.
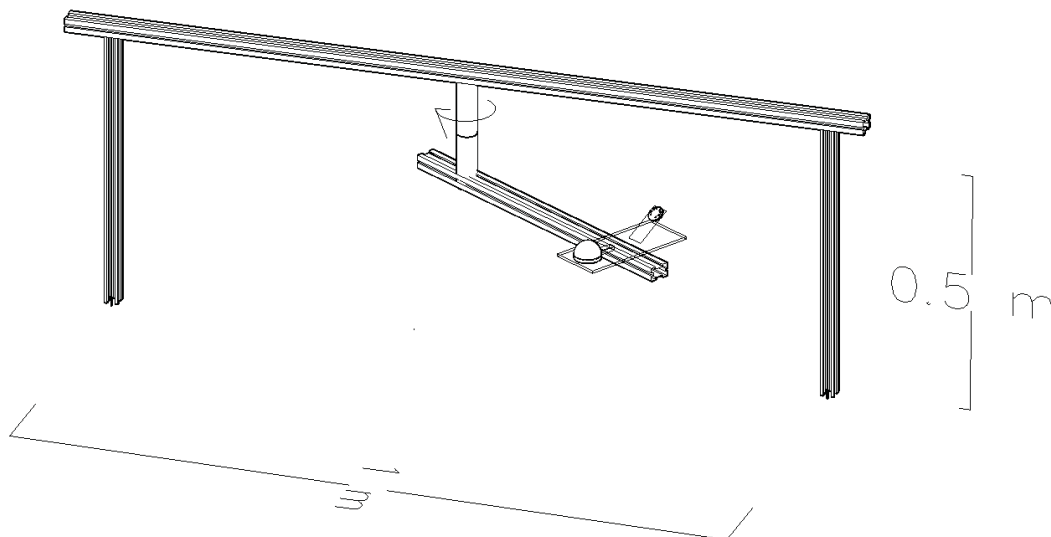
Figure 5.4: Rotating machine used to simulate car speed, with two optical sensors placed on the devices.

Figure 5.4 shows the rotating machine which has been used in the laboratory. The electrical motor of the machine is able to work with different speeds and as a result simulate car speeds. Two optical sensors are placed on a rotating machine. In order to simulate an average windshield angle, the Xanonex is placed at an angle of 45°. By changing the rotational speeds (ω) in the car speed simulator, different tangential speeds (u) are produced:

$$u = r\omega \qquad (5.1)$$

where "r" is the radial distance, which is constant.

In order to measure the rotational speed of the device, a digital laser based tachometer with the stated accuracy of $\pm\ 0.05\ \%\ +\ 1$ digit is used.

It is necessary to mention that the devices used here are under the rain without being cleaned off by the wiper system, unlike when implemented on cars with the wiper system cleaning off the droplets on the sensors repeatedly.

The experiments with the car speed simulator are carried out separately from the experiments for deriving the (*W-R*) relationships. For each individual run, the dynamic sensors are compared with the static ones of the same type. Speeds of up to 45 km h^{-1} are reached and tested.

The estimation of rainfall is affected by different factors including (a) the horizontal angle of the optical sensor which is representing the windshield angle, (b) the rain droplet velocity, and (c) the car speed. The rain droplet velocity can be interpreted as an indicator for the rain type. Considering the direction of the moving plane (car) as the (*x*) axis and the direction of the falling rain drops as the (*z*) axis, the windshield angle affects the projected area corresponding to both axes.

BOCCI (2012) introduced $v = (v_x, v_y, v_z)$ as the rain velocity where the vertical component, v_z, depends on the drop size. He called ρ the ratio between the mass of water drops that are found within a given volume and the volume itself. Afterwards, he defined the rain density as vector:

$$j_0 = \rho v \qquad (5.2)$$

He then introduced a vector for the moving objects, considered as a plane, representing the velocity $u = (u, 0, 0)$. Subsequently, for the moving objects, an apparent rain density j, which differs from j_0 can be defined:

$$j(u) = \rho(v - u) = \rho(v_x - u, v_y, v_z). \qquad (5.3)$$

He proposed the following equation representing the rain flux as the surface integral over the rain density j:

$$\Phi(u) = \oint_S j dA. \qquad (5.4)$$

Restricting the integration to the "wet surface" of the object, the rain flux is defined as

$$\Phi(u) = \oint_{S_w} |j dA|. \qquad (5.5)$$

Assuming always vertical rainfall (no horizontal effect of the wind, $v_x = 0$ and $v_y = 0$) and θ as the windshield angle, the ratio between the rain flux observed by the dynamic device and static device becomes

$$\eta = \frac{\Phi_{dynamic}(u)}{\Phi_{static}(u)} = \frac{u_x \cdot A \cdot sin(\theta) + v_z \cdot A \cdot cos(\theta)}{v_z \cdot A} = \frac{u_x \cdot sin(\theta)}{v_z} + cos(\theta). \qquad (5.6)$$

This theoretically obtained ratio η will be compared later against the empirically obtained results from the experiments with the rotating machine.

5.3.4 Data processing

The data from the dynamic optical sensors are transmitted using a wireless connection. Processing of the data by a single PC requires no further synchronization. In order to process the data from the tipping bucket and optical sensors, free data logger software (HTerm) has been used (HAMMER, 2006).

5.4 Analysis of the produced rainfall

5.4.1 Homogeneity of the produced rainfall

The measurement devices are placed under the rain simulator at different locations. Since the rain amounts on these points are compared, the homogeneity of the produced rainfall needed to be investigated. The homogeneity of the rainfall produced in the laboratory is verified with the help of 48 beakers. They are symmetrically placed at a distance of 50 cm from each other. For each individual setting of the rain simulator, the amount of water kept in each of the beakers after each run is measured. Figure 5.5 shows an example of the water depth distribution for a pressure of 2 bars and the nozzle combination class 6 in Table 5.2.
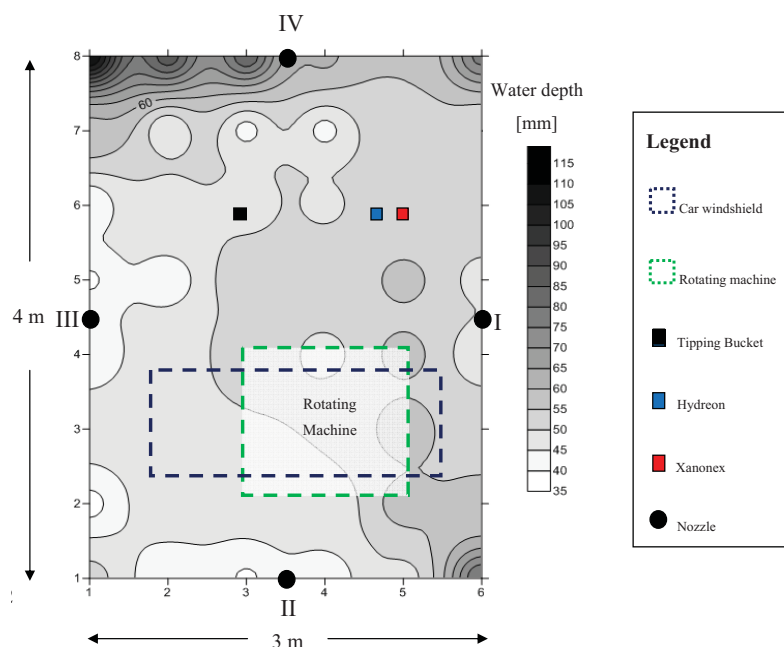
Figure 5.5: Distribution of the accumulated rainfall depth over the sprinkler area for the case of nozzle combination class 6 with 2 bar pressure and the permanent location of measurement devices.

It shows that the water amount kept in the beakers at the two locations, where tipping bucket and the optical sensors are located, is not identical but very similar (48 and 50 mm, respectively). However, the two optical sensors receive the same amount of water because of their proximity. The water depth distribution varies between the different cases of nozzle combinations and pressures. In order to assess the error resulting from non-homogeneous rainfall distribution the relative deviation in water depth between the two points at the locations of the tipping bucket and the optical sensors is calculated as follows:

Table 5.4: Homogeneity statistics related to 21 cases of nozzle combination and pressures applied in the laboratory experiments.

Class	Pressure [bar]	Mean [mm]	Std dev [mm]	CV [%]	RDev [%]
	1	9.25	3.48	37.6	00.00
Class 1	2	13.42	6.85	51.0	21.10
	2.5	17.46	7.82	44.7	35.00
	1	16.58	5.87	35.4	45.00
Class 2	2	32.04	8.75	27.3	14.30
	2.5	39.54	6.14	15.5	25.00
	1	26.67	7.84	29.3	25.90
Class 3	2	35.79	8.80	24.5	25.00
	2.5	46.04	12.72	27.6	6.70
	1	31.04	5.09	16.3	11.40
Class 4	2	57.21	10.31	18.0	15.70
	2.5	61.79	10.28	16.6	2.60
	1	37.08	6.26	16.8	22.60
Class 5	2	65.13	8.27	12.6	31.10
	2.5	65.42	9.66	14.7	4.80
	1	31.21	6.93	22.2	20.00
Class 6	2	49.63	5.28	10.6	4.20
	2.5	55.29	6.65	12.0	8.60
	1	46.63	6.01	12.8	0.00
Class 7	2	61.88	9.89	15.9	10.30
	2.5	–	–	–	–
	1	66.25	8.39	12.6	2.50
Class 8	2	–	–	–	–
	2.5	–	–	–	–

$$RDev = \frac{x_{tipp} - x_{opt.sensors}}{x_{tipp}} \times 100. \tag{5.7}$$

Table 5.4 shows statistical information of the produced rainfall for a selection of 21 cases of different pressures and nozzle combination classes. The rainfall amount at the points on the edges of the sprinkler area is much higher than at the inner points because of the proximity of these points to the nozzles and the wall. For this reason, the statistics in Table 5.4 are calculated without considering these outer points, including only the 24 inner measurements.

Considering the total sprinkler area covered by those 24 beakers the rainfall distribution is still

quite inhomogeneous as shown especially by the coefficient of variation (CV) in Table 5.4. Although the design of the rain simulator is based on 2 bar pressure, a pressure of 2 bars does not always provide the most homogeneous distribution. For example, a pressure of 1 bar in class 1 provides a more even rainfall depth distribution, whereas a pressure of 2 bars in class 5 provides more homogeneous rainfall than the other two pressures.

However, in order to assess the influence of the rainfall distribution on the (*W-R*) relationships the relative deviation RDev between the measurement points is relevant. Positive values of the RDev illustrate the situations in which the water depths in beakers at the tipping bucket location are larger than in beakers at the locations of the optical sensors, and vice versa. For example, the relative deviation RDev for class 1 at a pressure of 1 bar is about 0.0 % meaning that the amount of water kept in the beakers at the two points is identical,while at a pressure of 2 bars RDev is 21.1 % meaning more water has been kept in the beaker where the tipping bucket stands than in the beaker where the optical sensors are located. The average value of all the estimated relative deviations is − 5.8 %. This average error is most relevant to assess the influence of the non-homogeneous rainfall distribution on the estimation of the (*W-R*) relationships. A mean relative deviation of about −6 % in rainfall depth between reference and sensor locations is assumed to be acceptable and to have only little influence on estimation of the (*W-R*) relationships.

5.4.2 W-R relationship

5.4.2.1 Wiper frequency

First, the initial idea of considering wiper speed as an indicator for the rain intensity is investigated. Figure 5.6 shows the results of a linear regression for the (*W-R*) relationship of a Ford SMAX automobile with automatic wiper system where a tipping bucket gauge is taken as the reference device. Each point illustrates an individual run lasting between 10 and 15 min. The wiper speed is adjusted either completely manually (Fig. 5.6, left panel) or automatically (Fig. 5.6, right panel). The dashed lines illustrate the 95 % prediction limits for the prediction of an individual observation. Because of technical constraints and restrictions in using all the nozzles when placing the car, depending on its dimension, it was not possible to apply all the cases. As a result, the number of points in Fig. 5.6 differs from the number of possible runs provided in Table 5.3. The same is valid for the automatic wiper adjustment when the highest wiper frequency (when not moving) is 60 w min^{-1} ("w" represents the number of wipes). Here,

the experiment is stopped after reaching this threshold.
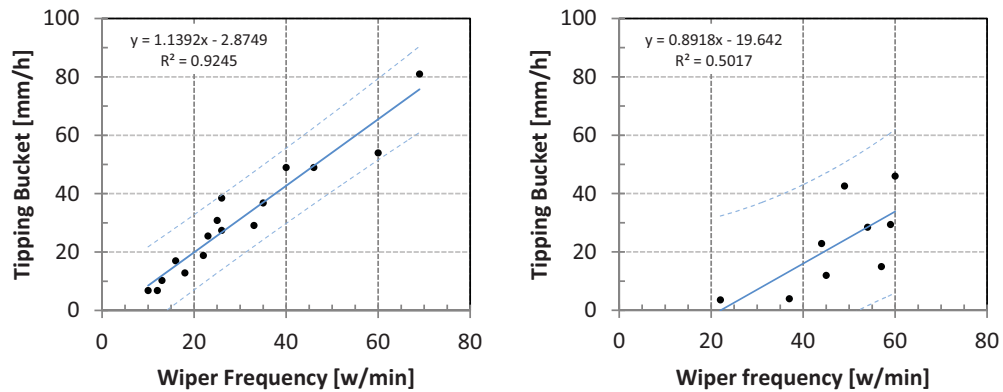
Figure 5.6: Relationship between wiper frequency (*W*) and rainfall intensity (*R*) using manually (left panel) and automatically (right panel) adjusted wiper activities and the tipping bucket as the reference using a Ford SMAX as test car.

There are different sensitivities defined for the automatic wiper system in this car, only one of the higher sensitivities is illustrated here.

Apparently, a relatively strong relationship exists between rainfall intensity and wiper speed for the manual adjustment. The result of the wiper activity adjustment, according to front visibility, supports the initial idea of considering wiper speed as an independent variable in the (*W-R*) relationship. The relationship between automatic wiper frequency adjustment and rainfall intensity shows much weaker correlation and higher uncertainty. Reasons for that may be (a) too simple data processing of data readings from the optical sensor controlling the wiper activity, and (b) the point measurement of the optical sensor which may not be representative for the total water amount on the windshield.

Apart from the better suitability of the manual wiper adjustment for the establishment of a (*W-R*) relationship, it may be concluded that the manual adjustment of the wiper speed is superior for drivers when compared to the automatic wiper system. So, it may be expected that advancements in the development of automatic wiper systems will provide better (*W-R*) relationships in the future. With the current sensors, the driver has to adjust the sensitivity manually for different conditions to have optimal front visibility. This should not be the case if the automatic wiper control system works optimally.

Here, at first a linear (*W-R*) relationship is assumed for all the analyses. However, since the lines do not pass the origin, the relationship between the two variables may be nonlinear especially for small intensities.

5.4.2.2 Optical sensors

Figure 5.7 shows the (*W-R*) relationships between the data readings from the optical sensors and the rainfall intensity measured by the tipping bucket. Each point in this figure represents one individual run lasting between 10 and 15 min; the dashed lines illustrate the 95% prediction intervals. Although the Hydreon sensor was considered as calibrated, Fig. 5.7b shows an underestimation of the rainfall by this device. However, the high coefficient of determination (R^2) shows that this underestimation could be interpreted as a systematic error which may be corrected by recalibration. The relationship between the data readings from the Xanonex optical sensor and the rainfall intensity from tipping bucket shows lower R^2 value (Fig. 5.7a) compared to the Hydreon. A possible reason for the lower R^2 value and the concentration of the data readings in the range between 20 and 40 [s min^{-1}], Fig. 5.7c) might be the nonlinear relationship between the signal lengths and measured rainfall intensities. The higher R^2 value for the Hydreon in comparison to Xanonex may also be due to a better calibration or a better suitability of the device. The correlation between the data readings from the two optical sensors (Fig. 5.7c) is not as strong as the former two. This shows the difference in the calibration procedure of the devices as well as their sensitivities.

The similarity of the derived (*W-R*) relationships for the automatic wiper adjustment (Fig. 5.6, right panel) and the Xanonex (Fig. 5.7a) shows the likely comparable data processing in both cases (i.e., a possible similar principle to the derived (*W-R*) relationship). It can be concluded that a better calibration (e.g., considering nonlinear relationship) for the optical sensors controlling the automatic wiper systems may improve the performance of the system resulting in more convenient automatic wiper system for drivers.

5.4.3 Car speed simulator

Car speed is one of the important influential factors for the estimation of rainfall by moving cars. Theoretically, there is a positive linear relationship between the velocity of an object with a plane surface under rain and the water mass hitting the object (BOCCI, 2012). This means when a car moves with higher speed the rainfall intensity measured by car sensors would be overestimated compared to a stationary ground reference value, linearly proportional to its speed.

Figure 5.8 illustrates the results of the car speed simulator in the laboratory. This does not
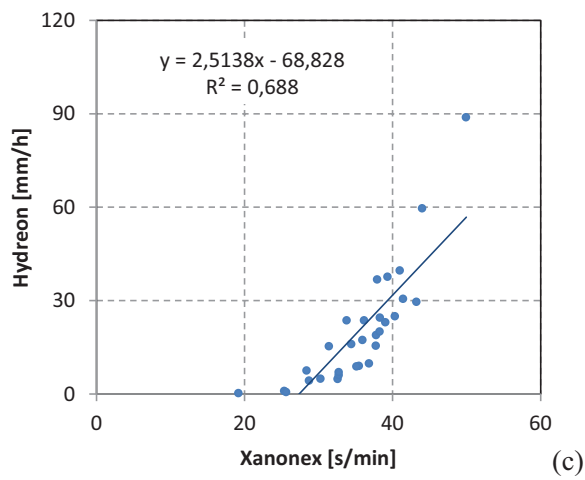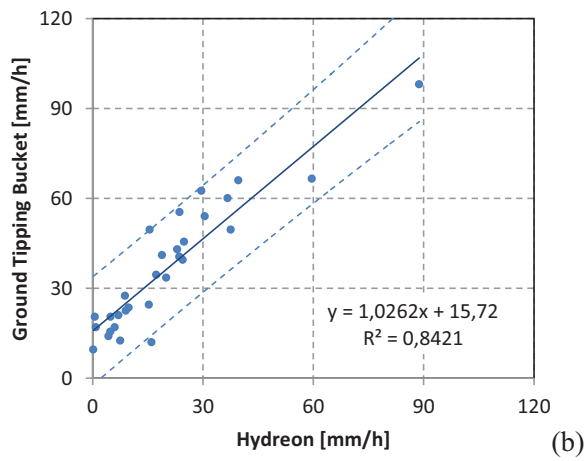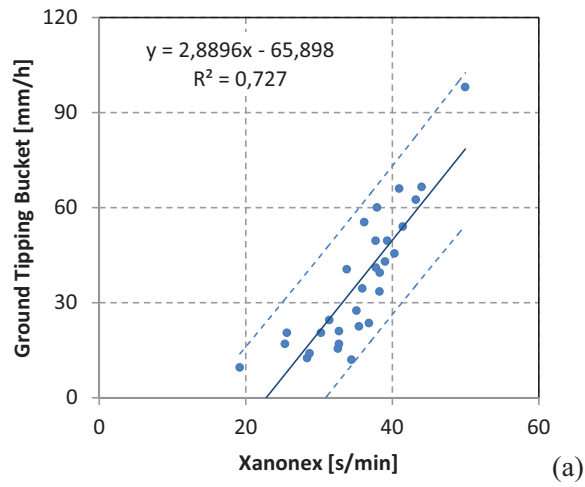
Figure 5.7: Comparison of the optical sensors with the reference device, tipping bucket, with 95 % prediction limits

involve using a car but the car speed simulator (see Fig. 5.3). The black line represents the mean ratio of the sensor readings from the dynamic and static device η (Eq. 5.6) versus the sensor speed in different rainfall intensities. The gray area shows the range between the upper and lower quartile considering 22 runs with different rainfall intensities. Apparently, the ratios derived in the laboratory are not linear and have a tendency to become constant after a certain speed. There may be three reasons explaining this behavior: (a) the shielding effect of the remaining drops after a certain speed, which introduces a hypothetical capacity for the sensor's surface (i.e., the accumulated drops may prevent the incoming drops from affecting the sensor readings); (b) the centrifugal force on the drops, which draws the remaining drops from the center of rotation and may cause noises in the sensor readings; and (c) the special aerodynamics of the small plane carrying the optical sensor in the laboratory experiments (see below). Assuming that the first linear part of the measurements (Fig. 5.8b up to 20 km h^{-1}) is correct; a linear extrapolation would provide the complete relationship which may be applied also for higher speeds.
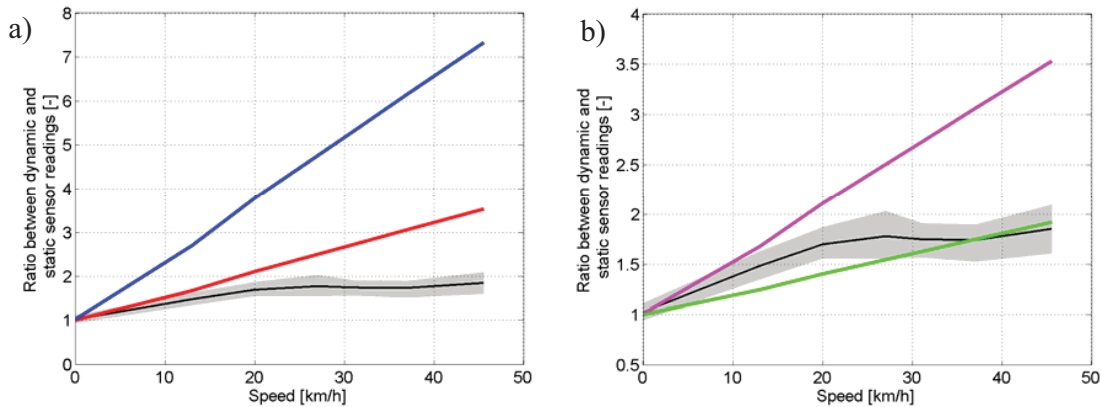
Figure 5.8: Black line: experimental results of the car speed simulator with gray uncertainty boundaries. a) Theoretical ratios for assumed rainfall velocity of 2 m s^{-1} (blue) and 5 m s^{-1} (red). b) Theoretical ratios for assumed windshield angle of 70° (green) and 45° (purple) at an assumed raindrop velocity of 5 m s^{-1}. The empirical relationship is derived by the car speed simulator and there is no car involved in this experiment.

It has been discussed that the ratio η (Eq. 5.6) between the dynamic device and the static device dependents on (a) rainfall velocity (v_z), (b) the horizontal angle (θ), and (c) the object speed (u_x). The rain drop velocity could be interpreted as the rain type. LULL (1959) has shown that there is a strong relationship between rain type and fall velocity; usually the higher the fall velocities, the heavier the rain. In his classification, velocities from 0.003 to 7.9 m s^{-1} cover the rain types from fog to extreme rain. Using Eq. (5.6) with $\theta = 45°$, the blue line and the red line in Fig. 5.8a show the theoretical ratios for assumed rainfall velocity of 2 and 5 m s^{-1},

respectively.

Due to the fact that the rainfall produced in the laboratory is from the nozzles with a height of 3 m only, the terminal velocity of the raindrops is lower than natural events. Knowing this, the black line in Fig. 5.8 should have a steeper slope compared with red and blue lines representing natural rain with higher velocities. This uncharacteristic behavior may be explained by aerodynamic effects. That is the small plane used in the laboratory may not receive all drops in the air volume in front, but several drops may be blown away.

The windshield angle is a factor which influences the rainfall estimation by the moving cars. By assuming the raindrop velocity at 5 m s^{-1} in Eq. (5.6), the green line and the purple line illustrate the effect of the angle on the ratio corresponding to an angle of 70° and an angle of 45° in Fig. 5.8b, respectively. Note that the black lines and the gray range in Fig. 5.8a and b represent the same data; the only difference between the two figures is the scaling of the *y* axis.

Figure 5.8 indicates also that the effect of rain type, in terms of rainfall velocity, on the overestimation of rainfall is likely larger than the influence of the windshield angle.

5.5 Summary and conclusions

The feasibility of considering moving cars as rain gauges to estimate areal rainfall is discussed in theory using computer experiments by HABERLANDT and SESTER (2010). The main objective of this study was to develop a relationship between sensor readings (*W*) and rain rate (*R*) based on laboratory experiments to quantify the errors. Therefore, a rainfall simulator with the ability to produce a wide range of rain intensities is designed and constructed. Analyses of the rainfall produced in the laboratory are accomplished using a tipping bucket as reference device. Two variables were considered as sensor readings in this study: wiper speed, and readings from two optical sensors which can be placed on cars to automate wiper activity. The use of wiper speed as an indicator for the rain intensity is investigated by adjusting the wiper speed either completely manually, which is executed by a person and might be subjective depending on the person in charge, or automatically. Additionally, the influence of the car speed on the estimation of the rainfall is investigated with the help of a car speed simulator.

The results of this investigation can be summarized as follows:

1. The result of the manual wiper activity adjustment, according to front visibility, shows a strong relationship between rainfall intensity and wiper speed. This supports the initial idea of considering wiper speed as the main independent variable in the (*W-R*) relationship.

2. The derived (*W-R*) relationship between automatic wiper frequency adjustment and rainfall intensity shows weaker correlation and higher uncertainty. Possible reasons for that include data processing of the readings from the optical sensor and the point measurement of the optical sensors controlling the wiper activity.

3. In addition to wiper activity analyses, the (*W-R*) relationship has been derived for optical sensors. The Hydreon sensor was considered as calibrated, but an underestimation of the rainfall sensed by the device has been observed. This underestimation may be interpreted as a systematic error considering a relatively strong (*W-R*) relationship for the Hydreon and the low relative deviation between the sensor and the tipping bucket. The derived (*W-R*) relationship for the Xanonex is weaker. Due to the narrow range of the data readings and also a large (non-zero) intercept in the (*W-R*) relationship, better calibration of the device may lead to better (*W-R*) relationships.

4. The similarity of the derived (*W-R*) relationship for automatic wiper adjustment and the Xanonex optical sensor shows possible similarity in data processing for both cases. It can be concluded that a better calibration of the optical sensor controlling the wiper activities may improve the (*W-R*) relationship as well as the performance of the automatic wiper system for drivers.

5. A positive relationship between the velocity of the optical sensor located on the car simulator under rain and the water mass hitting the sensor has been observed. Theoretically, a positive linear relationship exists between the two criteria, but in the laboratory the results are only approximately linear up to a speed of about 20 km h^{-1} and become almost constant after that. Assuming that the first part of the function is correct, a linear extrapolation would provide the complete relationship which may also be applied for higher speeds.

6. Interpreting the drop velocity as the rain type, it has been observed that the effect of rain type on the overestimation of rainfall is larger than the influence of the windshield angle. This means that by knowing the drop velocity, the rainfall overestimation could be corrected more accurately.

Altogether, the results of the laboratory experiments have shown that it is possible to derive (*W-R*) relationships from the sensor readings. However, there are many influential factors which need further investigation, for example, the aerodynamics of the plane in the car speed simulator or the droplet size distribution in the laboratory.

One limitation of this study is producing rainfall intensities only in the range from 9 to 98 mm h^{-1}. This range starts from a quite high rain intensity, compared with natural rain events, but it is quite wide for analyzing the sensor readings from optical sensors.

Equation (5.6) shows that by changing the windshield angle to 0°, the derived ratio between the dynamic optical sensor and static optical sensor becomes 1. This means that by placing an optical sensor completely horizontal, there would be no relative influence of the car speed on the sensor readings. Future work covers investigating an optical sensor when located horizontally in the laboratory, the influence of the droplet size distributions, different car types and other factors. Currently, field experiments are carried out to obtain (*W-R*) relationships in natural conditions especially for lower rain intensities. Results of the field experiments and comparisons with the laboratory derived (*W-R*) relationships will be reported elsewhere. Preliminary results and possible theoretical methods of the field experiments are investigated by FITZNER et al. (2013). The rainfall data obtained by car measurements might be used separately or more likely to be combined with other sources of rainfall observations like radar data and point measurements and need to be tested for different hydrological applications.

Edited by: L. Pfister

Chapter 6

Areal rainfall estimation using moving cars - computer experiments including hydrological modeling

Abstract

The need for high temporal and spatial resolution precipitation data for hydrological analyses has been discussed in several studies. Although rain gauges provide valuable information, a very dense rain gauge network is costly. As a result, several new ideas have been emerged to help estimating areal rainfall with higher temporal and spatial resolution. RABIEI et al. (2013) observed that moving cars, called RainCars (RCs), can potentially be a new source of data for measuring rain rate. The optical sensors used in that study are designed for operating the windscreen wipers and showed promising results for rainfall measurement purposes. Their measurement accuracy has been quantified in laboratory experiments. Considering explicitly those errors, the main objective of this study is to investigate the benefit of using RCs for estimating areal rainfall. For that, computer experiments are carried out, where radar rainfall is considered as the reference and the other sources of data, i.e. RCs and rain gauges, are extracted from radar data. Comparing the quality of areal rainfall estimation by RCs with rain gauges and reference data helps to investigate the benefit of the RCs. The value of this additional source of data is not only assessed for areal rainfall estimation performance, but also for use in hydrological modeling. The results show that the RCs considering measurement errors derived from laboratory experiments provide useful additional information for areal rainfall estimation as well as for hydrological modeling. Even assuming higher uncertainties for RCs as obtained

from the laboratory up to a certain level is observed practical.

6.1 Introduction

Rainfall data is one of the most important information in hydrological analyses. The spatial and temporal resolutions of the data are crucial for the quality of hydrological analyses. Different modeling scales usually require different resolutions of input data. A relatively high spatial and temporal resolution is required for smaller scale modeling such as in urban hydrology, whereas data with coarser resolution could be sufficient for larger scale hydrological modeling. Hypothetically, the performance of a model could be objectively judged when input data of a high quality is provided. In particular, the spatial and temporal resolution of rainfall data over a study area influences the model performance significantly. The quality of rainfall estimation depends, on the one hand, on the data availability, i.e. rain gauge network density, the temporal resolution of data and/or availability of additional information such as Digital Elevation Model (DEM) or radar data, and, on the other hand, on the interpolation techniques used for areal rainfall estimation.

Conventional rain gauges provide accurate point rainfall depth, but they are sparsely and irregularly located over the study area. This results in missing rainfall information where no rain gauge is available. On the other hand, a dense rain gauge network is costly. There are several innovative ideas discussing new manners of measuring rainfall. Weather radar data with relatively high spatial and temporal resolution are widely used for rainfall estimation purposes, but the data are subject to several sources of error. Besides, weather radar is not available all over the world. Estimating rainfall using satellite data has become of interest for practical purposes, in particular for remote areas, because of good spatial coverage and being freely available. The satellite data provide precipitation data globally, but they suffer from the intrinsic weakness of the principle behind estimating rainfall, i.e. finding the relationship between observable variables from space (e.g. cloud top temperature and the presence of frozen particles aloft) and rain intensity. The satellite data are relatively coarse for local use. The TRMM PR data, for example, is provided in 3-hour temporal resolution and a 0.25-degree by 0.25-degree spatial resolution. PRAKASH et al. (2016) compared the new GPM-based multi-satellite IMERG precipitation estimates with the TRMM Multi-satellite Precipitation Analysis (TMPA) in capturing heavy rainfall over India for the southwest monsoon season. They observed notably better estimation from the GPM data. KIDD and LEVIZZANI (2011) and KIDD and HUFFMAN (2011) have summarized some of the efforts given to improve the accuracy of satellite rainfall

estimation. Several studies investigated rainfall estimation using microwave links as another potential source of data (OVEREEM et al., 2013; RAHIMI et al., 2006; UPTON et al., 2005; ZINEVICH et al., 2009), where a line-averaged precipitation is estimated therefrom. Acoustic rain gauges are an economical alternative which analyses the raindrops sound similar to when one listens to rain in a tent (JONG, 2010). Most of the mentioned studies seek for alternatives which either are not initially intended for rainfall estimation or have low operational costs.

HABERLANDT and SESTER (2010) hypothetically presented the potential of using moving cars for rainfall measurement purposes, called RainCars (RCs). They pointed at the potential of using RCs because of the widespread availability of cars especially in countries such as Germany. They concluded that a large number of hypothetically inaccurate devices could help in improving the estimation of rainfall compared with just a few of accurate devices. RABIEI et al. (2013) investigated the possibility of using RCs for rainfall estimation with laboratory experiments. A strong relationship between rainfall intensity and the wiper speed, adjusted with front visibility, was observed. The rainfall estimation by the two optical sensors, HYDREON (2015) and XANONEX (2015), implemented in that study showed also promising results. Whether the derived accuracy of the sensors is sufficient for areal rainfall estimation or not is a question which is addressed in this study. Because of the low number of real observations with RCs available on roads, the investigations are carried out by computer experiments. A continuous investigation using RCs with the derived uncertainties from laboratory experiments for a long period of time as well as implementing the data in a hydrological model would answer three important scientific questions: 1) Is the accuracy of optical sensors investigated by RABIEI et al. (2013) sufficient for areal rainfall estimation as well as discharge simulation? 2) What is the minimum required accuracy of RCs measuring rain rate for estimation as well as for discharge simulation? and 3) What is the influence of using RCs over a longer period of time rather than just for certain events? These questions address the main objective of the study which is a better assessment of the value of the RCs for areal rainfall estimation rather than only for point measurement purposes.

The influence of input data quality on hydrological modeling performances has been under investigation by several studies. For example, SHRESTHA et al. (2006) investigated the influence of data resolution on the performance of a macro-scale distributed hydrological model (MaScOD). They split the factors influencing the quality of model performance into three categories: (1) the quality of the model, (2) the selected model parameters, and (3) the quality of the input data. The advantages of using RCs are assumed to provide a denser measurment network and additional information. XU et al. (2013) investigated the influence of rain gauge

density and network distribution on the Xinanjiang River in China by the Xinanjiang Model. They found that the probability of getting a poor model performance increases significantly when the number of rain gauges falls below a certain threshold. They also concluded that the number of rain gauges above a certain threshold does not improve the model performance meaningfully. They realized that not only the number of stations is important, but also the spatial configuration of rain gauges.

This paper is organized as follows. The methodologies implemented in this study are presented after the "Introduction". Chapter 3 provides detailed information regarding the study area and data used in this study. The results and corresponding discussions are provided in chapter 4. Thereafter, a summary of the work and comparison of the results is presented with a more general conclusion.

6.2 Methods

Since there are not enough observed data from RCs, this study uses computer simulation. In order to carry out the analyses, rainfall fields as reference data are required. The point data from stations and RCs are extracted from the reference data and compared accordingly. There are essentially two possibilities to obtain reference data: (1) simulating the rainfall field or (2) using an available data source such as radar data. The latter choice has the advantage of being closer to reality and avoiding additional rainfall modeling. As a result, it is decided to consider radar data as reference and to extract the point data from the radar data. As radar data has its deficiencies, the Mean Field Bias method is applied to correct the error in a straightforward way. The positions of RCs are provided by a traffic model and rainfall data are extracted from the reference data accordingly. The results are compared with what occurs in practice, i.e. using only the rain gauge network. The uncertainties for the rainfall measurement by RCs are taken from the results of the laboratory experiments (RABIEI et al., 2013). For a more general conclusion, larger uncertainties are also investigated.

6.2.1 Mean Field Bias correction

The Mean Field Bias (MFB) correction adjusts the radar data with the observed rain gauge data. Assuming that the rain gauge network provides accurate point precipitation data, the radar images could be corrected by:

$$B(t) = \frac{\sum_{i=1}^{n} \sum_{j=1}^{m} G(t_{i,j})}{\sum_{i=1}^{n} \sum_{j=1}^{m} R(t_{i,j})}$$

$$R^*(j) = B(t) \times R(j)$$

(6.1)

where $G(t_{i,j})$ is the precipitation amount from rain gauge i. j is the time step within a time interval t. $R(t_{i,j})$ represents the precipitation amount on the radar pixel where rain gauge i is located at the time j. In fact, the B coefficient represents the relationship between observation data $G(t_{i,j})$ and the corresponding extracted radar-point data $R(t_{i,j})$. R and R^* are the original and corrected radar rainfall, respectively. In this study, a daily time interval is considered for estimating the coefficient B for each time step, which results in having a constant correction factor for each day, individually. This means that m is 288 as the data are provided at a 5 minute temporal resolution. For the days on which Eq. 6.1 has an indeterminate form, i.e. when no rainfall is recorded by the rain gauge network, the B coefficient is set to 1.

Applying MFB does not have any smoothing effect, or, in other words, the structure of images after using MFB is very similar to that in the original radar data. Applying MFB to radar data was considered here to prevent unrealistic radar data values, whereas using radar data directly would also be possible since the relative errors obtained in the end would not change significantly.

6.2.2 Traffic model

The traffic model used in this study is similar to the one used by HABERLANDT and SESTER (2010). It is based on the road data derived from the Open Street Map (OSM). The traffic density is estimated using the data from the Federal Highway Research Institute (BASt) which provides the number of cars per day for certain points along federal roads and highways. For each particular catchment, those traffic count points within and close to the catchment, concerning federal roads (corresponding to the OSM road type "primary"), are selected. The traffic count number per catchment is estimated therefrom. Based on this number, cars are generated applying the methodology described in the following. The assumptions underlying the traffic model are always conservative assumptions concerning the number and distribution of cars. This means that the number and spatial distribution of the cars is considered lower and less dense in the model than in reality:

(a) Only larger roads on/and surrounding the study area are considered which includes the "*primary*" and "*secondary*" OSM road types (corresponding to the German "*Bundesstraßen*" and "*Landstraßen*" road types). Because of the relatively high practical uncertainties related to the RCs on highways, these road types are excluded. Smaller roads are also neglected due to the low traffic.

(b) An average speed of 80 km/h is considered to calculate the number of cars for each catchment. The assumed average speed is higher than in practice, which results in a lower number of cars than in reality (see Eq. 6.2). This follows the conservative assumption mentioned earlier.

(c) Due to the lack of traffic count data for the "secondary" OSM road type, the traffic count for this road type is calculated using half the "*federal roads*" (OSM "*primary*" roads) traffic count data. This also follows the conservative considerations for the traffic model assumptions.

In order to estimate the number of cars driving simultaneously within and around a catchment, the following equation is used for each catchment and each of the two road types separately:

$$t = \frac{X}{h}$$
$$z = t^{-1} \times \bar{v} \qquad (6.2)$$
$$n = \frac{l}{z}$$

where X is the number of cars from the traffic data over a certain time period h, $\bar{v}$ is the assumed average car speed and z is the space between two cars. The number of cars driving simultaneously in and around the catchment area n is then estimated using the total roads length l on a catchment. Due to the long period of time considered in this study, the day-night variation in traffic count is considered insignificant. However, different RC density scenarios address the possible change in the number of RCs. Therefore, the daily average number is used in this study. This number is subsequently used for generating cars randomly on the OSM road network at each time step. This means that the points representing RCs are not dependent in successive time steps, i.e. no car identities are modeled.

It is important to notice that car speed, wind speed and wind direction influence the performance of RainCars in practice. RABIEI et al. (2013) proposed using a linear relationship for taking the

effect of the car speed for RainCars into consideration. A similar approach could be applied for compensating the effect of wind speed, knowing the wind direction.

6.2.3 Network density of rain stations

In order to compare the network densities for rain gauges and RC scenarios, the network density of each subcatchment for each scenario is calculated in a similar way to that used by (HABERLANDT and SESTER, 2010). The network density is calculated using the kernel density estimator (SILVERMAN, 1986):

$$D_i = \frac{1}{\pi r^2} \sum_{j=1}^{n} k_j \text{ with } k_j = \begin{cases} 3\left(1 - \left(\frac{d}{r}\right)^2\right)^2 & \text{for } d \leq r \\ 0 & \text{for } d > r \end{cases} \tag{6.3}$$

where n is the number of observation points (either stations or RCs) within the search radius r = *20000 m* and d is the distance to subcatchment cells (the ones for which the density is being calculated). D_i is calculated for each subcatchment cell and averaged over all subcatchment cells. The kernel density estimator considers not only the observation points in the subcatchment, but also the ones within the search radius.

6.2.4 Uncertainties for RainCars

In order to consider the uncertainties in rainfall measurement using RCs, the results of laboratory experiments (RABIEI et al., 2013) are utilized. The relationship between sensor reading (W) and rainfall intensity (R) is named W-R relationship. Signal lengths from the optical sensors are considered as sensor readings.

$$\hat{R} = a + bW + \varepsilon \tag{6.4}$$

where $\hat{R}$ is the rainfall intensity, W is the sensor reading, a and b are the linear regression coefficients and ε represents the random error. The assumption behind the linear regression model is that the error is normally distributed, with mean = 0 and variance = σ^2. This provides a simple error model for the measured uncertainties from RCs.

Three different linear W-R relationships between sensor readings and rain rate are discussed by RABIEI et al. (2013). The first relationship considers wiper frequency as sensor. As wiper activity is influenced by several factors, such as driver preferences, car speed, number of wiper speed levels defined for each car type, etc, this alternative is considered as impractical. The two other remaining alternatives are the W-R relationships derived from the optical sensors. Two optical sensors, Hydreon and Xanonex, with promising results were investigated by RABIEI et al. (2013) and suggested for further use. The two sensors performed similarly, whereas the Hydreon performed slightly better. Because of the Xanonex shape and its ease of installation on cars, it is decided to investigate the Xanonex W-R relationship. The device bounces infrared beams within its lens. Rain drops escape some of the beams, and consequently, drops could be sensed when there is a change in beam intensity. This change could represent the rain rate observed by the sensor. More detailed information about the functionality of the device could be found in RABIEI et al. (2013).

Although a relatively strong relationship between the two variables exists, one encounters difficulties for smaller rain rates. According to the estimated regression line, negative rainfall could be obtained using Eq. 6.4, which is not possible. By neglecting the negative values, a systematic positive bias would enter the data. In addition, the uncertainties of the devices on the market are usually expressed as a percentage, which illustrates a smaller absolute error when smaller values are measured. Considering Eq. 6.4 does not account for those two problems. Therefore, in order to investigate the uncertainties for the sensor readings, a power regression model is used to describe the W-R relationship:

$$\hat{R} = a \times W^b \times \varepsilon \tag{6.5}$$

where $\hat{\boldsymbol{R}}$ is the rainfall intensity, W is the sensor reading, a and b are the regression coefficients and ε is the random error. Taking the logarithm of both sides of Eq. 6.5 gives:

$$log(\hat{R}) = log(a) + b \times log(W) + log(\varepsilon) \tag{6.6}$$

As is assumed for simple linear regression, a constant random error, here $log(\varepsilon)$, is considered. It should be noticed that the error variance is constant in log transformed space and variable in original space. The parameters of the linear regression in the Eq. 6.6 are optimal in the log space, nut not after back transformation, i.e. the original space.

Negative rain rates can no longer be estimated because of the log-log transformation to the data. Implementing this data transformation also leads to a more accurate performance for smaller rainfall values, which is different to the constant value considered by RABIEI et al. (2013).

The traffic model provides coordinates of the RCs for each time step. The rain rate for each RC is extracted from the reference data set, i.e. radar data. The device outputs are signal lengths related to rain intensities (RABIEI et al., 2013). In order to consider the uncertainties for RCs, the corresponding signal length of each extracted value would be estimated using the W-R relationship. A normally distributed error $log(\varepsilon)$ with mean = 0 and variance = σ^2 is randomly selected and added to $log(R)$ before re-transformation.

6.2.5 Areal rainfall estimation

Ordinary Kriging (OK) is an interpolation method which is widely used for several hydrological variables such as temperature, rainfall, wind etc. OK is implemented here for interpolating data from both RCs and rain gauges. It is worth noticing the fact that OK is only optimal when the data are Gaussian. However, the benefit of using RCs can be explored by comparing the quality of areal rainfall estimated by rain gauges with when only RCs are used instead. A relative comparison is carried out, resulting in trivializing the non-Gaussianity of the data. For a detailed description of the method, please refer to geostatistical text books such as ISAAKS and SRIVASTAVA (1990).

The experimental variogram is estimated using the following equation:

$$\gamma_k(h) = \left[\frac{1}{2 \times N(h)} \sum_{i=1}^{N(h)} (Z(x_i) - Z(x_i + h))^2 \right] \tag{6.7}$$

where *N(h)* represents the number of data pairs, h is the separating vector, x the location and. Similar as in RABIEI and HABERLANDT (2015), a seasonal average variogram is used here. The experimental variogram is estimated using radar data when 1000 random radar cells are taken. Only the time steps with an average rainfall above a defined threshold are selected for variogram estimation. The following equation is used for estimating climatological variograms over *n* time steps:

$$\gamma_{st}(h) = \frac{1}{n} \sum_{i=1}^{n} \frac{\gamma(h,i)}{var(i)} \tag{6.8}$$

where $\gamma(h,i)$ is the variogram for the h distance class and *var(i)* represents the variance in time step *i*. An exponential variogram is considered as the theoretical variogram model:

$$\gamma_h = c_0 + c \left[1 - exp \left(-\frac{h}{a} \right) \right] \tag{6.9}$$

where *a*, *c* and c_0 are the range, the sill and the nugget effect, respectively.

The variograms are fitted using radar data with 5 min temporal resolution as the goal is to interpolate rain gauges as well as RCs on 5 min temporal resolution.

6.2.6 The HBV hydrological model

The hydrological model used in this study, HBV-IWW, is a modified semi-distributed version of the HBV model (LINDSTRÖM et al., 1997). The model has a horizontal spatial discretization in subcatchments, which are linked to each other by river reaches. For each of the subcatchments a snow routine, a soil routine, a response routine and a transformation routine is applied. The snow routine classifies precipitation as rainfall or snowfall and also takes snow melt into account. After that, the sum of the rainfall and snowmelt passes the soil routine which consists of two modules. The first module calculates the actual evapotranspiration, while the second module calculates the contributing runoff depending on precipitation and actual soil water content. The contributing runoff is then directly linked to the upper groundwater layer of the response routine, where surface runoff, interflow, percolation and the actual water content of the upper groundwater layer are calculated. Percolation contributes to the lower groundwater layer wherefrom the base flow is calculated. Surface runoff, interflow and base flow are finally added together and transformed with a simple triangular unit hydrograph. If more subcatchments are connected to each other, the Muskingum method is used for river routing.

The model is calibrated using the Simulated Annealing algorithm (KIRKPATRICK, 1984) for which 1000 iterations are considered. The objective function is:

$$OF = (1 - NSE) + (1 - NSE_{Log}) \rightarrow min \qquad (6.10)$$

where *NSE* is the Nash-Sutcliffe coefficient after NASH and SUTCLIFFE (1970), and NSE_{Log} is the *NSE* with logarithm of discharges. A more detailed description of the parameter calibration procedure as well as further details of the HBV-IWW model can be found in WALLNER and HABERLANDT (2015). Unlike the common procedure of calibrating the parameters of a hydrological model and validating them afterwards, when two separate time periods are defined, in this study the whole time period is considered for calibrating the model parameters. The HBV parameters are calibrated lumped as only the rainfall data are to be investigated. This means that all the subcatchments of each catchment have the same model parameter set. For all the scenarios in the following, the same parameter sets are used for an explicit comparison of the results. As the main purpose of the study is to investigate the influence of different means of rainfall measurement, the model calibration is less important than in studies dealing with observation data.

6.2.7 Performance measures

A common way to evaluate the performance of interpolation is cross-validation, i.e. the leave-one-out approach. The resemblance of the estimations to the observations illustrates the quality of the interpolation technique. Since reference radar data are considered as the truth in this study, the areal rainfall estimated by each scenario is directly compared with the reference areal rainfall. The following criteria are used for evaluation.

The Root Mean Square Error is estimated by:

$$RMSE(i) = \left[\sqrt{\frac{\sum_{j=1}^{J}(Z_{i,j}^{*} - Z_{i,j})^2}{J}} \right], \qquad (6.11)$$

the Nash-Sutcliffe coefficient by:

$$NSE(i) = 1 - \frac{\sum_{j=1}^{J}(Z_{i,j}^* - Z_{i,j})^2}{\sum_{j=1}^{J}(Z_{i,j} - \bar{Z})^2} \qquad (6.12)$$

and the Percent Bias (*Pbias*) is estimated by:

$$Pbias(i) = 100 \times \frac{\sum_{j=1}^{J}(Z_{i,j}^* - Z_{i,j})}{\sum_{j=1}^{J}(Z_{i,j})} \qquad (6.13)$$

where Z^* is the estimated areal rainfall and Z is the corresponding reference areal rainfall. j is the number of time steps considered for the subcatchment i. These statistical measures are used also for evaluating the performance of the hydrological model where Z^* and Z are then the simulated discharges and reference discharges, respectively.

A positive *Pbias* indicates overestimation, whereas a negative value indicates underestimation.

6.3 Study area and data

A part of the state of Lower Saxony covered by the weather radar located at Hanover airport and the three catchments in Fig. 6.1 encompass the study area. As mentioned, the benefit of RCs is investigated by comparing with what occurs in practice, i.e. when only rain gauges are considered. In this study, it is assumed that the coordinates of rain gauges and the coordinates of 53 rain stations provided by the German Weather Service (DWD) are identical.

The transparent blue circle in Fig. 6.1 with a 128 km radius is the area being scanned by the Hanover weather radar, whereas the points represent the 53 rain gauges considered in this study. The Digital Elevation Model shows that the northern part of the study area is relatively flat and a region with mountainous characteristics is in the south-eastern part. The precipitation amount also varies within the study area from around 500 mm/yr in the north to 1700 mm/yr in the mountains (BERNDT et al., 2014). The mean annual rainfall in Fig. 6.1 for each subcatchment shows also the spatial rainfall variation over the study area. Those values are derived from radar data, from 2006 to 2010. This is more evident for the Nette catchment as the south-eastern subcatchment receives a larger amount of rainfall than the other subcatchments. Although the
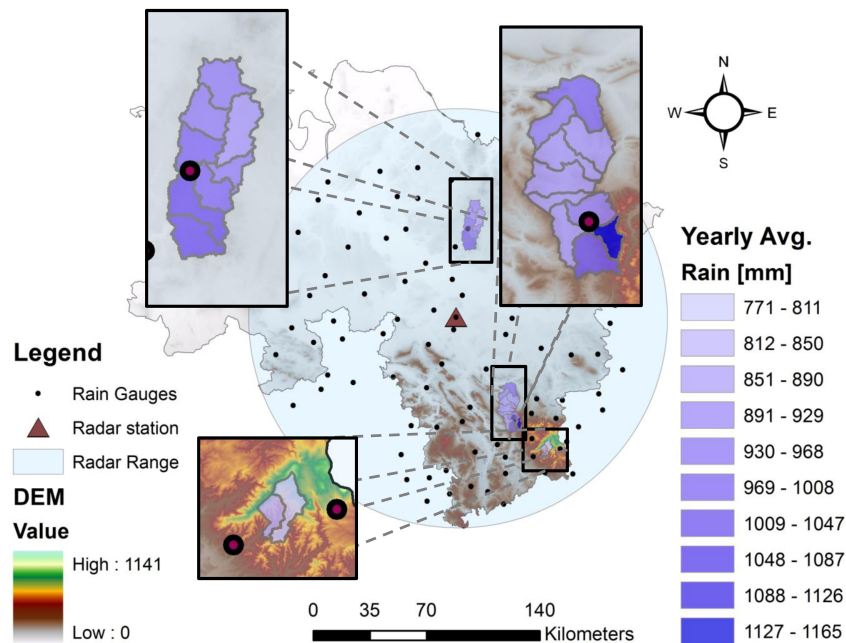
Figure 6.1: Study area, catchments, station network and mean annual precipitation (MAP) from 2006 to 2010 from radar data. From north to south: Böhme, Nette and Sieber catchments.

Sieber catchment is located in the mountainous area, the mean annual rainfall is relatively low. This could be explained by the fact that the catchment is located at the leeward side of the mountains considering the usual west-to-east weather front moving direction.

6.3.1 Catchments

Three catchments of the Aller-Leine river basin, which have different characteristics, are considered in this study, Fig. 6.1. Not only are the characteristics of the catchments important, but also are the locations of the rain gauges. The Böhme catchment located in the northern part, with a relatively flat terrain, contains eight subcatchments and covers 285 km^2. This catchment varies between 50 m and 150 m in elevation and contains one rainfall station. The Nette catchment has 10 subcatchments covering 309 km^2 and is partly located in the mountainous area, where the elevation reaches up to 550 m. In contrast, the northern part of this catchment is mostly flat. An important point worth mentioning here is that the only station available in this catchment is located in front of the hillside in the southern part. The Sieber catchment is located completely in the mountainous area and has two subcatchments covering 45 km^2. There are some stations close to the catchment, but no stations are available within it.

6.3.2 Radar rainfall

The C-band Hannover weather radar provides radar data with a 5-min temporal resolution and an azimuth resolution of $1°$. The spatial resolution along each beam is 1 km. The time period from 2006 to 2010 is considered in this study. The dx-radar product provided by the DWD is used and processed as following. First, the reflectivity (Z in $mm^6 m^{-3}$) is transformed to rain intensity (R in mm/hr) by the following relationship:

$$Z = a \times R^b. \tag{6.14}$$

Standard DWD parameters (RIEDL, 1986; SELTMANN, 1997) are used, where $a = 256$ and $b = 1.42$. A straightforward clutter detection similar to that of BERNDT et al. (2014) is applied thereafter. The final step is to interpolate the rain intensities on rectangular grids using the Inverse Distance Weighted (IDW) technique. This produces rainfall of 1 km $\times$ 1 km spatial resolution. Afterwards, the Mean Field Bias method (see section 6.2.1) is implemented to adjust radar data with the observed rain gauge data.

As the observed data are not used directly for the objectives of this study, it is decided not to describe them here to avoid any confusion.

6.3.3 W-R relationship

RABIEI et al. (2013) used a linear regression model to describe the W-R relationship between the Xanonex sensor readings and rain intensity. Fig. 6.2 illustrates this linear relationship with a = 0.2408 and b = -5.4915 (Eq. 6.4). The dots represent the observations in the laboratory whereas the dashed lines show the 95% prediction limits. A detailed description of the laboratory experiments is provided in RABIEI et al. (2013). The main disadvantage is when facing small rainfall values. As mentioned, by considering this relationship and the error distribution for linear regression, negative rain rates can be estimated.
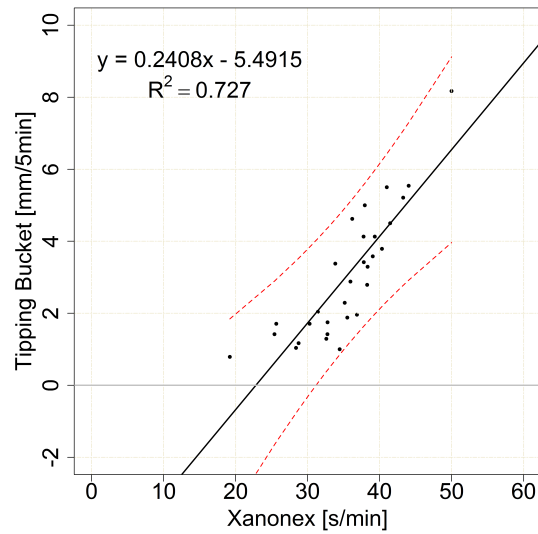
Figure 6.2: Xanonex W-R relationship (RABIEI et al., 2013)

Table 6.1: Number of cars driving at the same time for each RCs scenario on each catchment

	5%	4%	3%	2%	1%
Böhme	38	30	23	15	8
Nette	138	110	83	55	28
Sieber	14	11	8	6	3

6.4 Results and discussion

In the following, the results of the steps taken for investigating the benefit of using RCs for areal rainfall estimation as well as discharge simulation are presented and discussed.

6.4.1 Traffic model

The number of cars is estimated using Eq. 6.2. It is assumed that only a small portion of cars is equipped with sensors measuring rainfall. In this study, from 1% to 5% of all cars on the roads are considered to measure rainfall which describes all the RC scenarios. For each 5-minute time step, the number of cars is calculated for the 5% scenario. The other scenarios are generated therefrom. Table 6.1 depicts different RCs' scenarios considered in this study.

Fig. 6.3 shows the road network considered for the three catchments. As seen in Table 6.1, a denser network than for the other catchments is available for the Nette catchment. As the Nette

catchment is partly located in mountainous area, even this denser network might not provide enough information. This is due to the fact that the RCs are not available overall because of the road network. For that reason, in subcatchments such as the south-eastern subcatchment, the number of available RCs is lower than in the other subcatchments.
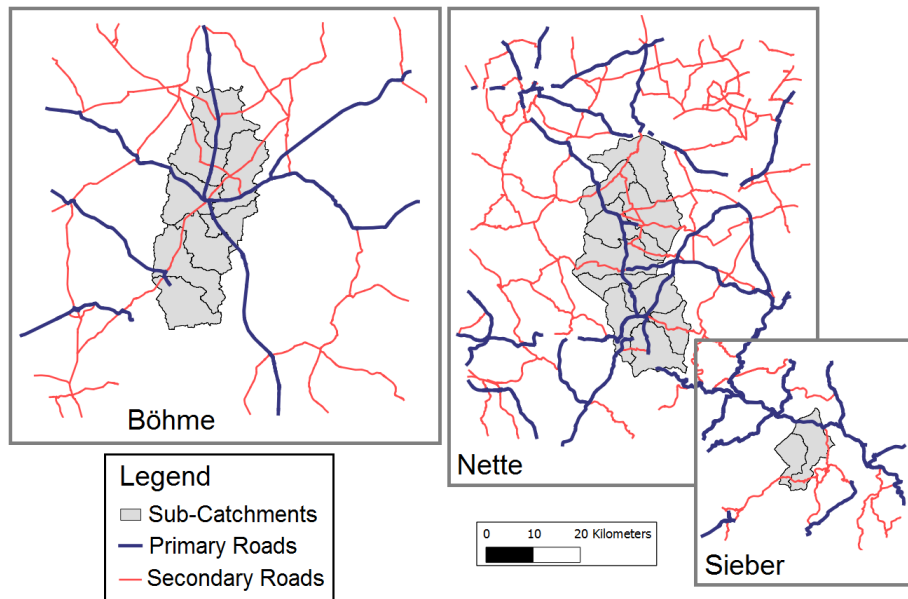
Figure 6.3: The road network on which the RCs are modeled.

6.4.2 Network density

Before illustrating the results of the simulations, i.e. areal rainfall as well as runoff simulation comparison, the network densities using Eq. 6.3 for different scenarios are presented. This helps to determine whether the network density influences the results.

Fig. 6.4 shows the network densities estimated for the scenarios being investigated in this study. Although the density varies among the catchments, Fig. 6.4 shows that all the RC scenarios have a higher density than the rain gauge network. Depending on the accuracy of the measurement devices, i.e. RCs or rain gauges, the network density has a variable influence. A more detailed investigation is provided in subsection 6.4.6.2.
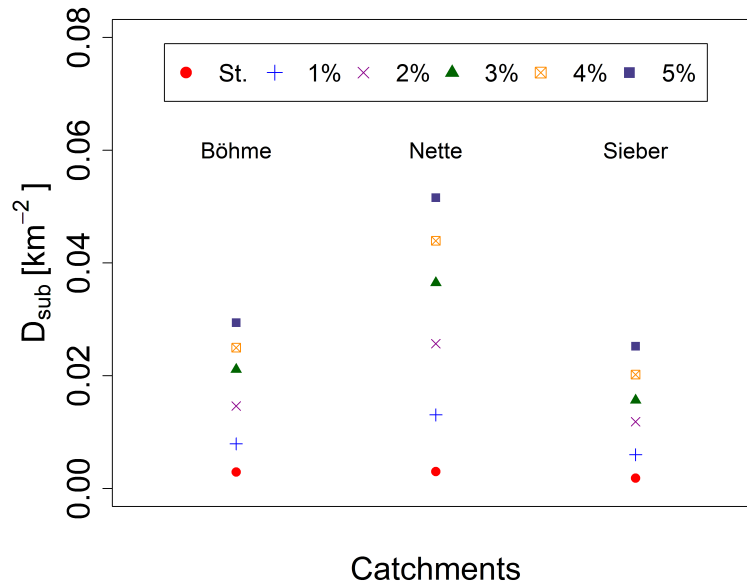
Figure 6.4: Network density of the catchments for different scenarios

6.4.3 RainCars Uncertainty

The uncertainty related to rain rate by RCs is described by Eq. 6.4 to Eq. 6.6 where ε represents the random error. The normal distribution that defines the random error for each signal reading (signal length) corresponding to each rainfall amount has the residual variance estimated by the vertical distances between the observations and the regression line. The random error, $\log(\varepsilon)$, is then simulated using the normal distribution. As discussed earlier, a power regression model describes the W-R relationship in this study.

Fig. 6.5 (a) shows the W-R relationship after log-log transformation. The same assumption as before is valid, namely that the random error is normally distributed and derived from the deviation between observation points and the linear regression model. Fig. 6.5 (b) illustrates the W-R relationship implemented in this study. It is derived using the following steps: 1) applying log-log transformation on both axes, 2) applying linear regression on the transformed data (Fig. 6.5 (a)), 3) estimating the residual variance for the normal distribution describing the random error for the linear regression model and 4) transferring the data back for practical use (Fig. 6.5 (b)).

The data transformation has, in general, two important effects on the W-R relationship: 1) preventing the estimation of unrealistic rain rates and 2) skewing the distribution of random
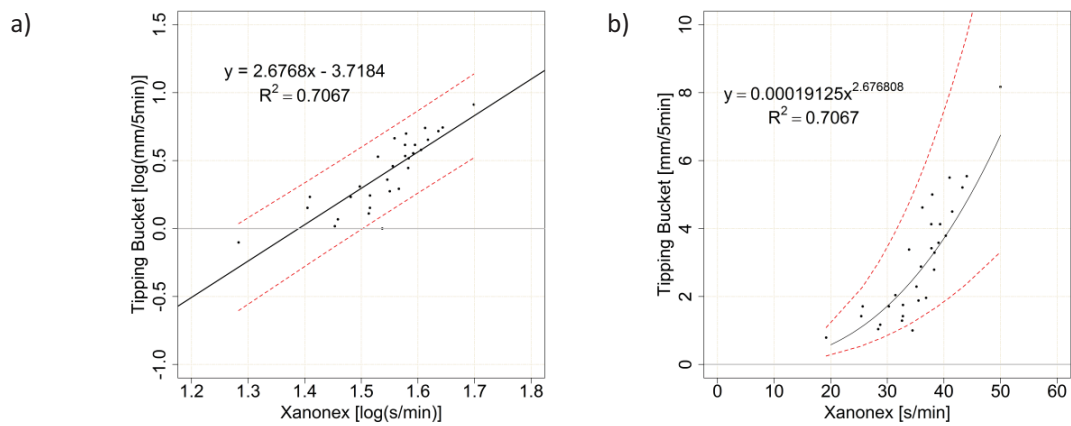
Figure 6.5: (a) Xanonex log transformed W-R relationship after Eq. 6.6 (b) Xanonex W-R relationship after Eq. 6.5; the red lines illustrate the 95% prediction limits

error. The latter aspect affects also the prediction limit in Fig 6.5. As can be seen in Fig. 6.5b, the upper and lower limits bend when further from the origin which results in larger inaccuracy for the rain rate estimated by RCs for higher rainfall intensities. On the other hand, the positive skewness introduces a positive bias that causes overestimation when estimating rain rate by RCs. This can be seen when comparing the distances from the model line to the upper and lower prediction limits. Although the W-R relationship has this deficiency, a larger number of RCs and more accurate optical sensors can help compensate this problem. These two aspects are addressed in section 6.4.6.2 and 6.4.6.3, respectively.

6.4.4 Variogram properties used in this study

The properties of the variograms used in this study are provided in Table 6.2.

The variograms are fitted using radar data with 5 min temporal resolution as the goal is to interpolate rain gauges as well as rainfall from RCs on a 5 min temporal resolution. A relative large range is estimated in winter time which illustrates different seasonal rainfall patterns. It supports the seasonal separation for interpolating the data which was discussed earlier. As can be seen, the properties of the variograms change even among the same seasons in different years. Therefore, it is decided to use the variable variograms provided in Table 6.2.

Table 6.2: Theoretical variogram model parameters used in this study, a_{eff} is the effective range, c_c the sill and c_0 the nugget effect

Time period:	2006 (01-03)	2006 (04-09)	2006-07 (10-03)	2007 (04-09)	2007-08 (10-03)	2008 (04-09)
c_0 (-)	0.2	0.1	0.17	0.1	0.13	0.3
c_c (-)	1	0.9	0.9	0.85	1	0.7
a_{eff} (m)	60000	24000	42000	24000	42000	36000

Time period:	2008-09 (10-03)	2009 (04-09)	2009-10 (10-03)	2010 (04-09)	2010 (10-12)
c_0 (-)	0.1	0.1	0.1	0.1	0.1
c_c (-)	1	0.85	1	0.87	1
a_{eff} (m)	48000	22500	45000	27000	48000

6.4.5 Reference discharge

As mentioned earlier, the simulated discharge for different scenarios will be compared with the reference discharge. The reference discharge, the benchmark, is simulated using radar data after applying Mean Field Bias correction (creating the reference rainfall data) as input to the HBV-IWW model using pre-calibrated model parameters. Because of the lumped approach for calibrating the model parameters and the subcatchments with relatively small size, the rainfall characteristics, especially its spatial pattern, are the highest influencing factor in discharge simulation.

The performance of the HBV-IWW model is evaluated on an hourly temporal resolution. Therefore, an aggregation of 5 min interpolation data to hourly data is carried out before using it in the hydrological model.

6.4.6 Areal rainfall and simulated discharge for different sources

The value of the RCs in comparison to the rain gauge network is assessed by comparing areal rainfall estimations as well as the simulated discharges using these data. First, the results of using only the rain gauge network are presented. Thereafter, the results of using RCs for rainfall observations are provided and compared with when only the rain gauge network is used.

6.4.6.1 Rain gauge network

Areal rainfall estimation
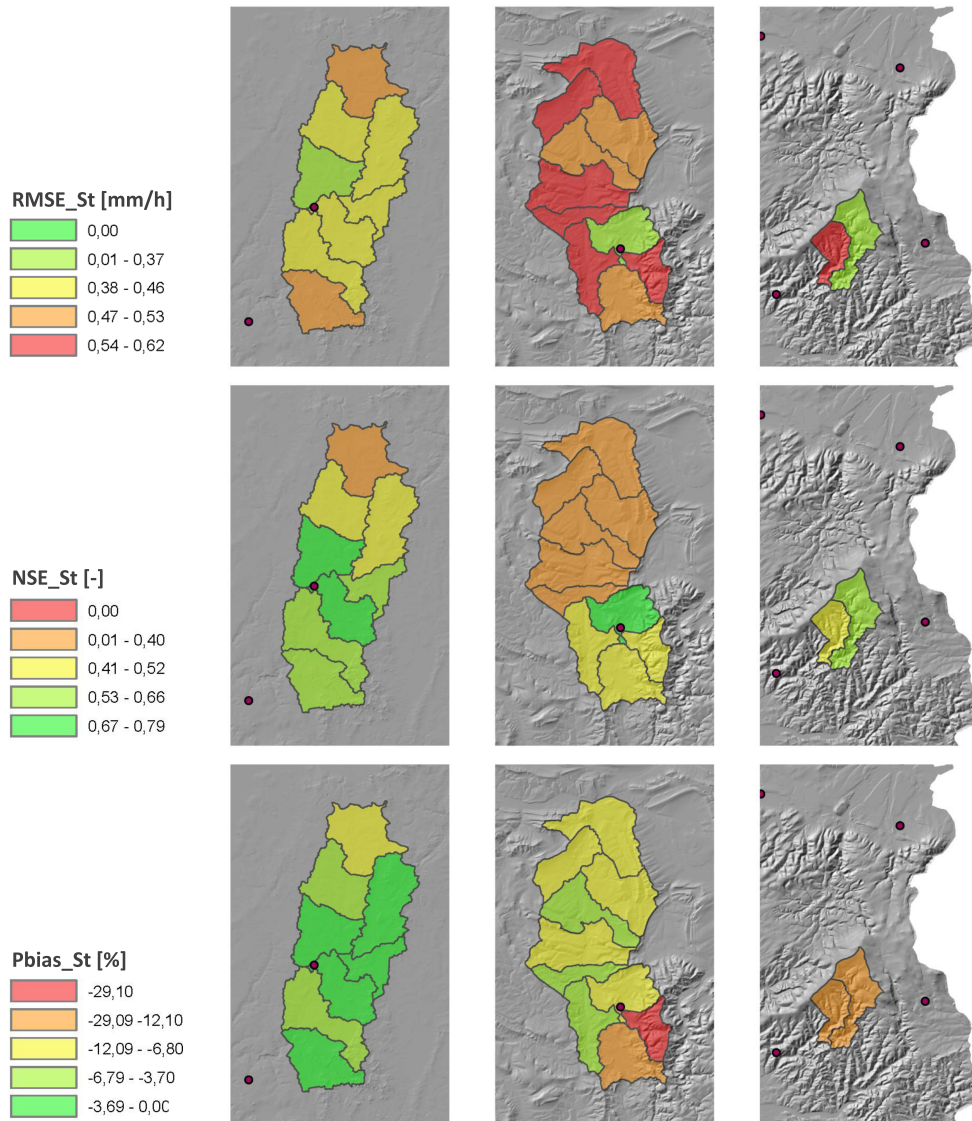
Figure 6.6: Areal rainfall estimation using rain gauges compared with the reference data in, from left to right, the Böhme, Nette and Sieber catchments. The polygons toward green colour present better results than the ones toward red colour.

The areal rainfall estimations corresponding to the three catchments shown in Fig. 6.1 are compared with the reference data. It should be noticed again that the comparison is carried out after interpolating the data with 5 min temporal resolution and aggregating the data to hourly

temporal resolution because of the required temporal resolution for the hydrological model.

Fig. 6.6 provides the statistical measures for the three catchments under study when evaluating the quality of areal rainfall estimation using only rain gauges. This is carried out by comparing the estimated areal rainfall using rain gauges and implementing OK with the reference data.

For the Böhme catchment having one station in the catchment and one close by provides sufficient rainfall information. As expected, the closer the subcatchments to the stations, the better the quality of areal rainfall estimation. The areal rainfall estimated for the northernmost subcatchment is not as good as for the other subcatchments because there is no station nearby. Although the potential for improving *RMSE* and *NSE* values exists, the *Pbias* criterion is in general relatively low. This means that the total water volume is estimated relatively well, and therefore for purposes such as hydrological modelling the quality of areal rainfall estimation might be sufficient.

Studying the Nette catchment, the subcatchment that includes a station has, as expected, a superior rainfall estimation quality to the other subcatchments. Unpredictably, the quality of areal rainfall estimation for the other subcatchments close to the station is weak. For example, although the two southern subcatchments are in the vicinity of a station, the statistical measures are relatively poor. A rapid change in elevation is evident when considering the DEM map in Fig. 6.1. Assuming that rainfall characteristics change along the elevation gradient, a change in the spatial rainfall pattern is expected. The single station is no longer able to provide the actual rainfall even for the surrounding subcatchments. This is in contrast to the Böhme catchment where the DEM map shows a flat catchment and the only station on the Böhme catchment is sufficient for areal rainfall estimation.

Although the Sieber catchment is smaller than the other two catchments and is expected to be more easily modelled, the catchment is located in a mountainous region and suffers from the fact that no rain gauge is available directly within the catchment. Owing these facts, the areal rainfall estimation is rather poor, especially when the *Pbias* is of concern. For such conditions, additional means of rainfall measurement would be beneficial.

Discharge simulation

The same statistical measures are used for evaluating the performance of the hydrological model. Depending on the location of stations, catchment characteristics and spatial rainfall

Table 6.3: Simulated discharge by rain gauges compared with the reference data

	Böhme	Nette	Sieber
RMSE (m^3/s)	0.98	2.8	0.51
NSE $(-)$	0.95	0.76	0.86
Pbias $(\%)$	-6.2	-22.5	-15.8

pattern, each catchment responds differently when only rain gauges are used. The reference discharge, the benchmark, is simulated using reference areal rainfall, i.e. radar data after MFB, and the pre-calibrated model parameters.

Table 6.3 provides the statistical measures of simulated discharges when only rain gauges are implemented. Although both the Böhme and Nette catchments benefit from having a station in the catchment, the two catchments responded differently. The Böhme catchment performs better than the other two catchments. From Fig. 6.7, it can be seen that the quality of the areal rainfall estimation for the Böhme catchment is the best. As discussed in the *study area and data* section (Fig. 6.1), the mountainous area receives more rainfall than the other parts of the catchment. The mountainous part of the catchment can cause a change in the spatial rainfall pattern. In other words, a fast elevation change (when the contour lines are tightly spaced together) can draw the isohyetal lines close together. This can explain the reason that the model performance in the Nette catchment is relatively poor. From the mean annual rainfall for each subcatchment provided in Fig. 6.1, it may also be concluded that the two southern subcatchments in the mountainous area produce a big share of the discharge. It is observed that one station can be sufficient for areal rainfall estimation for a flat catchment such as the Böhme catchment and would not be sufficient for a catchment such as the Nette catchment, which is partly located in the mountainous area. There is no station located in the Sieber catchment, which explains the poor *Pbias* in Table 6.3, although the other two criteria are rather good. In the Sieber catchment, not only the characteristics of the two subcatchments are similar, but also the spatial rainfall pattern over the two subcatchments which could explain the relatively good *NSE* values.

6.4.6.2 RCs against rain gauges using errors from laboratory experiments

Areal rainfall estimation

A similar strategy is pursued for the moving cars measuring rainfall. As before, the evaluation involves two parts. First, the areal rainfall estimation by implementing RCs is compared with

the reference rainfall. Thereafter, the simulated discharges are compared after using the data in the HBV-IWW hydrological model.

The benefit of using RCs for areal rainfall estimation can be assessed when their performance is compared with the standard approach, i.e. using only the rain gauges. To this end, after estimating the statistical measures by comparing with reference data, the difference between the statistical measures is addressed. This means that for example for the Root Mean Square Error $RMSE_{diff} = RMSE_{RCs} - RMSE_{St}$. As a result, negative $RMSE_{diff}$ values as well as positive NSE_{diff} values represent better areal rainfall estimation when using RCs compared to stations. For *Pbias*, the specific values are compared without building differences.
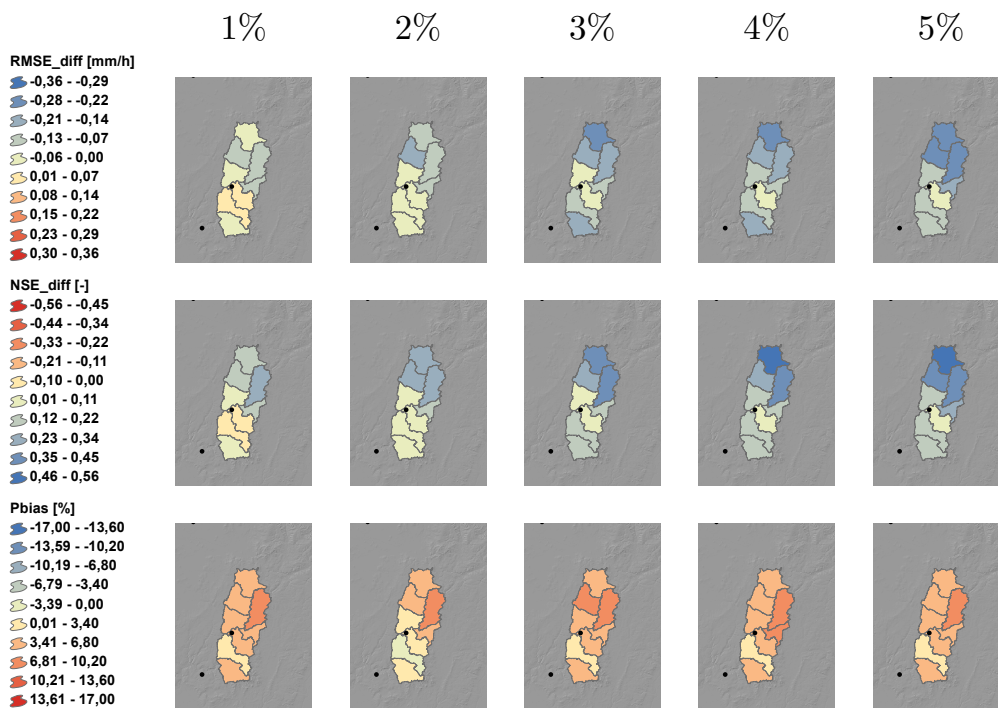
Figure 6.7: Areal rainfall estimation evaluation using RCs for the Böhme catchment. The blue colour for $RMSE_{diff}$ and NSE_{diff} illustrates the improvement of the areal rainfall estimation quality when RCs are used compared with when only rain gauges are considered.

Fig. 6.7 illustrates the statistical measures for the Böhme catchment when the RCs are used for areal rainfall estimation. Implementing RCs in general results in better areal rainfall estimation. As expected, the improvement in subcatchments away from the stations is more significant than the ones close to them. Also, the number of cars plays an important role. If the number of RCs increases, the quality of areal rainfall estimation improves. Considering only the two mentioned criteria, using RCs for areal rainfall estimation is always superior to using stations

in this catchment. The improvement for each subcatchment varies depending on the number of RCs as well as the location of the station. *Pbias$_{RCs}$* values show an overestimation of areal rainfall because of the positive skew of the error distribution as explained earlier (see Fig. 6.5b).
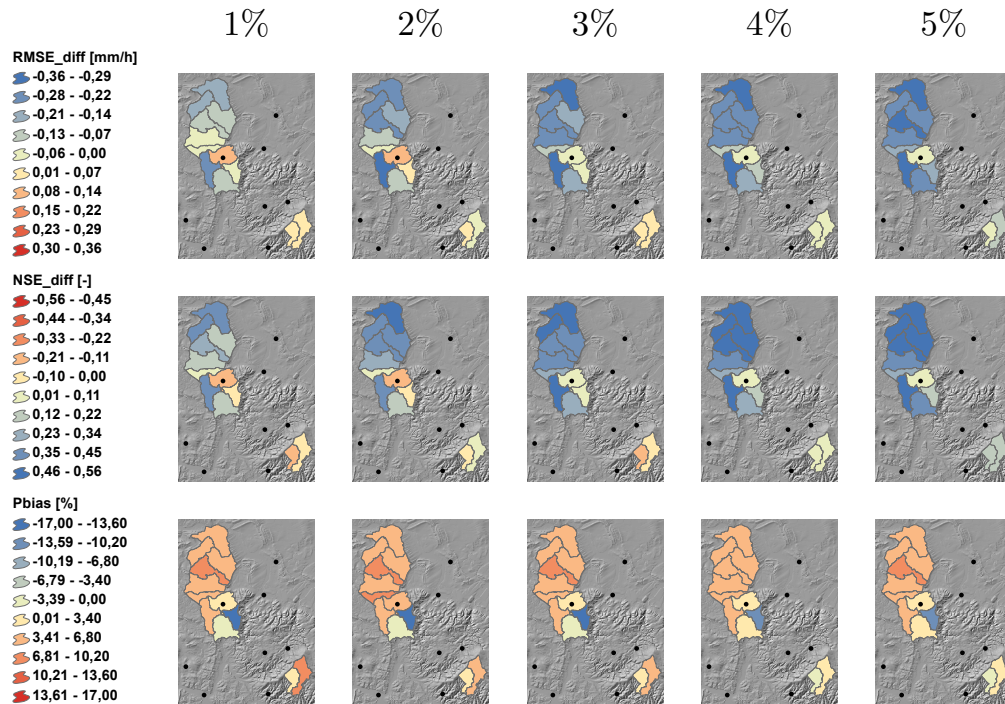
Figure 6.8: Areal rainfall estimation evaluation using RCs for the Nette and Sieber catchment. The blue colour for $RMSE_{diff}$ and NSE_{diff} illustrates the improvement of the areal rainfall estimation quality when RCs are used compared with when only rain gauges are considered.

Fig. 6.8 illustrates the statistical measures for different RC scenarios in the Nette and Sieber catchments.

The use of RCs for rainfall estimation in the Nette catchment has similar advantages as for the Böhme catchment. In contrast to that, RCs are not always beneficiary in the Nette catchment. A detailed investigation shows that the rainfall estimation for the subcatchment in which the station is located is hard to beat by using RCs. In contrast to all the subcatchments where an overestimation is observed, for the Nette basin, the subcatchment with red colour in *Pbias* responds differently. This can be explained by the RC network density. This part of the catchment suffers from the fact that RCs are rarely available because there are fewer roads as it is located in the mountainous part.

For the Sieber catchment using RCs also results in better areal rainfall estimation. Increasing

the number of RCs has again advantages. The improvement in areal rainfall estimation is not as strong as in the other catchments because of the existing stations in the vicinity of the catchment. Although *RMSE* and *NSE* do not vary significantly, comparing with Fig. 6.6, the *Pbias* criterion improves meaningfully.

It should be noted that although the Nette catchment benefits from a denser RC network (Fig. 6.4), because of the spatial rainfall pattern, the need for a higher number of RCs or a better location for the only station is evident.

Discharge simulation

Table 6.4: Simulated discharge by RCs compared with the reference data

Catchment		St.	1%RCs	2%RCs	3%RCs	4%RCs	5%RCs
	RMSE (m^3/s)	0.98	0.66	0.6	0.61	0.6	0.57
Böhme	NSE $(-)$	0.95	0.98	0.98	0.98	0.98	0.98
	Pbias $(\%)$	-6.2	6.4	6.1	7.4	7.6	7.4
	RMSE (m^3/s)	2.8	1.01	0.84	0.67	0.73	0.76
Nette	NSE $(-)$	0.76	0.97	0.98	0.99	0.98	0.98
	Pbias $(\%)$	-22.5	4.8	6.8	5	6.7	7.2
	RMSE (m^3/s)	0.51	0.55	0.58	0.53	0.48	0.37
Sieber	NSE $(-)$	0.86	0.83	0.81	0.84	0.88	0.92
	Pbias $(\%)$	-15.8	7.5	6	4.7	3.2	2.6

Table 6.4 provides the statistical measures of simulated discharges when RCs are implemented. The first column, titled "St.", refers to when only rain gauges are considered, which is included here again to facilitate easy comparison.

Although the Böhme catchment performs the best among the three catchments when only rain gauges are considered, using RCs is still useful. Fig. 6.8 shows that the areal rainfall estimation improves slightly when using RCs. For analyses requiring fine temporal and spatial resolution data, e.g. urban hydrology, using RCs may improve the simulation results more evident. Due to the fact that the improvement in discharge simulation is not very strong in this catchment, with the given temporal and spatial resolution, for such studies the need for using RCs can be considered inessential.

As discussed earlier, because of the characteristics of the Nette catchment, this catchment has the highest potential for improvement by RCs. Implementing even a small number of RCs

improves the results significantly. As seen in Fig. 6.4, the Nette catchment has the highest RC network density among the three catchments. This explains the better performance in this catchment. As expected, positive *Pbias* in the simulated discharge indicates overestimation, which follows the areal rainfall overestimation observed earlier.

Unlike the other catchments, the Sieber catchment is located in the mountainous area. The *NSE* and *RMSE* criteria do not improve significantly when using RCs. Taking a deeper look at the traffic model data, from 1% scenario to 5% scenario, the number of cars measuring rainfall is 3, 6, 8, 11 and 14, respectively (see Table 6.1). Only two scenarios can result in better discharge simulation, 4% and 5% indicating the least required RC network density for this catchment. As with the other two catchments, using RCs results in the overestimation of the discharge.

The network density of the 1% RCs scenario for the Nette catchment is similar to those of the Böhme and Sieber with 2% RCs scenarios (Fig. 6.4). Taking the similarity of the network densities into account, the improvement of the hydrological model performance in the Nette catchment is more evident than for the other two catchments. It shows that the RCs are more valuable in the catchments such as the Nette when the spatial rainfall pattern varies within the study area (see section 6.3). Improving the discharge simulation performance for bigger catchments such as the Nette and Böhme seems to be easier achievable with less density of RCs than for smaller catchments such as the Sieber. Additionally, even a small number of RCs can improve the discharge simulation significantly. Depending on the quality of the required hydrological analyses, the need for the use of RCs is open to discussion. Basically, a higher number of equipped cars are needed for mountainous catchments in this study area than for flat catchments. In other words, the need for increasing the number of observations is evident when the spatio-temporal variation of rainfall is high.

6.4.6.3 RCs against rain gauges using hypothetical errors

Areal rainfall estimation

The minimum rainfall measurement accuracy required for the RCs to be useful is investigated in this section. All the different accuracies are addressed for the 5% RCs scenario specifically.

The error for the linear model is estimated on the log-log transformed data, Fig. 6.5. The normal distribution was defined by the variance (σ^2), equal to 0.021, from laboratory experiment results. In order to investigate the importance of the error on the results, four other variances of 0.0,

Table 6.5: Uncertainties for RCs when estimating areal rainfall and averaging over all subcatchments; 5% traffic model is considered

		$\sigma^2 = 0.0$	$\sigma^2 = 0.01$	$\sigma^2 = 0.04$	$\sigma^2 = 0.09$	$\sigma^2 = 0.021$	St.
Böhme	RMSE (mm/h)	0.27	0.27	0.30	0.38	0.28	0.44
	NSE $(-)$	0.85	0.85	0.81	0.70	0.84	0.58
	Pbias $(\%)$	-0.49	2.19	10.56	26.26	5.19	-3.22
Nette	RMSE (mm/h)	0.28	0.29	0.32	0.42	0.30	0.53
	NSE $(-)$	0.84	0.83	0.80	0.65	0.82	0.43
	Pbias $(\%)$	-2.8	0.09	8.5	24.07	3.11	-10.21
Sieber	RMSE (mm/h)	0.37	0.37	0.38	0.43	0.37	0.46
	NSE $(-)$	0.69	0.69	0.68	0.6	0.69	0.53
	Pbias $(\%)$	-4.55	-1.7	6.4	21.5	1.2	-14.45

0.01, 0.04 and 0.09 are considered. At the end, the areal rainfall estimation quality as well as the performance of the hydrological model was compared with that of using the original variance from the laboratory.

Table 6.5 provides the averaged statistical measures for each catchment. The areal rainfall estimation considering different errors for RCs is compared with the reference data. The same assumptions as earlier (see section 6.4.3) are taken with different variances for the distribution function representing the error range. St. represents the areal rainfall estimation performance when only the rain gauges are implemented.

The rainfall overestimation by implementing higher σ^2 values is evident. For all catchments even assuming a relatively large uncertainty of $\sigma^2 = 0.09$, *NSE* and *RMSE* values improve compared with when only rain gauges are considered. As the *Pbias* is quite large for $\sigma^2 = 0.04$ and $\sigma^2 = 0.09$, the use of RCs for areal rainfall estimation is questionable. In fact, for such cases, rainfall data observed by RCs could be considered as additional information for areal rainfall estimation, e.g. in External Drift Kriging or Kriging with Uncertain Data.

Assuming no inaccuracy for the measurement devices, i.e. St. and $\sigma = 0.0$, a negative *Pbias* still exists representing an underestimation of areal rainfall. Although OK is an unbiased interpolation technique, its performance is strongly dependent on the measurement locations. In an ideal situation, measurements should take place in regard to the variation in spatial rainfall patterns. This can not be fulfilled in practice due to the dynamic nature of rainfall. Missing the minima and maxima over the study area can lead to overestimation and underestimation, respectively. It is more probable to miss maxima than minima due to the fact that high rainfall intensities may occur in places where no RCs or rain gauge observations are available. Minima can be captured easier than maxima as it covers a larger area, illustrating the positive skewness

of the rain rate distribution. This might explain the minor negative *Pbias* derived by RCs even if when $\sigma = 0.0$.

Discharge simulation

Table 6.6 provides the averaged statistical measures of the simulated discharges for each catchment when the 5% RC scenario is considered. As expected, the best performance belongs to the RCs scenario for which the measurement error is assumed to be zero ($\sigma^2 = 0.0$). The quality of the simulated discharge lowers by increasing the error of the measurement devices (RCs). A similar trend can be found as that for areal rainfall estimation, in that the discharge overestimation becomes meaningful by increasing the uncertainty of the RCs. Implementing RCs with large uncertainty for the measurement values leads to a relatively weak discharge simulation. On the other hand, even though using RCs results in discharge overestimation (*Pbias* criterion), the quality of simulated discharges for variances (σ^2) smaller than 0.04 improves in terms of *RMSE* and *NSE*, compared with when only rain gauges are considered (St.). As discussed before, in order to overcome the overestimation caused by RCs, one may consider RCs as additional information in interpolation techniques. RCs could be corrected in practice by implementing quantile mapping like the one introduced by RABIEI and HABERLANDT (2015).

Table 6.6: Investigating different uncertainties for RCs when simulating discharge compared with the reference discharge; 5% traffic model is considered

		$\sigma^2 = 0.0$	$\sigma^2 = 0.01$	$\sigma^2 = 0.04$	$\sigma^2 = 0.09$	$\sigma^2 = 0.021$	St.
	RMSE (m^3/s)	0.34	0.38	1.05	2.64	0.57	0.98
Böhme	NSE $(-)$	0.99	0.99	0.94	0.65	0.98	0.95
	Pbias $(\%)$	-1	2.9	15.5	40	7.4	-6.2
	RMSE (m^3/s)	0.65	0.52	1.56	4.19	0.76	2.8
Nette	NSE $(-)$	0.99	0.99	0.92	0.45	0.98	0.76
	Pbias $(\%)$	-4.9	0.9	18.6	52.6	7.2	-22.5
	RMSE (m^3/s)	0.37	0.36	0.43	0.71	0.37	0.51
Sieber	NSE $(-)$	0.93	0.93	0.9	0.72	0.92	0.86
	Pbias $(\%)$	-4.5	-1	9.1	28	2.6	-15.8
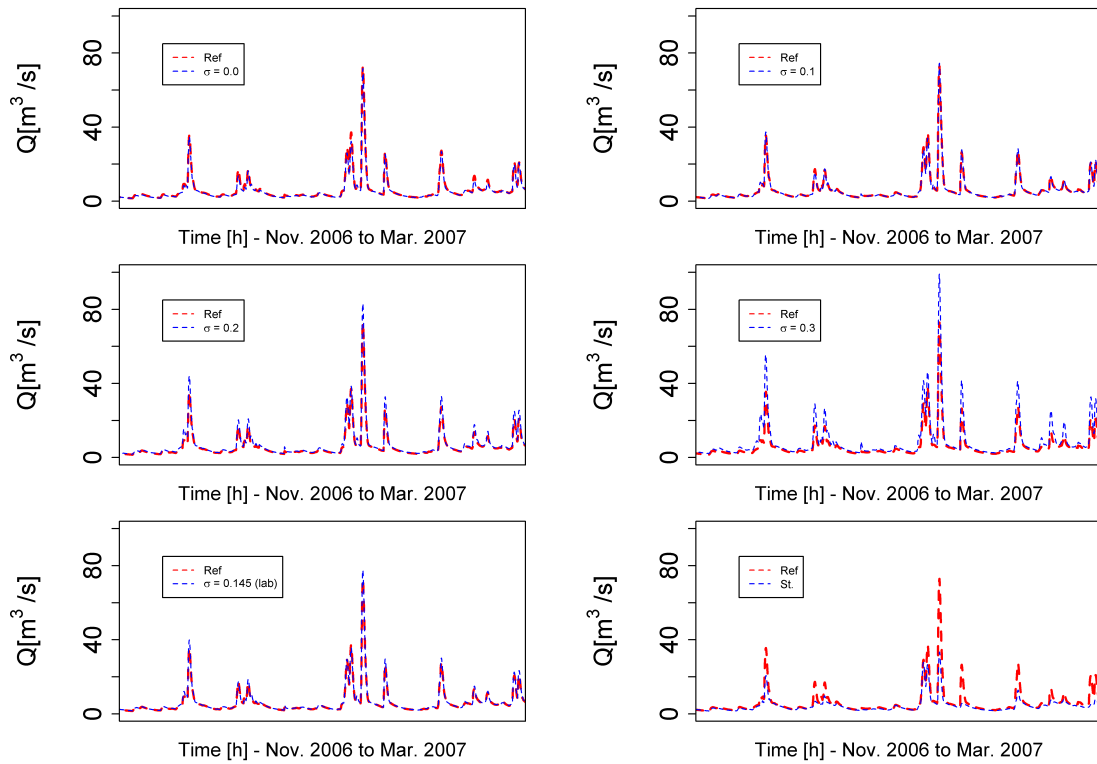
Figure 6.9: Discharge simulation using different sources of data for the Nette catchment. For RCs only 5% scenario is considered.

As observed, the improvement of model performance in the Nette catchment when using RCs is more evident than for the other two catchments. Therefore, it is decided to investigate the Nette catchment in more detail by analysing the hydrographs for all the scenarios given in Table 6.6.

Fig. 6.9 shows the simulated discharge between November 2006 and March 2007. It can be observed that when only rain gauges (St.) are used, the model misses some peaks and performs poorly. This illustrates that the local rainfall is often not captured. The model performance improves significantly when using RCs. By increasing the uncertainties, i.e. enlarging σ^2, the overestimation of rainfall affects the model performance as well. Considering the uncertainties larger than the uncertainty derived from laboratory experiments could in fact illustrate situations that we may encounter in practice and we did not take into account here.

6.5 Summary and conclusion

The value of using moving cars for rainfall measurement purposes (RCs) was investigated with laboratory experiments by RABIEI et al. (2013). They analysed the Hydreon and Xanonex optical sensors against different rainfall intensities. The optical sensors showed promising results when used for point rainfall measurement. Because of the low number of real RCs available on roads, the main objective of this study was to implement and investigate the errors derived from the laboratory experiments for areal rainfall estimation in a computer simulation. The errors were considered for the theoretical RCs, provided by a traffic model, and Ordinary Kriging (OK) is implemented for areal rainfall estimation. Thereafter, the data are also used for discharge simulations in the HBV hydrological model. The value of the RCs is compared with when only rain gauges are implemented. Radar data was considered as the reference data to directly evaluate the areal rainfall estimation rather than following the common approach for evaluating an interpolation technique, i.e. cross-validation. The other sources of data, i.e. RCs and rain gauges, were extracted from the reference data source, accordingly. A period of 5 years from 2006 to 2010 and three catchments with different characteristics are considered. The results of the study are as follows:

1. Implementing RCs with the uncertainties derived from the laboratory experiments improves the quality of modelled areal rainfall estimation compared with when only rain gauges are used. The same is valid for discharge simulation when the estimated areal rainfall is implemented in hydrological modeling. However, the improvement is observed to be strongly dependent on the catchment characteristics, RC network density and spatial rain variability.

2. Because of the positive bias of the error distribution when using a log-transformed W-R relationship, areal rainfall overestimation is, in general, observed which resulted in an overestimation of discharges as well. This can be compensated by either increasing the RC network density or implementing more accurate optical sensors.

3. By increasing the rainfall measurement uncertainty by RCs, i.e. assuming larger variances for the random error, rainfall overestimation increases significantly. Implementing errors up to a certain level is observed beneficiary whereas larger uncertainties resulted in deterioration of results. Although the RCs with large errors should not be considered directly for rainfall measurement, relatively good *NSE* values show the potential of RCs to be regarded as additional information in interpolation techniques.

4. It is observed that applying OK for areal rainfall estimation results in underestimation of rainfall. This was seen when no uncertainty was considered for RCs as well as for the case when only rain gauges were involved. Missing the rainfall maxima over the study area explains this phenomenon.

The hydrological simulations are carried out on hourly temporal resolution data with a lumped model parameter approach where the areal rainfall for each subcatchment is estimated separately. The conclusion of this study may not be valid for other cases when, for example, a distributed model or a different temporal resolution is being investigated. Depending on the target of each study, higher levels of data quality may be required. For instance, following the conclusions by SCHILLING (1991), in which he discussed implementing high spatial (1 km^2) and temporal (1 min) resolution data for urban hydrology, the quality of rainfall measurement by RCs might be insufficient. Furthermore, BERNE et al. (2004) also concluded that a temporal resolution of 5 min and a spatial resolution of about 3 km are required for urban catchments with an area about 1000 ha. They also stated that for smaller catchments with an area about 100 ha, higher resolution of about 3 min and 2 km are needed.

This study only shows the required accuracy that could be considered for RainCars as a future potential of crowdsourcing. Environmental factors such as road spray, car speed, wind direction, snow, night/day variation, etc. can influence the performance of RCs in practice. Although this study showed that the RCs are beneficiary, field experiments are necessary to better assess the measurement uncertainty.

Acknowledgment

Chapter 7

Summary and outlook

Improving rainfall estimation was the main objective of this study. Therefore, investigating the current means of measuring rainfall, on the one hand, and the need for using RainCars (RCs), on the other hand, are the topics discussed in this dissertation. The objectives of this dissertation were addressed separately in Chapters 3 to 6. Therefore, the summary and outlook of the work is also provided in a similar way.

Rainfall measurement and interpolation techniques

Considering the fact that the temporal resolution of data and the number of rain gauges play a crucial role in the quality of areal rainfall estimation, Chapter 3 discussed those factors in relation to using radar data as additional information in interpolation techniques. Three different geostatistical interpolation methods of (1) KED, (2) IKED and (3) CM were implemented to use radar data as additional information. The results were then compared with the reference technique, OK. Temporal resolutions from 10 min to 6 h and five different rain gauge network densities were addressed investigating the sensitivity of each method. Temporal and spatial smoothing of radar data is also addressed in order to investigate a possible improvement in interpolation performances when using radar data as additional information. The methods were evaluated by means of cross validation.

A spatio-temporal smoothing on radar data improved the merging performance the best among other smoothing techniques. However, a consistent improvement was not observed. It was concluded that too much smoothing can result in reduction of the preservation of the observation variance and is not recommended. Furthermore, too much smoothing might also result in a loss

of information. As the correlation between rain gauge values and the corresponding radar-pixels declines for high temporal resolution data, smoothing radar data was observed to be more important for such resolutions. The CM was observed to outperform the KED and IKED in all the scenarios under study. Considering relatively low performance of CM when using original radar data, smoothing radar data was strongly recommended when using CM. Investigating the performance of interpolation techniques in high temporal resolution, it was observed that CM using original radar data performed poorer than OK whereas CM using smoothed radar data outperformed OK. Using radar in CM was generally observed to be more appropriate than other approaches. The numerical instabilities are not expected when implementing CM, whereas they can cause problems in KED. The CM and IKED were observed to be less sensitive to radar data quality than KED, especially when the number of stations is relatively low. In addition to the facts that KED is more time consuming and might face numerical instabilities, if the assumption of having a linear relationship between observation and additional information is not met, the performance of the method can deteriorate. Because of the difficulties radar data has, this could be more dominant for high resolution data, where the additional information might even have an inverse relationship with the observation values. For such conditions, CM is more suitable. Although this might be a problem for high resolution data, KED in coarse temporal resolution data could outperform CM, as a strong linear relationship between the observation values and radar data is expected and problems such as attenuation are more observable. It is worth noticing that all the conclusions are for continuous time series and a similar conclusion might not be valid for single events.

Weather radar is an important source of data with very high temporal and spatial resolution. The data could be considered either directly as input in hydrological analyses or as additional information in interpolation techniques. Although using radar data directly for hydrological analyses was pointed out in several studies, radar data has problems. Smoothing radar data was observed advantageous and resulted in a better performance of geostatistical interpolation techniques. This illustrates the need for correcting radar data even when they are considered as additional information. Several studies have tried to propose methods correcting radar data. Most of the studies try to find a relationship between observations and the corresponding radar-point values. As mentioned earlier, relating these two sources of data might be improper, in particular for high temporal resolutions. This could be explained by the principles describing rainfall estimation by radar, such as the fact that measurements take place at a certain height from the ground.

The method proposed in Chapter 4 assimilates the CDF derived from radar data to the CFD

derived from rain gauges. Applying quantile-quantile (Q-Q) transformation, used usually for scaling and bias correction purposes in climate impact studies, was implemented for correcting radar data. The main assumption is that the spatial statistical variability derived by the CDF from rain gauges is more realistic than the one from radar data. An important advantage of this method is that the observation values are not directly compared with the corresponding radar points for correcting radar data. This makes the method more suitable for high temporal resolution. It is worth mentioning that a specific Q-Q transformation is carried out for each time step, separately. In addition to comparing the rain gauge values with the corresponding radar-pixels for evaluating the method, the performance of CM and KED are also investigated after applying the correction method. The two interpolation techniques were evaluated by means of cross validation. Using radar data for disaggregating non-recording rain gauges is another possible application which is addressed also in this study. The findings of this part of the study are as follows.

It was observed that the radar data quality improved after implementing the quantile mapping correction technique. Furthermore, a better Q-Q transformation was observed when adding 3 time steps before and after the current time step (7 time steps in total) for creating the CDF from rain gauge network. This is more significant for fine temporal resolution when a high number of observations at each time step could have zero values over the study area. However, if too many time steps are taken into consideration, unrealistic CDFs may be set. The seasonal variation observed in interpolation performance in general (using radar data or not) followed the assumption of seasonal changes in types of rainfall events and radar data quality. A better performance was observed in winter time than in summer. This was explained by the fact that the majority of convective events occur in summer. Implementing radar data in interpolation techniques in summer was observed to be useful and correcting radar data was observed to be more important for summer rainfall events. The CM performed better than KED after implementing bias correction. The CM was observed to be more sensitive towards radar data quality compared to EDK, especially when the number of observations is large. Although radar data was observed to be a useful source of data for disaggregating non-recording rain gauges, the correction method was not seen as essential for such purposes.

In general, using bias corrected radar data in CM is recommended when comparing with the other techniques used in this study. This conclusion is only valid for the temporal resolutions considered in this study. GOUDENHOOFDT and DELOBBE (2009), for example, observed that KED performed better than CM for daily temporal resolution. It should be noticed that implementing bias corrected radar data might result in losing information. This could become

more evident for fine temporal resolution and sparse rain gauge network where the rain gauge network is not able to capture events properly.

RAFIEEINASAB et al. (2015) also investigated different merging techniques for improving high resolution quantitative precipitation estimation. They implemented four different methods based on Fisher estimation and its conditional bias-penalized variant for merging available sources of data in north Texas, USA. Although some improvements were observed, the high temporal resolution was 15-min. The DWD weather radar network provides data with 5-min temporal resolution. The data are not accurate and could be improved when merging with rain gauges. It is important to notice that merging rain gauge data with radar data becomes very difficult for fine temporal resolution data. Implementing quantile mapping technique could also result in deteriorating the quality of rainfall estimation if a rain event is not observed by rain gauge network. In this case, applying quantile mapping results in rainfall underestimation. The latter aspect could become less significant by either building a denser rain gauge network or optimizing rain gauge locations for better capturing rain events. The estimated rainfall amounts should always be verified with reliable sources such as rain gauges. It is recommended to verify each time step even separately when it comes to sensitive analyses and fine temporal resolutions.

Some new studies also pointed to the importance of disaggregating daily rain gauge network for increasing rain gauge network density, such as in BÁRDOSSY and PEGRAM (2016). They proposed recently a method for disaggregating the daily rainfall data via simulation. The method is proposed for disaggregating daily records to 1.5 h and hourly amount. They used a Gaussian copula-based model when the temporal information of the records are used to define the marginal distributions and censored values representing the dry periods. They point the fact that although high spatial precipitation variability is a known problem, a strong temporal coherence exists. They assumed that a specific distribution of precipitation could be determined for each time step using all recording rain gauges. They compared the method with Rescaled Ordinary kriging (ROK) and Rescaled Nearest Neighbors (RNN). They believe that their approach is superior to any of previously known methods.

CM is also used recently for merging rain gauge data with satellite data, for example, JONGJIN et al. (2016) tried to merge satellite-based and ground-based data using CM, Geographic Differential Analysis (GDA), and Geographic Ratio Analysis (GRA) methods. They also recommend implementing CM for merging the two sources, in particular for regions with sparse rain gauges. However, the finest temporal resolution investigated in that study was 1 hour. By accumulating the temporal resolution to daily, OK outperformed the other methods.

Moving cars measuring rainfall

After hypothetically investigating the potential of using RainCars by HABERLANDT and SESTER (2010), the main objective of Chapter 5 was to investigate RainCars for point measurement purposes. Consequently, wiper activity and signals coming from optical sensors indicating rainfall intensity are analyzed. The relationship between sensor readings (W) and rain intensity (R) is derived by laboratory experiments. Two readings of (1) wiper speed adjusted both manually and by optical sensors and (2) optical sensors designed for automating wiper activities were considered to indicate rainfall intensity. The sensor readings were analyzed considering tipping bucket readings as reference. Another important factor influencing the readings in practice is the car speed. This issue was also addressed using a car speed simulator.

It was observed that manual adjustment of wiper activity, according to front visibility, has a stronger relationship than when the wiper activity is adjusted by the optical sensor installed in the car. This was explained by the relatively inaccurate data processing of the readings from the optical sensor and point measurement of the optical sensor adjusting wiper activity. Therefore, it was concluded that a better calibration of the optical sensor when adjusting wiper speed may result in better efficiency of the sensor, and therefore, a better W-R relationship. On the other hand, the two extra optical sensors (Hydreon and Xanonex) showed promising results. Although the hydreon sensor is a calibrated optical sensor, an underestimation of rainfall amount was observed. The device observed also to have a systematic error in the derived W-R relationship. The other optical sensor, the Xanonex, was observed to be useful for rainfall measurement, but less accurate than Hydreon. The influence of the car speed on sensor readings could be explained by a linear regression model, whereas the empirical relationship followed the theoretical relationship up to a certain speed. The theoretical relationship was observed to be strongly dependent upon two important factors of drop velocity and windshield angle. However, the drop velocity was observed to be more influential. The drop velocity can be interpreted as representing rain type. This means that the W-R relationship may vary for different rain events similar to the Z-R relationship for radar data.

The measurement uncertainty of RainCars was investigated in Chapter 5. Due to the difficulties that wiper adjustment had, it was decided to investigate the benefit of using optical sensors when installed in RainCars for rainfall estimation. As the number of RainCars available on streets is not sufficient to be investigated directly for rainfall estimation, computer experiments are set up to investigate the uncertainties observed earlier in the laboratory for both areal rainfall estimation and discharge simulation. This was described in more detail in Chapter 6. Although

both optical sensors showed promising results, the Xanonex optical sensor was selected for further investigation. This decision was made because of the ease of installing the device in cars. The benefit of using RainCars could be observed when comparing the results with when only rain gauges are implemented for both areal rainfall estimation and discharge simulation. The discharge is simulated by the HBV-IWW hydrological model, using a constant parameter set for all the sources. Rather than investigating the interpolation performances by means of cross-validation, radar data (as the reference) was compared with the areal rainfall estimation using the other sources, i.e. RainCars and rain gauges, where RainCars and values for rain gauges were extracted from radar data. A random error was introduced into the RainCars' values on the log-transformed W-R relationship. On the contrary, the extracted values for rain gauges were used directly. OK was applied for areal rainfall estimation. In a similar way, discharge simulations by RainCars and rain gauges were compared with the reference discharge simulated by radar. Higher and lower uncertainties for RainCars were also addressed in addition to investigating the uncertainties derived in laboratory experiments in order to make a more general conclusion. Furthermore, due to the fact that the number of RainCars is an influencing factor, different scenarios addressed different hypothetical numbers of RainCars in the streets. A period of five years from 2006 to 2010 and three catchments with different characteristics were considered in this part of the study.

It was observed that using RainCars with uncertainties derived from laboratory experiments resulted in a better areal rainfall estimation compared with when only rain gauges are used. A similar conclusion is valid for discharge simulation when using the data in the HBV-IWW hydrological model. However, factors such as the number of RainCars, spatial rainfall variability and catchment characteristics were observed to be influential on the improvement of discharge simulation. An overestimation of rainfall was observed when using RainCars, which was explained by the W-R relationship used for transforming signal readings to rain intensities. By increasing the uncertainty for RainCars (larger σ in random error), rainfall overestimation increased significantly. RainCars up to a certain uncertainty were observed to be still beneficial for using directly for areal rainfall estimation, whereas larger uncertainties deteriorated the results. However, because of the relatively good *NSE* values, RainCars with large errors could still be suggested to be considered as additional information in interpolation techniques. Applying OK was observed to underestimate the rainfall amount. Missing the rainfall maxima over the study area could justify this phenomenon.

Although RainCars were observed to be useful in this study, the results might not be valid for other study areas, temporal resolutions or model structures. It is worth mentioning again that

all the results were under certain conditions in computer experiments. Not only several factors, such as road spray, car speed and wind direction could influence the performance of RainCars, but also some soft issues, such as hydrological model interactions. Some investigations for analyzing the RainCars data from field experiments were provided by FITZNER et al. (2013). However, wiper frequency, used in that study, was not observed to be a strong rainfall intensity indicator.

RainCars could be a very important potential for crowdsourcing. MULLER et al. (2015) described the current status and future potential of crowdsourcing for climate and atmospheric sciences. They pointed at the benefits of using such data sources as they are cost-effective. However, they are of the opinion that more research is required for evaluation. ALLAMANO et al. (2015) introduce a technique for satisfying the need for larger number of observations by estimating instantaneous rain rates using pictures of rainy scenes. They pointed to the fact that even defining a region of influence with a 5 km radius for each rain gauge could be insufficient for short rainfall events. They described the image processing steps as follows: (1) drop detection, (2) blur effect removal, (3) estimation of the drop velocity, (4) drop positioning in the control volume, and (5) rain rate estimation. However, they realised that the quality of the results is strongly dependent on the setting of the camera during the shooting. BERNE et al. (2004) concluded that the region of influence becomes larger for longer aggregation intervals. MULLER et al. (2015) stated also the fact that depending on the scale of analyses different scales are required. Five min resolution, for example, for urban hydrology and hourly data for other regional hydrological applications. It can be concluded that RainCars could improve the analyses under certain conditions. The number of observations becomes more important when spatio-temporal variation of rainfall is large. For fine temporal analyses and/or convective rain events, a denser network of observations is required. For such analyses, in fact, RainCars may improve the quality of the analyses.

A higher number of RainCars and more attention need to be given to the field experiments for a better conclusion. One of the problems in the field experiments when evaluating RainCars is finding a reliable reference data source. Radar data can not be considered as the reference for real RainCars due to all the deficiencies related to this data source. On the other hand, increasing the number of rain gauges is not feasible. By increasing the number of RainCars, evaluating the moving sensors would be more plausible as it is more likely that a RainCar is in the vicinity of a station. This is also less costly comparing with increasing the number of rain gauges. In such a way, similar approaches to FITZNER et al. (2013) could be more useful. Furthermore, considering a certain study area (a city) for evaluating different approaches

similar to RainCars (such as acoustic rain gauges) could help to compare their performances. Consequently, the number of reliable observations, e.g. rain gauges, for such a study area should be large enough, so that they could act as the reference.

In general, it could be concluded that the need for better rainfall data quality, in particular for fine temporal resolution, is evident. This might not be fulfilled using available sources of data, whereas using new ideas such as RainCars could help for better estimating areal rainfall. This need could also be satisfied using X-Band radar devices scanning with very high temporal and spatial resolution. CLEMENS (2013), for example, described the X-Band radar devices investigated in the University of Hamburg. The temporal resolution of 30 s and spatial resolution of 60 m along each beam (with azimuth resolution of 1°) provides a unique data source. However, the data are subject to several errors. Merging such a high resolution data source with RainCars (and if possible with rain gauges) might help to better estimate rainfall amount over certain areas.

Bibliography

ADAM, J. C., E. A. CLARK, D. P. LETTENMAIER, and E. F. WOOD (2006). "Correction of global precipitation products for orographic effects". *Journal of Climate* 19.1, pp. 15–38.

ALFIERI, L., P. CLAPS, and F. LAIO (2010). "Time-dependent ZR relationships for estimating rainfall fields from radar measurements". *Natural Hazards and Earth System Science* 10.1, pp. 149–158.

ALLAMANO, P, A CROCI, and F LAIO (2015). "Toward the camera rain gauge". *Water Resources Research* 51.3, pp. 1744–1757.

AUSTIN, P. M. (1987). "Relation between measured radar reflectivity and surface rainfall". *Monthly Weather Review* 115.5, pp. 1053–1070.

AZIMI-ZONOOZ, A, W. KRAJEWSKI, D. BOWLES, and D. SEO (1989). "Spatial rainfall estimation by linear and non-linear co-kriging of radar-rainfall and raingage data". *Stochastic Hydrology and Hydraulics* 3.1, pp. 51–67.

BÁRDOSSY, A and T DAS (2008). "Influence of rainfall observation network on model calibration and application". *Hydrology and Earth System Sciences Discussions* 12.1, pp. 77–89.

BÁRDOSSY, A. and J. LI (2008). "Geostatistical interpolation using copulas". *Water Resources Research* 44.7.

BÁRDOSSY, A. and G. PEGRAM (2011). "Downscaling precipitation using regional climate models and circulation patterns toward hydrology". *Water Resources Research* 47.4.

BÁRDOSSY, A. and G. PEGRAM (2013). "Interpolation of precipitation under topographic influence at different time scales". *Water Resources Research* 49.8, pp. 4545–4565.

BÁRDOSSY, A. and G. PEGRAM (2016). "Space-time conditional disaggregation of precipitation at high resolution via simulation". *Water Resources Research*.

BATTAN, L. J. (1973). "Radar Observation of the Atmosphere".

BERNDT, C., E. RABIEI, and U. HABERLANDT (2014). "Geostatistical merging of rain gauge and radar data for high temporal resolutions and various station density scenarios". *Journal of Hydrology* 508, pp. 88–101.

BERNE, A., G. DELRIEU, J.-D. CREUTIN, and C. OBLED (2004). "Temporal and spatial resolution of rainfall measurements required for urban hydrology". *Journal of Hydrology* 299.3, pp. 166–179.

BIEMANS, H, R. HUTJES, P KABAT, B. STRENGERS, D GERTEN, and S ROST (2009). "Effects of precipitation uncertainty on discharge calculations for main river basins". *Journal of Hydrometeorology* 10.4, pp. 1011–1025.

BOCCI, F. (2012). "Whether or not to run in the rain". *European Journal of Physics* 33.5, p. 1321.

CARACCIOLO, C, F PORCU, and F PRODI (2008). "Precipitation classification at mid-latitudes in terms of drop size distribution parameters". *Advances in Geosciences* 16, pp. 11–17.

CHANDRASEKAR, V, H. CHEN, and M. MAKI (2012). "Urban flash flood applications of high-resolution rainfall estimation by X-band dual-polarization radar network". *SPIE Asia-Pacific Remote Sensing*. International Society for Optics and Photonics, 85230K–85230K.

CHEN, J., F. P. BRISSETTE, D. CHAUMONT, and M. BRAUN (2013). "Finding appropriate bias correction methods in downscaling precipitation for hydrologic impact studies over North America". *Water Resources Research* 49.7, pp. 4187–4205.

CHUMCHEAN, S., A. SHARMA, and A. SEED (2003). "Radar rainfall error variance and its impact on radar rainfall calibration". *Physics and Chemistry of the Earth, Parts A/B/C* 28.1, pp. 27–39.

CHUMCHEAN, S., A. SEED, and A. SHARMA (2004). "Application of scaling in radar reflectivity for correcting range-dependent bias in climatological radar rainfall estimates". *Journal of Atmospheric and Oceanic Technology* 21.10, pp. 1545–1556.

CHUMCHEAN, S., A. SHARMA, and A. SEED (2006). "An integrated approach to error correction for real-time radar-rainfall estimation". *Journal of Atmospheric and Oceanic Technology* 23.1, pp. 67–79.

CIACH, G. J. (2003). "Local random errors in tipping-bucket rain gauge measurements". *Journal of Atmospheric and Oceanic Technology* 20.5, pp. 752–759.

CLEMENS, M. (2013). "Wetterradar–Eine Gerätevorstellung". *Wetterradar – Anwendungen und neue Entwickelungen*, pp. 91–98.

DWD (2016). "DWD FTP". *ftp://ftp-cdc.dwd.de/*.

DELRIEU, G., H. ANDRIEU, and J. D. CREUTIN (2000). "Quantification of path-integrated attenuation for X-and C-band weather radar systems operating in Mediterranean heavy rainfall". *Journal of Applied Meteorology* 39.6, pp. 840–850.

DEUTSCH, C. and A. JOURNEL (1992). *GSLIB: Geostatistical Software Library and User's Manual*.

DIOP, M and D. GRIMES (2003). "Satellite-based rainfall estimation for river flow forecasting in Africa. II: African Easterly Waves, convection and rainfall". *Hydrological sciences journal* 48.4, pp. 585–599.

DUBOIS, G, J MALCZEWSKI, and M. CORT (1998). "Spatial interpolation comparison 97: special issue". *Journal of Geographic Information and Decision Analysis* 2.1-2.

EHRET, U. (2002). *Rainfall and flood nowcasting in small catchments using weather radar*. Eigenverlag des Instituts für Wasserbau an der Universität Stuttgart.

ERDIN, R., C. FREI, and H. R. KÜNSCH (2012). "Data transformation and uncertainty in geostatistical combination of radar and rain gauges". *Journal of Hydrometeorology* 13.4, pp. 1332–1346.

FIENER, P, S. SEIBERT, and K AUERSWALD (2011). "A compilation and meta-analysis of rainfall simulation data on arable soils". *Journal of hydrology* 409.1, pp. 395–406.

FITZNER, D., M. SESTER, U. HABERLANDT, and E. RABIEI (2013). "Rainfall Estimation with a Geosensor Network of Cars – Theoretical Considerations and First Results". *Photogrammetrie - Fernerkundung - Geoinformation* 2013.2, pp. 93–103.

GERMANN, U. and J. JOSS (2001). "Variograms of radar reflectivity to describe the spatial continuity of Alpine precipitation". *Journal of Applied Meteorology* 40.6, pp. 1042–1059.

GOOVAERTS, P. (1997). *Geostatistics for natural resources evaluation*. Oxford university press.

GOOVAERTS, P. (2000). "Geostatistical approaches for incorporating elevation into the spatial interpolation of rainfall". *Journal of hydrology* 228.1, pp. 113–129.

GOUDENHOOFDT, E and L DELOBBE (2009). "Evaluation of radar-gauge merging methods for quantitative precipitation estimates". *Hydrology and Earth System Sciences* 13.2, pp. 195–203.

GRIFFITH, R. (1995). "Weather radar and strategic urban drainage in real time." PhD thesis. University of Salford.

GUPTA, H. V., S. SOROOSHIAN, and P. O. YAPO (1999). "Status of automatic calibration for hydrologic models: Comparison with multilevel expert calibration". *Journal of Hydrologic Engineering* 4.2, pp. 135–143.

GYASI-AGYEI, Y. and G. PEGRAM (2014). "Interpolation of daily rainfall networks using simulated radar fields for realistic hydrological modelling of spatial rain field ensembles". *Journal of Hydrology* 519, pp. 777–791.

HABERLANDT, U. and M. SESTER (2010). "Areal rainfall estimation using moving cars as rain gauges–a modelling study". *Hydrology and Earth System Sciences* 14.7, pp. 1139–1151.

HABERLANDT, U. (2007). "Geostatistical interpolation of hourly precipitation from rain gauges and radar for a large-scale extreme rainfall event". *Journal of Hydrology* 332.1, pp. 144–157.

HAGEN, M. (2013). "Wetterradar–Eine Gerätevorstellung". *Wetterradar – Anwendungen und neue Entwickelungen*, pp. 23–34.

HAMMER, T. (2006). "Hammer". *http://www.der-hammer.info/*.

HAYKIN, S., B. W. CURRIE, and S. B. KESLER (1982). "Maximum-entropy spectral analysis of radar clutter". *Proceedings of the IEEE* 70.9, pp. 953–962.

HELMERT, K., P. TRACKSDORF, J. STEINERT, M. WERNER, M. FRECH, N. RATHMANN, T. HENGSTEBECK, M. MOTT, S. SCHUMANN, and T. MAMMEN (2014). "DWDs new radar network and post-processing algorithm chain". *8th Europ. Conf. on Radar in Meteorology and Hydrology, Garmisch-Partenkirchen*, pp. 1–6.

HOFSTRA, N., M. NEW, and C. MCSWEENEY (2010). "The influence of interpolation and station network density on the distributions and trends of climate variables in gridded daily data". *Climate dynamics* 35.5, pp. 841–858.

HUTCHINSON, M. F. (1998a). "Interpolation of rainfall data with thin plate smoothing splines. Part I: Two dimensional smoothing of data with short range correlation". *Journal of Geographic Information and Decision Analysis* 2.2, pp. 139–151.

HUTCHINSON, M. F. (1998b). "Interpolation of rainfall data with thin plate smoothing splines. Part II: Analysis of topographic dependence". *Journal of Geographic Information and Decision Analysis* 2.2, pp. 152–167.

HYDREON (2012). "Rain Gauge Model RG-11 Instructions". *http://www.rainsensors.com/*.

HYDREON (2015). "Rain Gauge Model RG-11 Instructions". *http://www.rainsensors.com/*.

INES, A. V. and J. W. HANSEN (2006). "Bias correction of daily GCM rainfall for crop simulation studies". *Agricultural and forest meteorology* 138.1, pp. 44–53.

ISAAKS, E. H. and R. M. SRIVASTAVA (1990). "An introduction to applied geostatistics".

JAKOB THEMESSL, M., A. GOBIET, and A. LEUPRECHT (2011). "Empirical-statistical downscaling and error correction of daily precipitation from regional climate models". *International Journal of Climatology* 31.10, pp. 1530–1544.

JASPER, K., J. GURTZ, and H. LANG (2002). "Advanced flood forecasting in Alpine watersheds by coupling meteorological observations and forecasts with a distributed hydrological model". *Journal of hydrology* 267.1, pp. 40–52.

JAVIER, J. R. N., J. A. SMITH, K. L. MEIERDIERCKS, M. L. BAECK, and A. J. MILLER (2007). "Flash flood forecasting for small urban watersheds in the Baltimore metropolitan region". *Weather and Forecasting* 22.6, pp. 1331–1344.

JONG, S. DE (2010). "Low cost disdrometer". *Master thesis report, TU Delft, the Netherlands*.

JONGJIN, B., P. JONGMIN, R. DONGRYEOL, and C. MINHA (2016). "Geospatial blending to improve spatial mapping of precipitation with high spatial resolution by merging satellite-based and ground-based data". *Hydrological Processes*.

KAVETSKI, D., F. FENICIA, and M. P. CLARK (2011). "Impact of temporal data resolution on parameter inference and model identification in conceptual hydrological modeling: Insights from an experimental catchment". *Water Resources Research* 47.5.

KIDD, C. and G. HUFFMAN (2011). "Global precipitation measurement". *Meteorological Applications* 18.3, pp. 334–353.

KIDD, C. and V LEVIZZANI (2011). "Status of satellite precipitation retrievals". *Hydrology and Earth System Sciences* 15.4, pp. 1109–1116.

KIRKPATRICK, S. (1984). "Optimization by simulated annealing: Quantitative studies". *Journal of statistical physics* 34.5-6, pp. 975–986.

KITANIDIS, P. (1997). *Introduction to geostatistics: applications in hydrogeology*. Cambridge University Press.

KITCHEN, M, R BROWN, and A. DAVIES (1994). "Real-time correction of weather radar data for the effects of bright band, range and orographic growth in widespread precipitation". *Quarterly Journal of the Royal Meteorological Society* 120.519, pp. 1231–1254.

KRAJEWSKI, W. F. (1987). "Cokriging radar-rainfall and rain gage data". *Journal of Geophysical Research: Atmospheres (1984–2012)* 92.D8, pp. 9571–9580.

KUMMEROW, C., W. BARNES, T. KOZU, J. SHIUE, and J. SIMPSON (1998). "The tropical rainfall measuring mission (TRMM) sensor package". *Journal of atmospheric and oceanic technology* 15.3, pp. 809–817.

LANZA, L, M LEROY, C ALEXANDROPOULOS, L STAGI, and W WAUBEN (2006). "WMO laboratory intercomparison of rainfall intensity gauges". *Final report, WMO, Geneva*.

LEIJNSE, H, R UIJLENHOET, and J. STRICKER (2007). "Rainfall measurement using radio links from cellular communication networks". *Water resources research* 43.3.

LENGFELD, K., M. CLEMENS, H. MÜNSTER, and F. AMENT (2014). "Performance of high-resolution X-band weather radar networks – the PATTERN example". *Atmospheric Measurement Techniques* 7.12, pp. 4151–4166.

LI, M. and Q. SHAO (2010). "An improved statistical approach to merge satellite rainfall estimates and raingauge data". *Journal of Hydrology* 385.1, pp. 51–64.

LI, Y., G. ZHANG, and R. J. DOVIAK (2014). "Ground clutter detection using the statistical properties of signals received with a polarimetric radar". *Signal Processing, IEEE Transactions on* 62.3, pp. 597–606.

LINDSTRÖM, G., B. JOHANSSON, M. PERSSON, M. GARDELIN, and S. BERGSTRÖM (1997). "Development and test of the distributed HBV-96 hydrological model". *Journal of hydrology* 201.1, pp. 272–288.

LIU, M., A. BÁRDOSSY, and E. ZEHE (2013). "Interaction of valleys and circulation patterns (CPs) on spatial precipitation patterns in southern Germany". *Hydrology and Earth System Sciences* 17.11, pp. 4685–4699.

LULL, H. W. (1959). *Soil compaction on forest and range lands*. 768. Forest Service, US Department of Agriculture.

MAIDMENT, D. R. et al. (1992). *Handbook of hydrology*. McGraw-Hill Inc.

MATHERON, G. (1963). "Principles of geostatistics". *Economic geology* 58.8, pp. 1246–1266.

MAY, R. M. (2014). "Estimating and Mitigating Errors in Dual-Polarization Radar Attenuation Correction".

MESSER, H., A. ZINEVICH, and P. ALPERT (2006). "Environmental monitoring by wireless communication networks". *Science* 312.5774, pp. 713–713.

MULLER, C., L CHAPMAN, S JOHNSTON, C KIDD, S ILLINGWORTH, G FOODY, A OVEREEM, and R. LEIGH (2015). "Crowdsourcing for climate and atmospheric sciences: current status and future potential". *International Journal of Climatology* 35.11, pp. 3185–3203.

NASH, J. and J. V. SUTCLIFFE (1970). "River flow forecasting through conceptual models part IŮA discussion of principles". *Journal of hydrology* 10.3, pp. 282–290.

OUBEIDILLAH, A. A., S.-C. KAO, M. ASHFAQ, B. S. NAZ, and G. TOOTLE (2014). "A large-scale, high-resolution hydrological model parameter data set for climate change impact assessment for the conterminous US". *Hydrology and Earth System Sciences* 18.1, pp. 67–84.

OVEREEM, A., H. LEIJNSE, and R. UIJLENHOET (2013). "Country-wide rainfall maps from cellular communication networks". *Proceedings of the National Academy of Sciences* 110.8, pp. 2741–2745.

PEGRAM, G., X. LLORT, and D. SEMPERE-TORRES (2011). "Radar rainfall: separating signal and noise fields to generate meaningful ensembles". *Atmospheric Research* 100.2, pp. 226–236.

PHOCAIDES, A (2000). *Technical hand book on pressurized irrigation techniques, food and agriculture organization of the United Nations*.

PRAKASH, S., A. K. MITRA, D. PAI, and A. AGHAKOUCHAK (2016). "From TRMM to GPM: How well can heavy rainfall be detected from space?" *Advances in Water Resources* 88, pp. 1–7.

PRICE, K., S. T. PURUCKER, S. R. KRAEMER, J. E. BABENDREIER, and C. D. KNIGHTES (2014). "Comparison of radar and gauge precipitation data in watershed models across varying spatial and temporal scales". *Hydrological Processes* 28.9, pp. 3505–3520.

QUIRMBACH, M and G SCHULTZ (2002). "Comparison of rain gauge and radar data as input to an urban rainfall-runoff model". *Water Science & Technology* 45.2, pp. 27–33.

RABIEI, E. and U. HABERLANDT (2015). "Applying bias correction for merging rain gauge and radar data". *Journal of Hydrology* 522, pp. 544–557.

RABIEI, E, U. HABERLANDT, M. SESTER, and D. FITZNER (2013). "Rainfall estimation using moving cars as rain gauges–laboratory experiments". *Hydrology and Earth System Sciences* 17.11, pp. 4701–4712.

RAFIEEINASAB, A., A. NOROUZI, D.-J. SEO, and B. NELSON (2015). "Improving high-resolution quantitative precipitation estimation via fusion of multiple radar-based precipitation products". *Journal of Hydrology* 531, pp. 320–336.

RAHIMI, A., A. HOLT, G. UPTON, S KRÄMER, A REDDER, and H. VERWORN (2006). "Attenuation calibration of an X-band weather radar using a microwave link". *Journal of Atmospheric and Oceanic Technology* 23.3, pp. 395–405.

RIEDL, J (1986). "Radar-Flächenniederschlagsmessung". *Promet* 2.3, pp. 20–23.

ROGELIS, M. and M. WERNER (2013). "Spatial interpolation for real-time rainfall field estimation in areas with complex topography". *Journal of Hydrometeorology* 14.1, pp. 85–104.

SALLES, C and J. POESEN (1999). "Performance of an optical spectro pluviometer in measuring basic rain erosivity characteristics". *Journal of Hydrology* 218.3, pp. 142–156.

SCHILLING, W. (1991). "Rainfall data for urban hydrology: what do we need?" *Atmospheric Research* 27.1, pp. 5–21.

SELTMANN, J (1997). "Radarforschung im DWD: Vom Scan zum Produkt". *Promet* 26, pp. 32–42.

SEO, D.-J., J. BREIDENBACH, and E. JOHNSON. "Real-time estimation of mean field bias in radar rainfall data". *Journal of Hydrology*.

SERRA, Y. L., P. A'HEARN, H. P. FREITAG, and M. J. MCPHADEN (2001). "ATLAS self-siphoning rain gauge error estimates*". *Journal of Atmospheric and Oceanic Technology* 18.12, pp. 1989–2002.

SHARPLEY, A. and P. KLEINMAN (2003). "Effect of rainfall simulator and plot scale on overland flow and phosphorus transport". *Journal of Environmental Quality* 32.6, pp. 2172–2179.

SHEPARD, D. (1968). "A Two-dimensional Interpolation Function for Irregularly-spaced Data". *Proceedings of the 1968 23rd ACM National Conference*. ACM '68. New York, NY, USA: ACM, pp. 517–524.

SHRESTHA, R., Y. TACHIKAWA, and K. TAKARA (2006). "Input data resolution analysis for distributed hydrological modeling". *Journal of Hydrology* 319.1, pp. 36–50.

SILVERMAN, B. W. (1986). *Density estimation for statistics and data analysis*. Vol. 26. CRC press.

SINCLAIR, S. and G. PEGRAM (2005). "Combining radar and rain gauge rainfall estimates using conditional merging". *Atmospheric Science Letters* 6.1, pp. 19–22.

SMITH, E. A., G. ASRAR, Y. FURUHAMA, A. GINATI, A. MUGNAI, K. NAKAMURA, R. F. ADLER, M.-D. CHOU, M. DESBOIS, J. F. DURNING, et al. (2007). "International global precipitation measurement (GPM) program and mission: An overview". *Measuring precipitation from space*. Springer, pp. 611–653.

TEEGAVARAPU, R. S. (2014). "Statistical corrections of spatially interpolated missing precipitation data estimates". *Hydrological Processes* 28.11, pp. 3789–3808.

THORNDAHL, S., J. E. NIELSEN, and M. R. RASMUSSEN (2014). "Bias adjustment and advection interpolation of long-term high resolution radar rainfall series". *Journal of Hydrology* 508, pp. 214–226.

UPTON, G., A. HOLT, R. CUMMINGS, A. RAHIMI, and J. GODDARD (2005). "Microwave links: The future for urban rainfall measurement?" *Atmospheric research* 77.1, pp. 300–312.

VELASCO-FORERO, C. A., D. SEMPERE-TORRES, E. F. CASSIRAGA, and J. J. GÓMEZ-HERNÁNDEZ (2009). "A non-parametric automatic blending methodology to estimate

rainfall fields from rain gauge and radar data". *Advances in Water Resources* 32.7, pp. 986–1002.

VERWORN, A and U HABERLANDT (2011). "Spatial interpolation of hourly rainfall–effect of additional information, variogram inference and storm properties". *Hydrology and Earth System Sciences* 15.2, pp. 569–584.

VOGL, S, P LAUX, W QIU, G MAO, and H KUNSTMANN (2012). "Copula-based assimilation of radar and gauge information to derive bias-corrected precipitation fields". *Hydrology and Earth System Sciences* 16.7, pp. 2311–2328.

WALLNER, M. and U. HABERLANDT (2015). "Non-stationary hydrological model parameters: a framework based on SOM-B". *Hydrological Processes*.

WALLNER, M., U. HABERLANDT, and J. DIETRICH (2013). "A one-step similarity approach for the regionalization of hydrological model parameters based on Self-Organizing Maps". *Journal of Hydrology* 494, pp. 59–71.

WEIGL, E. (2013). "Wetterradar–Eine Gerätevorstellung". *Datenprodukte und Datenaufbereitung beim Deutschen Wetterdienst*, pp. 37–43.

WILSON, J. W. and E. A. BRANDES (1979). "Radar measurement of rainfall-A summary". *Bulletin of the American Meteorological Society* 60.9, pp. 1048–1058.

WOLDEMESKEL, F. M., B. SIVAKUMAR, and A. SHARMA (2013). "Merging gauge and satellite rainfall with specification of associated uncertainty across Australia". *Journal of Hydrology* 499, pp. 167–176.

XANONEX (2012). "Xanonex Funktionsweise". *http://www.xanonex.de/*.

XANONEX (2015). "Xanonex Funktionsweise". *http://www.xanonex.de/*.

XU, H., C.-Y. XU, H. CHEN, Z. ZHANG, and L. LI (2013). "Assessing the influence of rain gauge density and distribution on hydrological model performance in a humid region of China". *Journal of Hydrology* 505, pp. 1–12.

YOON, S.-S., A. T. PHUONG, and D.-H. BAE (2012). "Quantitative comparison of the spatial distribution of radar and gauge rainfall data". *Journal of Hydrometeorology* 13.6, pp. 1939–1953.

ZINEVICH, A., H. MESSER, and P. ALPERT (2009). "Frontal rainfall observation by a commercial microwave communication network". *Journal of Applied Meteorology and Climatology* 48.7, pp. 1317–1334.